PLOS ONE

RESEARCH ARTICLE

Co-expression analysis identifies neuro-inflammation as a driver of sensory neuron aging in *Aplysia californica*

N. S. Kron*, L. A. Fieber

Department of Marine Biology and Ecology, Rosenstiel School of Marine and Atmospheric Science, University of Miami, Miami, FL, United States of America

* n.kron@umiami.edu

OPEN ACCESS

Citation: Kron NS, Fieber LA (2021) Co-expression analysis identifies neuro-inflammation as a driver of sensory neuron aging in *Aplysia californica*. PLoS ONE 16(6): e0252647. https://doi.org/10.1371/journal.pone.0252647

Editor: Jian Jing, Nanjing University, CHINA

Received: September 21, 2020

Accepted: May 20, 2021

Published: June 11, 2021

Data Availability Statement: The BioProject in which our sequencing data is archived can be accessed here: https://www.ncbi.nlm.nih.gov/bioproject/PRJNA639857. The project has Accession: PRJNA639857, ID: 639857, and title: Aplysia californica Sensory Neuron Time Series Transcriptome.

Funding: This work was funded by the National Institutes of Health Grant (P40OD010952). The funders had no role in study design, data collection and analysis, decision to publish, or preparation of the manuscript. This work was made possible, in part, through access to the Genomics High

Abstract

Aging of the nervous system is typified by depressed metabolism, compromised proteostasis, and increased inflammation that results in cognitive impairment. Differential expression analysis is a popular technique for exploring the molecular underpinnings of neural aging, but technical drawbacks of the methodology often obscure larger expression patterns. Co-expression analysis offers a robust alternative that allows for identification of networks of genes and their putative central regulators. In an effort to expand upon previous work exploring neural aging in the marine model *Aplysia californica*, we used weighted gene correlation network analysis to identify co-expression networks in a targeted set of aging sensory neurons in these animals. We identified twelve modules, six of which were strongly positively or negatively associated with aging. Kyoto Encyclopedia of Genes analysis and investigation of central module transcripts identified signatures of metabolic impairment, increased reactive oxygen species, compromised proteostasis, disrupted signaling, and increased inflammation. Although modules with immune character were identified, there was no correlation between genes in Aplysia that increased in expression with aging and the orthologous genes in oyster displaying long-term increases in expression after a virus-like challenge. This suggests anti-viral response is not a driver of Aplysia sensory neuron aging.

1 Introduction

As an organ composed of long-lived cells, the brain is uniquely susceptible to the deleterious effects of aging, the outcome of which is often cognitive impairment [1,2]. Common hallmarks of brain aging include impaired metabolism, compromised proteostasis, mitochondrial dysfunction, and neuro-inflammation [3–5]. However, what causes these hallmark phenotypes is not well understood and still debated [6–8]. Due to the complexity of mammalian brains, invertebrate models are often employed for the study of aging in the nervous system at the neuronal level.

The marine model *Aplysia californica* is well suited for study of aging neurons. These mollusks live approximately one year in the wild and mariculture setting and have relatively simple nervous systems of only approximately 10,000 neurons grouped into well mapped circuits [9–11].

Throughput Facility Shared Resource of the Cancer Center Support Grant (P30CA-062203) at the University of California, Irvine and NIH shared instrumentation grants 1S10RR025496-01, 1S10OD010794-01, and 1S10OD021718-01.

Competing interests: The authors have declared that no competing interests exist.

Studies on the life history and reflex behaviors of these animals in controlled environments have described weight loss and cognitive impairment in old age similar to that of other animals and humans [12–16]. Investigation of physiology and transcriptomics in easily identifiable neurons and neuron clusters during aging have elucidated neuronal correlates that underpin aging phenotypes at the behavior and organism level [17–23]. Indeed, it is the capacity for vertical integration of investigation, from molecular to behavioral, that makes Aplysia such an effective model for the aging nervous system. Previously, transcriptomic studies in aging sensory neurons of Aplysia identified signatures of common aging hallmarks, namely metabolic and proteostatic impairment [20,24]. However, due to the limitations of differential expression analysis (DEA), including log fold change thresholds and multiple comparison [25], the driving mechanism behind these transcriptional changes could not be identified. A common alternative analysis that can overcome these limitations is weighted gene correlation network analysis (*WGCNA*).

WGCNA is able to lessen the impact of correction for multiple tests by comparing changes in groups of genes, called modules, as opposed to individual genes and does not employ the strict fold change thresholds used in DEA [25,26]. This method can capture network level changes that integrate the small, coordinated changes of many genes that would otherwise be below the thresholds employed in DEA [27]. Furthermore, *WGCNA* allows for the identification of putative central driver genes in co-expression networks and inference of putative function for genes that are undescribed or have yet to be experimentally verified via guilt-by-association [26,28,29]. In this study we used *WGCNA* and eigengene network analysis to identify the central drivers of the transcriptional aging phenotype of Aplysia SN.

2 Methods

2.1 Experimental design

Sequencing data for this study were generated in our previous study [24]. RNA was extracted from *A*. *californica* Buccal S Cluster (BSC) and Pleural Ventral Caudal (PVC) sensory neurons across the adult aging spectrum (6–12 months).

2.2 Raw read processing

Raw, 150 base pair, paired end RNA reads from our previous study, available at the NCBI (PRJNA639857), were processed as described previously [24]. Briefly, raw reads were adapter trimmed and quality filtered using the *BBDUK* software [30] and then quantified by the *Salmon* software package [31] using the *Aplysia californica* reference transcriptome from the NCBI ftp site (AplCal3.0 GCF000002075.1).

Salmon derived transcript abundances were imported into the R statistical environment via the *tximport* R package [32]. Transcripts with a sum total abundance of less than 1 transcript per million (TPM) across all samples were considered not expressed and filtered out. The R package *geneFilter* was used to remove low variance transcripts using the function varFilter() with the default parameters var.func = IQR and var.cutoff = 0.5 to filter out transcripts with interquartile range (IQR) smaller than the median of all IQR in the expression data [33]. Surrogate variables were identified using the *SVA* R package [34]. Abundances were then variance stabilized using the vst() function from the *DESeq2* R package, with surrogate variables incorporated into the model design and the *blind* parameter set to *FALSE* to account of said surrogate variables *[35]*.

2.3 Co-expression analysis

Variance stabilized counts from BSC and PVC samples were used to construct sensory neuron type specific co-expression networks using the *WGCNA* R package. Briefly, Biweighted

midcorrelation in *WGCNA* was used to construct adjacency matrices for each sensory neuron type independently. A soft power of 16 was used for both PVC and BSC networks to achieve at least 0.8 metric for scale free topology and to minimize mean connectivity (S1 Fig). Adjacency matrices were used to construct signed topological overlap matrices (TOM) for each sensory neuron type. The sensory neuron type-specific TOMs were centered and scaled and combined to make a consensus TOM by taking the minimum of the two modules. Transcripts were hierarchically clustered with the average method using a distance metric of 1-consensus TOM and a minimum module size of 30.

Initial module eigengenes were hierarchically clustered to determine module similarity. Modules with a branch height of 0.25 or less were deemed insufficiently different from their neighbors and merged. Module eigengenes for merged modules were then recalculated (S2 and S3 Figs). Consensus module eigengenes were then correlated to animal chronological age.

Individual transcripts in each module were then correlated to the module eigengene, referred to as module membership, as a measure of the transcript centrality.

Similarly, transcripts were correlated with chronological age, referred to as transcript-age significance (TAS), as a measure of the influence of chronological age on the expression of that transcript. Correlation of module membership with TAS of all transcripts within a module (MM-TAS) was calculated to describe the influence of chronological age on the module as a whole. Only modules with high magnitude ($|\text{Pearson cor}| \geq 0.5$) and high degree of significance ($p \leq 0.01$) of MM-TAS were considered for further downstream analysis. Module hub transcripts were identified using the *WGCNA* function chooseTopHubInEachModule().

2.4 Module enrichment analysis

Transcript sets of each module were tested for enrichment for Kyoto Encyclopedia of Genes and Genomes (KEGG) canonical pathways using the *clusterProfiler* R package [36].

All software used and version information is available in Supplementary Table S1 Table and Supplementary Information **S1 File**. All scripts used for this analysis can be found in the following GitHub repository: [https://github.com/Nicholas-Kron/Kron_Cohort77_CoExpression_Analysis]

2.5 Comparison to immune response in *Crassostrea gigas*

To assess whether the observed module immune signatures suggested mapping to KEGG orthology and the UNIPROT human proteome represented a bona fide molluscan immune signature, module transcript sets were compared to differential expression resulting from immune challenge in the pacific oyster *Crassostrea gigas* by Lafont et al (2020) [37].

The Aplysia RefSeq proteome for the current genome build (AplCal3.0, GCF_000002075.1) was downloaded from the RefSeq database. Similarly, the proteome for the *C.gigas* genome build used by Lafont et al (2020, oyster_v9, GCA_000297859.1) [37] was downloaded from the Ensemble FTP site. The Aplysia proteome was BLASTed against local BLAST database built from said *C.gigas* proteome using an e value cutoff of less than 0.001 and selecting only the top hit.

The resultant putative protein orthologs between Aplysia and *C.gigas* were then mapped to their respective gene and transcripts identifiers using the respective genome build gene feature format annotation files (AplCal3.0_genomic.gff version 1.21 and oyster_v9.49.gff3). The new Aplysia to *C. gigas* mapping file was used to determine the proportion of each co-expression module that mapped to genes differentially expressed in response to immune challenge either due to exposure to poly(I·C) priming, viral challenge, or both [37]. Enrichment for *C. gigas*

orthologs in each module was calculated by Fisher's exact test with Bonferroni multiple test correction in R using the *dhyper* function.

3 Results

3.1 Filtering

Removal of transcripts with zero total count and variance filtering with the *geneFilter* package yielded 11,703 analysis ready transcripts, out of approximately 12,000 transcripts expressed in these sensory neuron types described previously [24]. SVA identified one surrogate variable which was included in the DESeq2 model design.

3.2 Clustering

Hierarchical clustering of transcripts and module merging resulted in 12 consensus co-expression modules, which were assigned arbitrary color names by *WGCNA*. A thirteenth module wastebasket module was assigned the "grey" designation and not evaluated in downstream analysis. The *royalblue*, *saddlebrown*, *orange*, and *pink* module eigengenes exhibited significant correlation with chronological age ($p \leq 0.05$; Fig 1). Module-trait correlations in both PVC and BSC individually can be found in Supplementary Figure **S4 Fig**. The hub transcript for each module can be found in Table 1.

3.3 Modules of interest

The expression of each transcript in a module was correlated with the module eigengene, called module membership (MM), and with age, called transcript-age significance (TAS). Modules for which MM and TAS were highly correlated ($|\text{Pearson cor}| \geq 0.5$, $p \leq 0.01$) were investigated further.

Both the *royalblue* and *saddlebrown* modules were significantly anti-correlated with age. Eigengene expression trend of both modules was stable until age nine months when expression decreased monotonically (Fig 2). Module membership was highly correlated with the transcript-age significance for age (TAS) in the *royalblue* module (Pearson cor ≥ 0.8, $p \leq 0.001$, Fig 3). However, MM-TAS was not strongly correlated for the *saddlebrown* module and thus this module was not investigated further (Pearson cor = 0.35, p = 0.004, Fig 3).

Eigengenes of the *pink*, *orange*, *darkgreen*, and *greenyellow* modules exhibited increasing expression trends with increasing chronological age for at least some portion of the age span (Fig 2). The *pink* and *orange* module eigengenes were significantly correlated with chronological age ($p \leq 0.05$, Fig 1) and both modules exhibited high MM-TAS correlation (Pearson cor ≥ 0.7, $p \leq 0.001$; Fig 2). Notably, the expression profile of the *orange* and *pink* eigengenes resemble the *royalblue* and *saddlebrown* eigengene mirrored over the x-axis, exhibiting a linear increase in expression after age 9 months. The *greenyellow* module exhibited a linear increase in eigengene expression with age across the entire aging span, while *darkgreen* exhibited increasing expression from ages 6–9 months (Fig 2). While the module eigengenes of these two modules were not significantly correlated with age, both modules exhibited strong MM-TAS correlation (Pearson cor ≥ 0.7, $p \leq 0.001$; Fig 3). This suggests aging strongly affects the central regulators of these modules, a notion sufficiently interesting to justify further investigation of these modules.

Many of the age associated modules overlapped with transcriptional trajectories of transcripts differentially expressed in aging in our previous study (Supplementary table S2 Table).

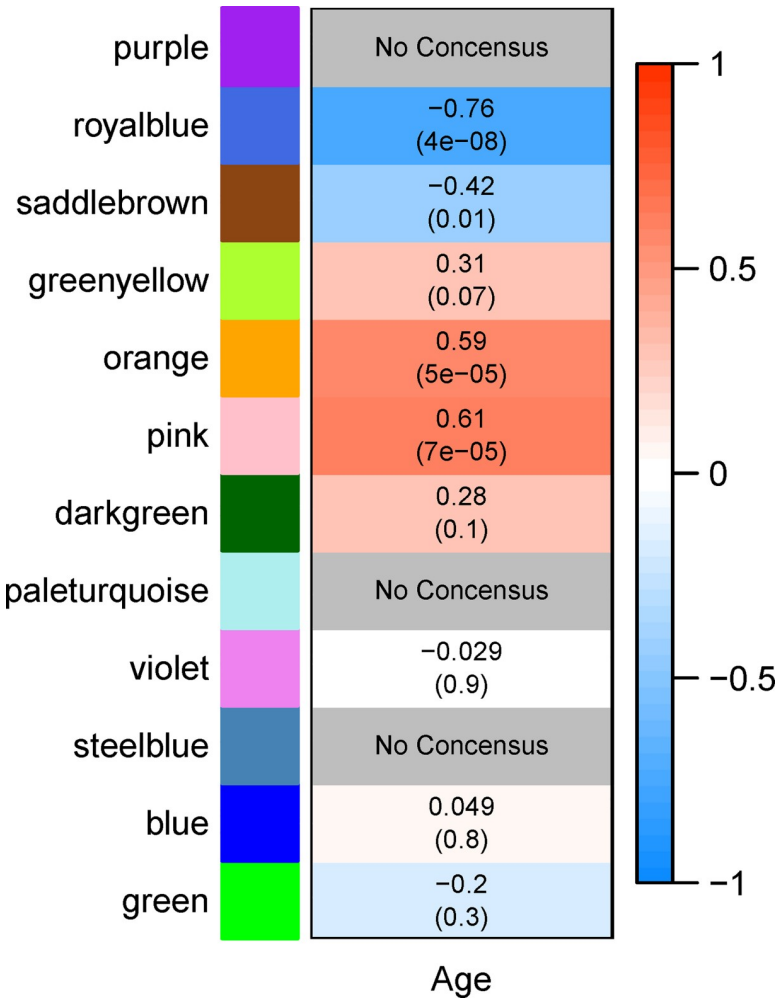

Fig 1. Correlation in *Aplysia californica* sensory neurons between consensus co-expression modules and animal age. Each module is arbitrarily assigned a color to assist in reference. This color is denoted on the heatmap row labels of Fig 1 and referred to throughout the figures and tables. Each cell of the heatmap represents the Pearson correlation between a module eigengene (row) and age (column). The upper value within a cell represents the magnitude of correlation. The lower value in parentheses in each cell represents the p-value of the correlation. Cell color denotes direction of correlation (red = positive, blue = negative) and saturation represents magnitude of correlation, with greater magnitude of correlation (top value in each cell) represented by higher saturation. Modules for which sign of eigengene correlation with age between PVC and BSC was inconsistent were colored grey and marked as "No Consensus" due to lack of consensus. *Orange* and *pink* modules are significantly correlated with age, while *royalblue* and *saddlebrown* are significantly anti-correlated.

https://doi.org/10.1371/journal.pone.0252647.g001

3.4 Enrichment analysis of modules of interest

3.4.1 Royalblue. The *royalblue* module, which exhibited decreasing eigengene expression trend with age, was enriched for a diverse set of KEGG pathways (Fig 4). Most prominent were the canonical energy metabolism pathways of *glycolysis* (ko00010), *TCA cycle* (ko00020), and *fatty acid metabolism* (ko01212). Amino acid metabolism related pathways such as *biosynthesis of amino acids* (ko01230) and *alanine, aspartate, and glutamate metabolism* (ko00250 were also enriched. Another set of enriched KEGG pathways represent elements important to neuronal function such as *synaptic vesicle cycle* (ko04721), *long-term potentiation* (ko04720), *MAPK signaling* (ko04013), and *calcium signaling* (ko04020). Several enriched pathways represent human neurodegenerative diseases that sit at the nexus of neuronal dysfunction and

Table 1. Co-expression modules identified in *Aplysia californica* sensory neurons.

Module	Module n	Hub gene RefSeq ID	Human Ortholog	Ortholog Name
blue	1581	XM_013088909.1	MGA	MAX gene-associated protein
darkgreen	225	XM_013082889.1	RPA2	Replication protein A 32 kDa subunit
green	2387	NM_001204703.1	GNAO1	G-protein G(o) subunit alpha
greenyellow	329	XM_005110768.2	ZNFX1	NFX1-type zinc finger-containing protein 1
orange	166	XM_005096841.2	CREB3L3	Cyclic AMP-responsive element-binding protein 3-like protein 3
paleturquoise	41	XM_013087385.1	-	-
pink	1255	XM_005111489.2	NFKBIA	NF-kappa-B inhibitor alpha
purple	3036	XM_005095177.2	PSMB7	Proteasome subunit beta type-7
royalblue	561	XM_005101095.2	-	-
saddlebrown	65	XM_005089315.2	-	-
steelblue	64	XM_013083399.1	EBF3	Transcription factor COE3
violet	36	XM_013085790.1	ATXN10	Ataxin-10

Modules were identified using the weighted gene correlation network analysis (*WGCNA*) R package. The most connected transcript, called the hub gene, is listed by its RefSeq identifier, as well as its BLASTx assigned human ortholog. Hub transcripts with a "-" in the Human Ortholog and Ortholog Name columns could not be mapped to any known human protein, and thus are of unknown function.

https://doi.org/10.1371/journal.pone.0252647.t001

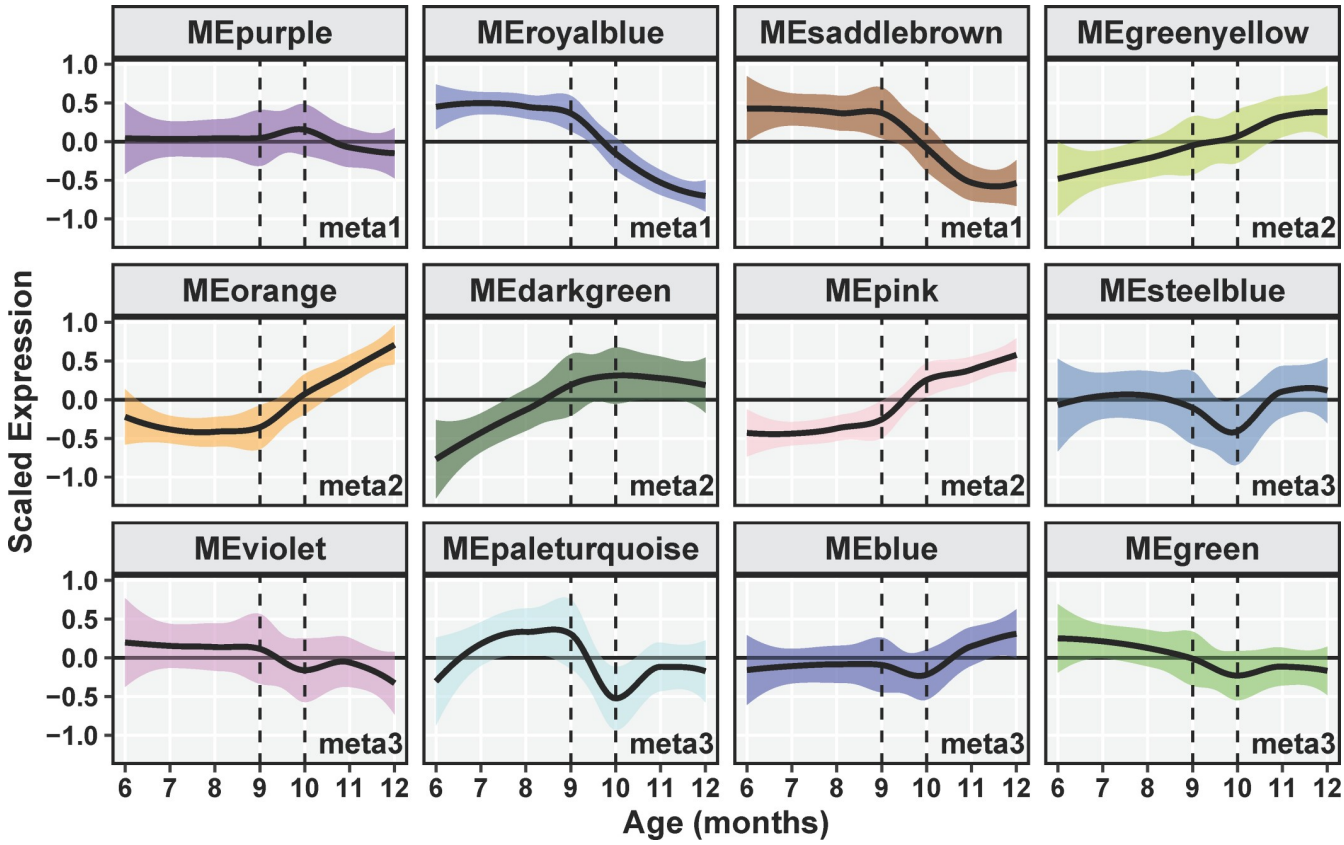

Fig 2. Expression trajectories of consensus co-expression module eigengenes of *Aplysia californica* sensory neurons over the adult lifespan. Each cell represents the mean centered and variance scaled expression of a module eigengene, with the solid line the monthly average with colored bounding area representing the standard error. Dotted lines highlight the transition at age 9–10 months, during which most module eigengenes exhibit perturbations of their expression trends.

https://doi.org/10.1371/journal.pone.0252647.g002

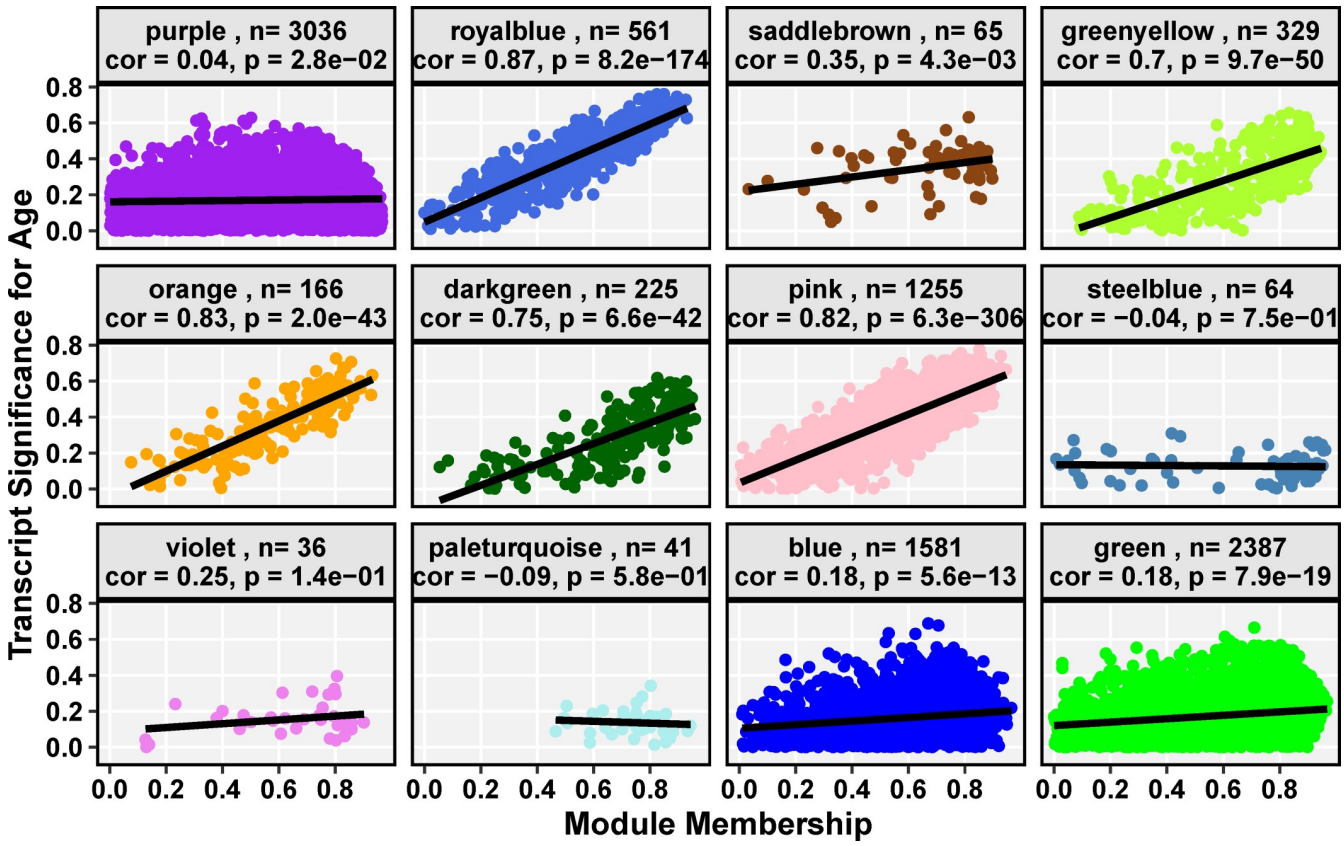

Fig 3. Trait significance–module membership correlation (TS-MM) for each co-expression module of *Aplysia californica* sensory neurons over the adult lifespan. The x-axis of each cell is the Pearson correlation of the expression of a transcript and the module eigengene. The y-axis of each cell is the Pearson correlation of the expression of a transcript and chronological age in months. Each module transcript is plotted as a colored point, while the line of best fit, which represents the TS-MM, is rendered in black. Header strips detail the module name, the number of transcripts in that module (n), the TS-MM Pearson correlation value, and the p-value significance of that correlation for each module as calculated by the WGCNA R package. The *darkgreen*, *greenyellow*, *orange*, *pink*, and *royalblue* modules have a significant TS-MM $\geq$ 0.7.

https://doi.org/10.1371/journal.pone.0252647.g003

metabolic failure such as *Alzheimer's disease* (ko05010), *Huntington's disease* (ko05016), and *Parkinson's disease* (ko05012).

Orthologs also involved in anterograde or retrograde movement of cellular cargo featured prominently among the transcripts with highest module membership in this module. Metabolic enzymes associated with TCA cycle, glycolysis, and mitochondrial fatty acid beta oxidation were also prominent. Reactive oxygen species (ROS) detoxification enzymes and other mitochondrial homeostasis maintenance orthologs were also present (Table 2).

3.4.2 Pink. The *pink* module, which was positively correlated with age, was significantly enriched for KEGG pathways related to translation, such as *ribosome biogenesis in eukaryotes* (ko03008) and *aminoacyl-tRNA biosynthesis* (ko00970), and proteostatic mechanisms, such as *lysosome* (ko04142), *protein processing in the endoplasmic reticulum* (ko04141), and *ubiquitin mediated proteolysis* (ko04120, Fig 5).

Investigation of individual transcripts with the highest module membership for the *pink* module similarly revealed several transcripts annotated to human orthologs involved in transcription, translation, and ribosome biogenesis, as well as modulation of innate immunity and NFkB signaling (Table 3).

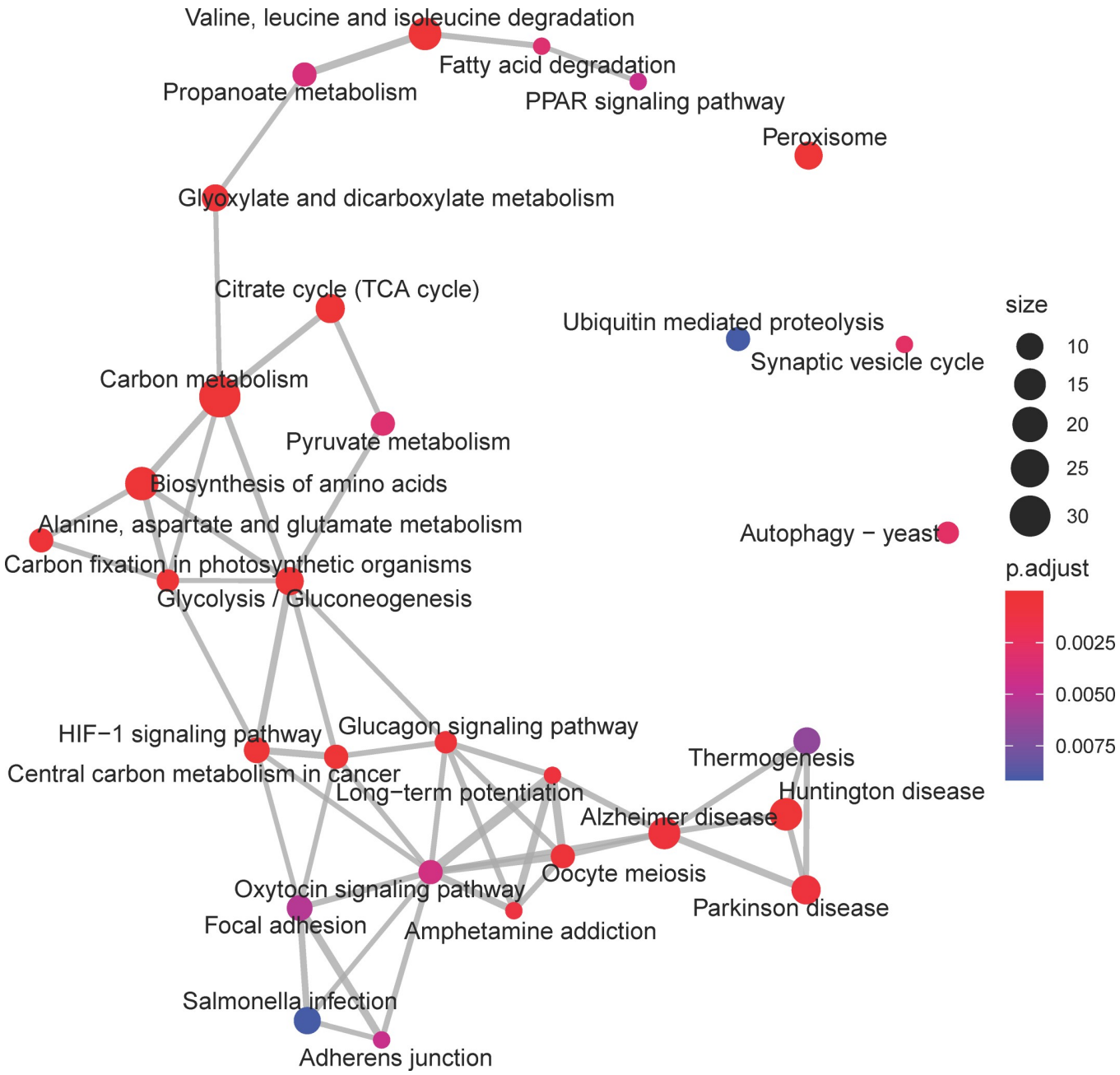

Fig 4. Enrichment map of Kyoto Encyclopedia of Genes and Genomes (KEGG) pathways for the *royalblue* consensus co-expression module from *Aplysia californica* sensory neurons. Each node represents a KEGG pathway, with node size representing the number of transcripts annotated to that pathway, and color denoting the significance of that enrichment (brighter red is most significant). KEGG pathways with overlapping transcripts sets are connected by grey lines, or edges. Edge width is determined by the number of overlapping transcripts. This module exhibits a high degree of gene set overlap between most of the enriched KEGG pathways. Metabolic pathways such as *TCA cycle*, *Glycolysis*, and *fatty acid degradation* are among the largest and most significantly enriched. The module eigengene trend of this module was negatively correlated with age, indicating downregulation of these pathways.

https://doi.org/10.1371/journal.pone.0252647.g004

3.4.3 Orange. The three KEGG pathways significantly enriched in the *orange* module, which was positively correlated with age, all participate in proteostasis, whether that is proper protein folding localized to the Endoplasmic Reticulum (ER) in the case of *protein processing in the endoplasmic reticulum* (ko04141) and *N-glycan biosynthesis* (ko00510), or in protein

Table 2. Selection of transcripts with highest correlation to transcript co-expression module eigengene (module membership, MM) in the *royalblue* consensus module identified in *Aplysia californica* sensor neurons by *WGCNA*.

Refseq ID	MM	MM p value	TAS	TAS p value	Human Ortholog	Ortholog Name	Ortholog Function
*XM_005096347.2***	0.93	9.9E-33	-0.63	2.95E-09	DCTN6	Dynactin subunit 6	Transport of cellular cargo [38]
*XM_005105237.1***	0.93	6.4E-32	-0.73	2.46E-13	GPI	Glucose-6-phosphate isomerase	glycolysis, neurotrophic factor [39]
*XM_005093202.2***	0.89	2.8E-25	-0.70	7.42E-12	NAPG	Gamma-soluble NSF attachment protein	Required for vesicular transport between the endoplasmic reticulum and the Golgi apparatus. (UniProt)
*XM_005101715.2***	0.88	1.1E-24	-0.70	6.98E-12	EXOC2	Exocyst complex component 2	Component of exocyst complex (UniProt)
*XM_005096859.2***	0.86	1.1E-22	-0.67	1.09E-10	GPX4	Phospholipid hydroperoxide glutathione peroxidase	Antioxidant [40]
*XM_005089329.2***	0.86	3.2E-22	-0.71	1.84E-12	MAP2K1	Dual specificity mitogen-activated protein kinase kinase 1	MEK 1
*XM_005105342.2**	0.85	2.2E-21	-0.76	5.45E-15	SNX30	Sorting nexin-30	Possibly intracellular trafficking (UniProt)
*XM_005103941.2**	0.84	5.9E-21	-0.55	4.21E-07	SDHAF2	Succinate dehydrogenase assembly factor 2, mitochondrial	Assembly and function of succinate dehydrogenase complex [41]
*XM_013079678.1**	0.84	1.0E-20	-0.66	1.71E-10	VAPA	Vesicle-associated membrane protein-associated protein A	vesicular transport between the endoplasmic reticulum and the Golgi apparatus [42]
*XM_005106229.2***	0.84	2.9E-20	-0.57	1.83E-07	ACADS	Short-chain specific acyl-CoA dehydrogenase, mitochondrial	catalyze the first step of mitochondrial fatty acid beta-oxidation [43]
*XM_005112738.2***	0.83	5.4E-20	-0.59	4.64E-08	ENO1	Alpha-enolase	glycolysis
*XM_013088411.1***	0.83	6.5E-20	-0.59	3.18E-08	CCDC151	Coiled-coil domain-containing protein 151	dynein arm assembly [44]
*XM_005098999.2***	0.83	8.4E-20	-0.61	7.88E-09	PARK7	Protein/nucleic acid deglycase DJ-1	Antioxidant, neuroprotection [45–47]
*XM_005096727.2***	0.83	2.7E-19	-0.61	1.13E-08	GDAP1	Ganglioside-induced differentiation-associated protein 1	Regulator of mitochondrial network [48]
XM_005111161.2	0.79	7.9E-17	-0.56	2.47E-07			
*XM_005109966.2***	0.82	3.2E-19	-0.76	6.07E-15	HADHA	Trifunctional enzyme subunit alpha, mitochondrial	catalyzes the last three of the four reactions of the mitochondrial beta-oxidation pathway [49]
XM_005098946.2	0.82	1.3E-18	-0.54	7.55E-07	C1orf194	Uncharacterized protein C1orf194	Ca^{2+} homeostasis [50]
*XM_013081239.1***	0.82	1.3E-18	-0.53	1.23E-06	PGK1	Phosphoglycerate kinase 1	glycolysis
*XM_005089581.2**	0.82	1.5E-18	-0.56	2.27E-07	EFCAB1	EF-hand calcium-binding domain-containing protein 1	Also called calaxin, binds Ca^{2+} and dynein [51]
XM_005092435.2	0.81	1.9E-18	-0.57	1.84E-07	CHMP6	Charged multivesicular body protein 6	ESCR-III complex, endosomal cargo sorting [52]
*NM_001204580.1**	0.81	2.1E-18	-0.53	1.59E-06	CALM2	Calmodulin-2 (Fragment)	Ca^{2+} homeostasis [53]
*XM_005104646.2***	0.81	2.2E-18	-0.55	4.29E-07	SOD2	Superoxide dismutase [Mn], mitochondrial	ROS defense [54]
XM_005090003.2	0.81	3.1E-18	-0.57	1.39E-07	CAT	Catalase	ROS defense [55]
*XM_005097336.2**	0.81	3.2E-18	-0.55	3.87E-07	BLOC1S1	Biogenesis of lysosome-related organelles complex 1 subunit 1	anterograde transport [56]
*XM_005089746.2***	0.81	3.8E-18	-0.58	5.48E-08	PGAM2	Phosphoglycerate mutase 2	glycolysis

(*Continued*)

Table 2. (Continued)

Refseq ID	MM	MM p value	TAS	TAS p value	Human Ortholog	Ortholog Name	Ortholog Function
*XM_005108968.2***	0.81	4.0E-18	-0.64	1.09E-09	GPS2	G protein pathway suppressor 2 (Fragment)	mitochondrial retrograde signaling, mitochondrial biogenesis, transcriptional activator of nuclear-encoded mitochondrial genes [57]
*NM_001280826.1***	0.81	5.0E-18	-0.57	1.90E-07	GAPDH	Glyceraldehyde-3-phosphate dehydrogenase	glycolysis
*XM_005097828.2***	0.81	5.5E-18	-0.57	1.92E-07	PDHB	Pyruvate dehydrogenase E1 component subunit beta, mitochondrial	pyruvate dehydrogenase
*XM_005104734.2***	0.81	7.3E-18	-0.55	3.70E-07	SDHA	Succinate dehydrogenase [ubiquinone] flavoprotein subunit, mitochondrial	TCA and OXPHOS
*XM_005100966.2***	0.80	1.9E-17	-0.62	6.83E-09	DECR2	Peroxisomal 2,4-dienoyl-CoA reductase	mitochondrial fatty acid beta-oxidation [58]
*XM_013090573.1**	0.80	2.1E-17	-0.56	2.64E-07	DLST	Dihydrolipoyllysine-residue succinyltransferase component of 2-oxoglutarate dehydrogenase complex, mitochondrial	TCA
*XM_005091339.2***	0.80	2.2E-17	-0.61	8.96E-09	ETFA	Electron transfer flavoprotein subunit alpha, mitochondrial	Electron acceptor, mitochondrial fatty acid beta-oxidation [59]
*XM_013079116.1**	0.80	2.3E-17	-0.54	6.66E-07	SYT4	Synaptotagmin-4	Retrograde signaling, endocytosis, Ca^{2+} sensing [60,61]
*XM_005106740.2***	0.80	2.8E-17	-0.64	8.87E-10	FUNDC1	FUN14 domain-containing protein 1	mitochondrial maintenance [62]
*XM_005112721.2***	0.80	3.6E-17	-0.59	5.11E-08	KCNC2	Potassium voltage-gated channel subfamily C member 2	ion channel [63]
XM_013088705.1	0.80	4.2E-17	-0.52	2.53E-06	MFN2	Mitofusin-2	mitochondrial fusion [64,65]
XM_005105274.2	0.79	4.8E-17	-0.63	3.04E-09	CCDC39	Coiled-coil domain-containing protein 39	Inner dynein arm assembly [66]
*XM_013084603.1**	0.79	6.4E-17	-0.62	6.02E-09	VPS26B	Vacuolar protein sorting-associated protein 26B	Endosome retromer complex [67,68]
*XM_013079609.1***	0.79	7.4E-17	-0.56	3.10E-07	IDH3G	Isocitrate dehydrogenase [NAD] subunit gamma, mitochondrial	TCA
*XM_005091388.2***	0.79	8.9E-17	-0.68	5.00E-11	NXNL2	Nucleoredoxin-like protein 2	ROS defense, neurotrophic factor [69]
*XM_013087736.1**	0.79	1.0E-16	-0.52	2.89E-06	NDUFAF2	NADH dehydrogenase [ubiquinone] 1 alpha subcomplex assembly factor 2	Mitochondrial complex I assembly and function [70,71]
*XM_005090280.2***	0.79	1.6E-16	-0.68	2.75E-11	PDCD6	Programmed cell death protein 6	calcium sensor, ER to golgi transport, interacts with ESCRT-III [72]
*XM_005097549.2**	0.78	2.5E-16	-0.45	5.60E-05	FMC1	Protein FMC1 homolog	Plays a role in the assembly/stability of the mitochondrial membrane ATP synthase [73]
*XM_013084592.1***	0.78	8.4E-16	-0.56	2.79E-07	ACO2	Aconitate hydratase, mitochondrial	TCA
*XM_013086643.1**	0.76	4.3E-15	-0.55	3.79E-07	KCNAB2	Voltage-gated potassium channel subunit beta-2	ion channel subunit, regulates other KCN [74]
XM_005110731.2	0.76	9.3E-15	-0.50	5.63E-06	SDHC	Succinate dehydrogenase cytochrome b560 subunit, mitochondrial	TCA and OXPHOS
XM_005108990.2	0.75	3.4E-14	-0.44	9.78E-05	ETFRF1	Electron transfer flavoprotein regulatory factor 1	regulator of the electron transfer flavoprotein [75]
XM_005104950.2	0.74	4.2E-14	-0.53	1.70E-06	KIF3A	Kinesin-like protein	anterograde transport [76]
*NM_001204727.1**	0.74	9.7E-14	-0.52	2.29E-06	STAU2	Double-stranded RNA-binding protein Staufen homolog 2	transport of neuronal RNA from the cell body to dendrites [77]

(*Continued*)

Table 2. (Continued)

Refseq ID	MM	MM p value	TAS	TAS p value	Human Ortholog	Ortholog Name	Ortholog Function
*XM_013089873.1***	0.74	1.3E-13	-0.61	1.08E-08	ITCH	E3 ubiquitin-protein ligase Itchy homolog	ROS defense [78], Involved in the negative regulation antiviral responses [79]
*XM_005103012.2***	0.71	3.1E-12	-0.48	2.02E-05	PRDX5	Peroxiredoxin-5, mitochondrial	Antioxidant [80]

The RefSeq ID of each transcript is paired with a human protein ortholog gene symbol and name annotated by BLASTn mapping to the UNIPROT human proteome (UP000005640). The function of each ortholog is detailed in the final column. Correlation of transcript expression and chronological age, transcript-Age correlation (TAS), and significance (TAS p-value) are also listed. Transcripts are marked with "*" if they were among significantly downregulated transcripts in Kron et al 2020 [24] in one neuron type and with "**" if in both. All subsequent tables are organized identically. Common functions include TCA cycle, glycolysis, retrograde and anterograde transport, and calcium homeostasis. The module eigengene trend of this module was negatively correlated with age, indicating downregulation of these processes in aging.

https://doi.org/10.1371/journal.pone.0252647.t002

degradation, in the case of *lysosome* (ko04142). Transcripts with highest module membership were associated with ER stress or the endoplasmic reticulum associated protein degradation (ERAD) pathway (Table 4).

3.4.4 Darkgreen. For the *darkgreen* module, which exhibited an increasing eigengene expression trend until age 10 months after which the trend stabilized, KEGG enrichment analysis highlighted processes involved in nucleic acid metabolism, namely *DNA replication* (ko03030), *Nucleotide excision repair* (ko03420), and *mismatch repair* (ko03430) for DNA and *RNA transport* (ko03013) and *RNA degradation* (ko03018) for RNA (Fig 6).

Many of the transcripts with highest module membership were involved with DNA damage response, as well as formation of the nuclear pore, mRNA quality control and export, and immune signaling cascades such as the JAK/STAT cascade, NFkB signaling, and RIG-1 signaling (Table 5).

3.4.5 Greenyellow. Pathways associated with viral infection and immune signaling dominated the KEGG enrichment results of the *greenyellow* module, which exhibited an increasing eigengene expression trend with age (Fig 7). Highly significant pathways included classical immune response associated pathways such as *NF-kappa-Beta signaling pathway* (ko04064), *RIG-1-like receptor signaling pathway* (ko04622), and *NOD-like receptor signaling* (ko04621). Transcripts with highest module membership in the *greenyellow* module mapped to human orthologs involved in the interferon and NFkB signaling pathways (Table 6).

A full list of KEGG enrichment results can be found in Supplementary Datasheet **S1 Dataset**. Full transcript sets and their respective module membership values can be found in Supplementary Datasheet **S2 Dataset**.

3.5 Module enrichment for *C. gigas* immune response genes

BLAST annotation of Aplysia proteins to the *C. gigas* proteome and subsequent annotation resulted in 22,715 unique Aplysia transcripts mapped to 10,112 unique *C. gigas* proteins. Of these 22,715 transcripts, 7,359 were present in one of the identified co-expression modules. Among the 1,547 genes marked as exhibiting coherent regulation profiles following priming with poly(I·C)and viral challenge in Lafont et al (2020) [37], 697 were also present in Aplysia co-expression modules. Enrichment tests for each module revealed that the *greenyellow*, *darkgreen*, and *pink* modules were significantly enriched for *C. gigas* immune response genes (Fisher's exact test, $p <= 0.00385$, Table 7). A full mapping of co-expression module genes to genes DE in Lafont et al (2020) [37] can be found in supplementary file **S3 Dataset**.

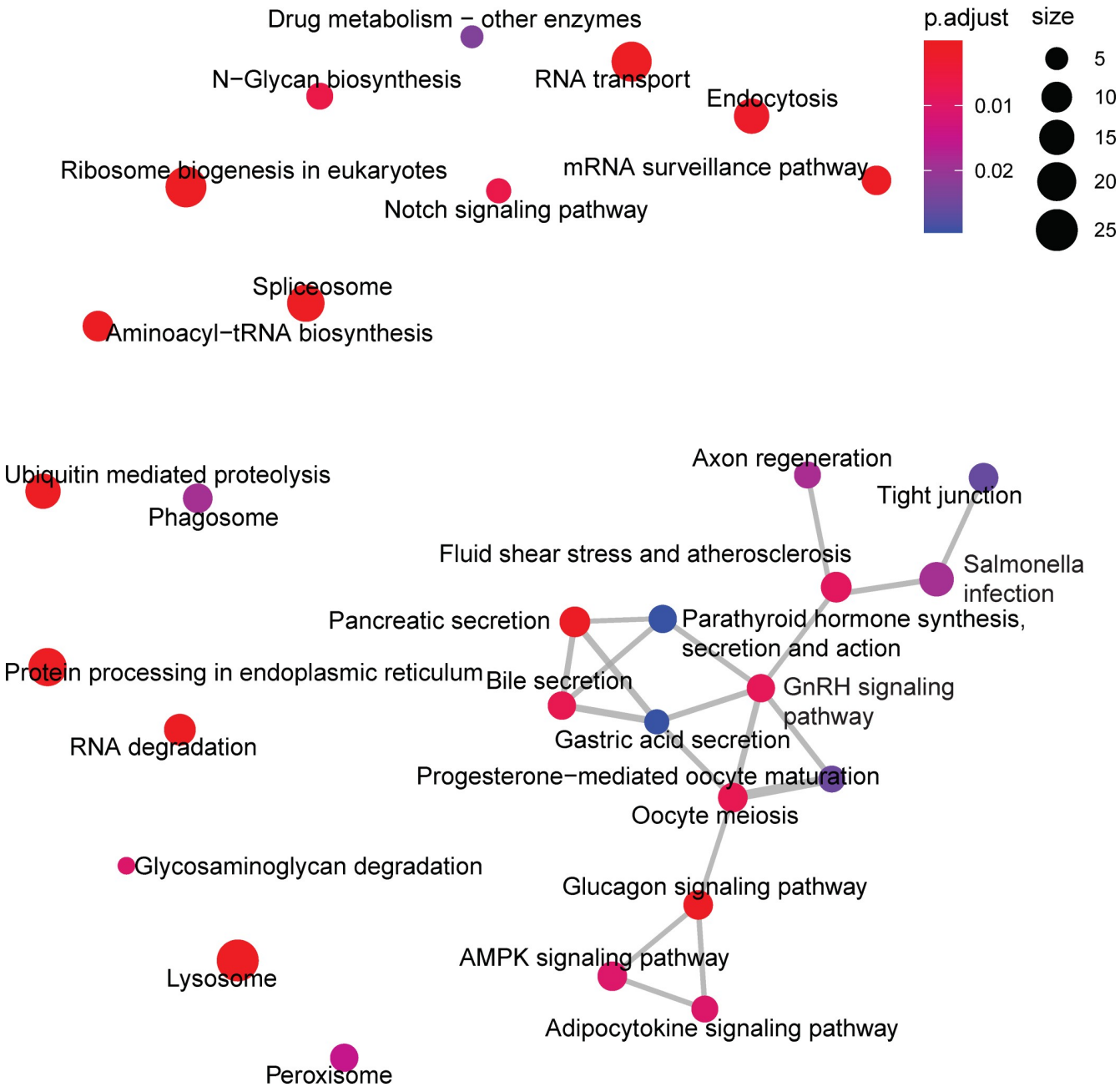

Fig 5. Enrichment map of Kyoto Encyclopedia of Genes and Genomes (KEGG) pathways for the *pink* consensus co-expression module. Symbol explanation as in Fig 4. The *Protein processing in the endoplasmic reticulum*, *Lysosome*, and *Ribosome biogenesis in eukaryotes* pathways are among the largest and most significantly enriched pathways. This module was positively correlated with age, suggesting these pathways are upregulated in aging.

https://doi.org/10.1371/journal.pone.0252647.g005

Of the transcripts in the *greenyellow*, *darkgreen*, and *pink* modules, 17, 7, and 8 respectively exhibited a module membership greater than 0.8 for their respective modules and mapped to a *C. gigas* gene with a log 2 fold change of greater than or equal to 1 in response to immune priming and/or viral challenge in Lafont et al (2020) [37] (Table 8). Of those, transcripts from the *greenyellow* and *darkgreen* modules mapped primarily to *C. gigas* genes with putative viral function. Furthermore, the *greenyellow* transcripts mapped to C. gigas genes assigned by

Table 3. Selection of transcripts with highest correlation to transcript co-expression module eigengene (module membership, MM) in the *pink* consensus module identified in *Aplysia californica* sensory neurons by *WGCNA*.

RefSeq ID	MM	MM p value	TAS	TAS p value	Human Ortholog	Ortholog Name	Ortholog Function
XM_005111489.2**	0.95	1.8E-36	0.66	1.4E-10	**NFKBIA**	**NF-kappa-B inhibitor alpha**	NF-kappa-B inhibition [81], anti-inflammatory [82]
*XM_005111747.2**!*	0.93		0.74	6.8E-14	BIRC3	Baculoviral IAP repeat-containing protein 3	E3 ubiquitin-protein ligase, NF-kappa-B signaling regulation [83], innate immunity regulation [84]
*XM_005106964.2**	0.84	4.1E-32	0.56	2.3E-20			
XM_013081148.1	0.78	3.15E-16	0.48	2.1E-05			
*XM_005098591.2***	0.93	1.5E-31	0.68	5.6E-11	ZUP1	Zinc finger-containing ubiquitin peptidase 1	Deubiquitination, DNA damage, replication stress [85]
XM_005098861.2	0.92	1.2E-30	0.63	2.3E-09	UBC	Polyubiquitin-C (Fragment)	Ubiquitination [86]
XM_005098862.2	0.87	5.6E-23	0.53	1.7E-06			
*XM_005105067.2**!*	0.91	6.5E-29	0.65	7.3E-10	HERC4	Probable E3 ubiquitin-protein ligase HERC4	E3 ubiquitin-protein ligase [87]
*XM_005112342.2***	0.91	6.6E-29	0.66	1.4E-10	ZNF343	Zinc finger protein 343	transcriptional regulation
*XM_005108387.2***	0.91	2.1E-28	0.63	1.7E-09	ACP7	Acid phosphatase type 7	Iron transport, innate immunity, ROS generation [88]
*XM_005092478.2**	0.90	7.5E-27	0.47	2.4E-05	INTS1	Integrator complex subunit 1	snRNA [89], eRNA [90], transcriptional attenuation [91,92]
*XM_005097515.2***	0.90	9.3E-27	0.63	2.3E-09	GM2A	Ganglioside GM2 activator	Ganglioside metabolism [93]
*XM_005111000.2***	0.90	1.3E-26	0.61	1.1E-08	GCN1	eIF-2-alpha kinase activator GCN1	Global translation repression, gene-specific mRNA translation [94]
*XM_005090686.2***	0.89	5.2E-26	0.60	2.4E-08	SLC16A5	Monocarboxylate transporter 6	Glucose and lipid metabolism, possible immune regulation [95]
*XM_005104555.2***	0.89	6.9E-26	0.59	3.5E-08	EFL1	Elongation factor-like GTPase 1	Ribosome biogenesis [96]
*XM_005093568.2***	0.89	7.1E-26	0.53	1.3E-06	NAT10	RNA cytidine acetyltransferase	Ribosome biogenesis [97], E3 ubiquitin-protein ligase, cellular stress sensor [98], translation efficiency [99]
*XM_005095929.2***	0.89	8.2E-26	0.58	7.5E-08	MOS	Proto-oncogene serine/threonine-protein kinase mos	Serine/threonine-protein kinase, MAPK pathway [100]
*XM_005093424.2**!*	0.89	1.8E-25	0.66	1.5E-10	BIRC7	Baculoviral IAP repeat-containing protein 7	E3 ubiquitin-protein ligase, apoptosis inhibitor [101]
*XM_005094992.2**!*	0.81	2.81E-18	0.66	1.9E-10			
*XM_005102721.2**	0.89	2.0E-25	0.63	3.4E-09	GIMAP4	GTPase IMAP family member 4	Apoptosis [102], cytokine signaling [103]
*XM_005106556.2***	0.88	6.1E-25	0.60	2.3E-08	ETF1	Eukaryotic peptide chain release factor subunit 1	Translation termination [104]
XM_005093041.2	0.88	1.3E-24	0.62	5.5E-09	RNASET2	Ribonuclease T2	Innate immunity [105], mtRNA degradation [106]
*XM_005104568.2***	0.88	3.1E-24	0.61	1.0E-08	PLIN2	Perilipin-2	Lipid storage, ROS defense [107]
*XM_013087467.1***	0.88	3.2E-24	0.60	1.7E-08	EIF4A2	Eukaryotic initiation factor 4A-II	Translation initiation [108], Translation inhibition [109]
*XM_013087273.1***	0.87	7.7E-24	0.56	2.4E-07	HEATR1	HEAT repeat-containing protein 1	Ribosome biogenesis [110]
XM_005101849.2	0.87	8.5E-24	0.57	1.3E-07	EXOSC10	Exosome component 10	RNA metabolism [111]
*XM_005099415.2***	0.87	1.1E-23	0.63	2.3E-09	DUSP7	Dual specificity protein phosphatase 7	MAPK pathway [112]
*XM_005088796.2**!*	0.87	1.2E-23	0.64	1.4E-09	IRF8	Interferon regulatory factor 8	Microglia activation and neuroinflammation [113]
*XM_013084591.1***	0.87	1.6E-23	0.64	1.5E-09	PSAP	Prosaposin	Sphingolipid metabolism [114]
*XM_013087976.1***	0.87	2.9E-23	0.60	1.9E-08	EEF2	Elongation factor 2	Translation [115]
*XM_005097092.2***	0.86	6.1E-23	0.66	2.1E-10	CTSL	Cathepsin L1	Lysosomal protease [116], neuropeptide processing [117]
*XM_005094650.2**!*	0.86	6.8E-23	0.69	2.1E-11	CYLD	Ubiquitin carboxyl-terminal hydrolase CYLD	NF-kappa-B regulation, deubiquitination [118], Negative regulation of innate immunity [119]
*XM_005090468.2***	0.86	9.1E-23	0.71	2.6E-12	PDE12	2',5'-phosphodiesterase 12	Negative regulation of innate immunity
*XM_005099805.2**	0.86	1.3E-22	0.49	9.2E-06	CASP3	Caspase-3	Apoptosis [120]
*XM_013087138.1***	0.86	2.6E-22	0.50	6.1E-06	GRN	Granulins	Lysosome biogenesis and homeostasis [121]
*XM_013083177.1***	0.85	6.4E-22	0.59	5.0E-08	SIGIRR	Single Ig IL-1-related receptor	Negative regulation of immune signaling [122]
*XM_005110683.2***	0.84	2.0E-20	0.62	5.0E-09	FTH1	Ferritin heavy chain	Iron storage, ROS defense [123]

(*Continued*)

Table 3. (Continued)

RefSeq ID	MM	MM p value	TAS	TAS p value	Human Ortholog	Ortholog Name	Ortholog Function
*XM_013089050.1**	0.81	1.8E-18	0.56	3.2E-07	MAP3K8	Mitogen-activated protein kinase kinase kinase 8	MAPK signaling, NFkB signaling [124]
XM_005112843.2!*	0.81	2.2E-18	0.50	6.3E-06	RIOK1	Serine/threonine-protein kinase RIO1	Ribosome biogenesis [125], p38 MAPK innate immune response suppressor [126]
*XM_005105539.2**	0.8	2.3E-17	0.45	6.9E-05	RIOK3	Serine/threonine-protein kinase RIO3	Ribosome biogenesis [127], INF signaling [128], NFkB inhibitor [129], innate immune response [130]
*XM_005102490.2**	0.79	8.4E-17	0.60	1.6E-08	JKAMP	JNK1/MAPK8-associated membrane protein	MAPK signaling, inhibits MAPK8 [131]
*XM_005092503.2***	0.78	2.3E-16	0.66	2.3E-10	TNIP1	TNFAIP3-interacting protein 1	NFkB inhibitor [132,133]
*XM_013087081.2**	0.78	5.3E-16	0.48	2.15E-05	DUOX1	Dual Oxidase 1	ROS production [134]
XM_013088029.1!	0.69	1.3E-11	0.54	8.6E-07			

See Table 2 for description of organization. Transcripts are marked with "*" if they were among significantly upregulated transcripts in Kron et al 2020 [24] in one neuron type and with "**" if in both. Transcripts identified as orthologs to genes differentially expressed due to immune challenge in *C. gigas* are marked with a "!"in the first column. Common categories include ubiquitination, NFkB signaling, innate immunity, ribosome biogenesis, and regulation of transcription and translation. This module was positively correlated with age, suggesting these processes are upregulated in aging.

https://doi.org/10.1371/journal.pone.0252647.t003

Lafont et al (2020) [37] primarily to the interferon-like and RIG-like receptor recognition pathways, while many *darkgreen* transcripts were assigned to the JAK/STAT signaling.

Of those *Crassostrea gigas* transcripts that exhibited a greater than two-fold increase in expression 10 days after treatment with a viral analog, 84 had clear orthologs in Aplysia. Of those 84 orthologous transcripts in Aplysia, only two exhibited a significant increase in expression in aging sensory neurons in our previous study: an IRF8 ortholog and an uncharacterized protein (S4 Dataset).

4 Discussion

While enrichment analysis and eigengene expression profiles suggested strong overlap with our previous study, several modules and enrichment results identified many facets to the transcriptional dynamics in aging of these sensory neurons not detected in our previous DEA study [24].

Enrichment analysis and eigengene expression trend of the *royalblue* module strongly resembles that observed in Kron et al (2020) [24] of expression clusters with decreasing expression trends in aging. Key enzymes in glycolysis such as *GPI*, *PGK1*, *PGAM2*, *GAPDH*, and *ENO1*, as well as *PDHB*, which is part of the pyruvate dehydrogenase complex that links glycolysis to the TCA cycle, were among the transcripts with the highest module membership in the *royalblue* module. Key TCA enzymes *DLST*, *IDH3G*, and *AOC2*, as well as two members of the succinate dehydrogenase complex, *SDHA* and *SDHC*, which function as a nexus between the TCA and OXPHOS, were also present. Downregulation of these transcripts suggests decreased TCA cycle activity, and decreased NADH generation for use in OXPHOS. The presence of orthologs to OXPHOS complex assembly proteins *SDHAF2*, *NDUFA2*, and *FMC1*, as well as electron transport chain regulator *ETRF1* among transcripts with high module membership may suggest further disruptions of OXPHOS at the complex level [41,71,73,75]. Mitochondria depleted of NADH exhibit impaired antioxidant capacity and increased ROS generation [258].

Several orthologs of major ROS detoxification enzymes, namely GPX4, SOD2, CAT, and *PRDX5* are present in the downregulated *royalblue* module [40,54,55,80]. The further presence of *PARK7*, *NXNL2*, and *ITCH*, which stimulate antioxidant activity, in this downregulated

Table 4. Selection of transcripts with highest correlation to transcript co-expression module eigengene (module membership, MM) in the *orange* consensus module identified in *Aplysia californica* sensory neurons by *WGCNA*.

Refseq ID	MM	MM p value	TAS	TAS p value	Human Ortholog	Ortholog Name	Ortholog Function
XM_005096841.2*	0.93	6.27E-33	0.63	1.8E-09	**CREB3L3**	**Cyclic AMP-responsive element-binding protein 3-like protein 3**	ER stress response transcription factor, acute inflammation [135]
NM_001204489.1*	0.93	4.47E-32	0.52	2.0E-06	PSEN2	Presenilin-2	Endoprotease, Ca^2+ homeostasis as ER leak channel [136], ER-Mitochondrial Ca^2+ shuttle [137]
XM_005101813.2*	0.89	6.49E-26	0.56	2.5E-07	LGMN	Legumain	Endopeptidase [138]
XM_013080474.1*	0.89	7.70E-26	0.60	2.0E-08	EIF2AK3	Eukaryotic translation initiation factor 2-alpha kinase 3	Known as PERK, ER stress response [139]
XM_005108642.2*	0.87	2.24E-23	0.54	7.4E-07	MACO1	Macoilin	ER localized regulator of neuronal activity [140]
XM_013081341.1	0.86	7.08E-23	0.51	4.6E-06	DESI2	Deubiquitinase DESI2	Deubiquitinase [141]
XM_013088003.1**!	0.86	4.35E-22	0.71	2.7E-12	BIRC3	Baculoviral IAP repeat-containing protein 3	E3 ubiquitin-protein ligase, NF-kappa-B signaling regulation [83], innate immunity regulation [84]
XM_005105526.2**	0.85	1.13E-21	0.56	2.8E-07	ABCA3	ATP-binding cassette sub-family A member 3	Lipid transporter [142]
XM_005113508.1**	0.85	4.97E-21	0.57	1.0E-07	PSAP	Prosaposin	Sphingolipid metabolism [114]
XM_013086889.1	0.84	6.78E-21	0.45	6.2E-05	SPTLC2	Serine palmitoyltransferase 2	Sphingolipid de-novo synthesis
XM_013079527.1*	0.84	1.12E-20	0.55	5.8E-07	SUN1	SUN domain-containing protein 1	Neurogenesis and neuron and glial migration [143], telomere attachment [144]
XM_005100110.2*	0.83	6.91E-20	0.41	3.0E-04	MBOAT7	Lysophospholipid acyltransferase 7	Regulation of free polyunsaturated fatty acids levels [145,146]
XM_013085224.1**	0.83	1.34E-19	0.68	5.7E-11	VCAN	Versican core protein	Diverse roles [147], including inflammation [148]
XM_005096173.2**	0.83	1.71E-19	0.58	6.3E-08	BCL3	B-cell lymphoma 3 protein	Enhances or inhibits NFkB signaling depending on phosphorylation state [149,150]
XM_005102600.2*	0.82	1.24E-18	0.48	1.7E-05	SLC39A2	Zinc transporter ZIP2	Zinc transporter
XM_013083287.1*	0.81	4.10E-18	0.51	4.0E-06	ADGRG6	Adhesion G-protein coupled receptor G6	Schwann cell differentiation and myelination [151]
XM_005101146.2*	0.81	4.14E-18	0.57	1.7E-07	C16orf62	UPF0505 protein C16orf62	Cell surface recycling, including of signaling receptors [152]
XM_005095917.2	0.79	1.10E-16	0.36	1.8E-03	STT3B	Dolichyl-diphosphooligosaccharide—protein glycosyltransferase subunit STT3B	N-glycosylates unfolded proteins [153], plays role in ERAD [154]
XM_005103010.2	0.78	3.77E-16	0.45	7.5E-05	TXNDC16	Thioredoxin domain-containing protein 16	ERAD [155], humoral immune response [156]
XM_005100158.2*	0.78	7.92E-16	0.43	1.4E-04	UGGT1	UDP-glucose:glycoprotein glucosyltransferase 1	ER glycoprotein quality control [157]

See Table 2 for description of organization. Common functions include Endoplasmic Reticulum (ER) stress response, ER associated protein degradation (ERAD), sphingolipid metabolism, and immune regulation. This module was positively correlated with age, suggesting these process are upregulated in aging.

https://doi.org/10.1371/journal.pone.0252647.t004

module suggest that the antioxidant system of these neurons is impaired in age [45,47,69,78]. The presence of ortholog mediators of mitochondrial fission-fusion dynamics such as *GDAP1* and *MFN2*, mediator of mitophagy *FUNDC1*, and promoter of mitochondrial biogenesis *GPS2*, which plays a role in mitochondrial stress signaling, suggests that maintenance of mitochondrial homeostasis is downregulated in aging [48,57,62,64,65]. Mitochondria act as key

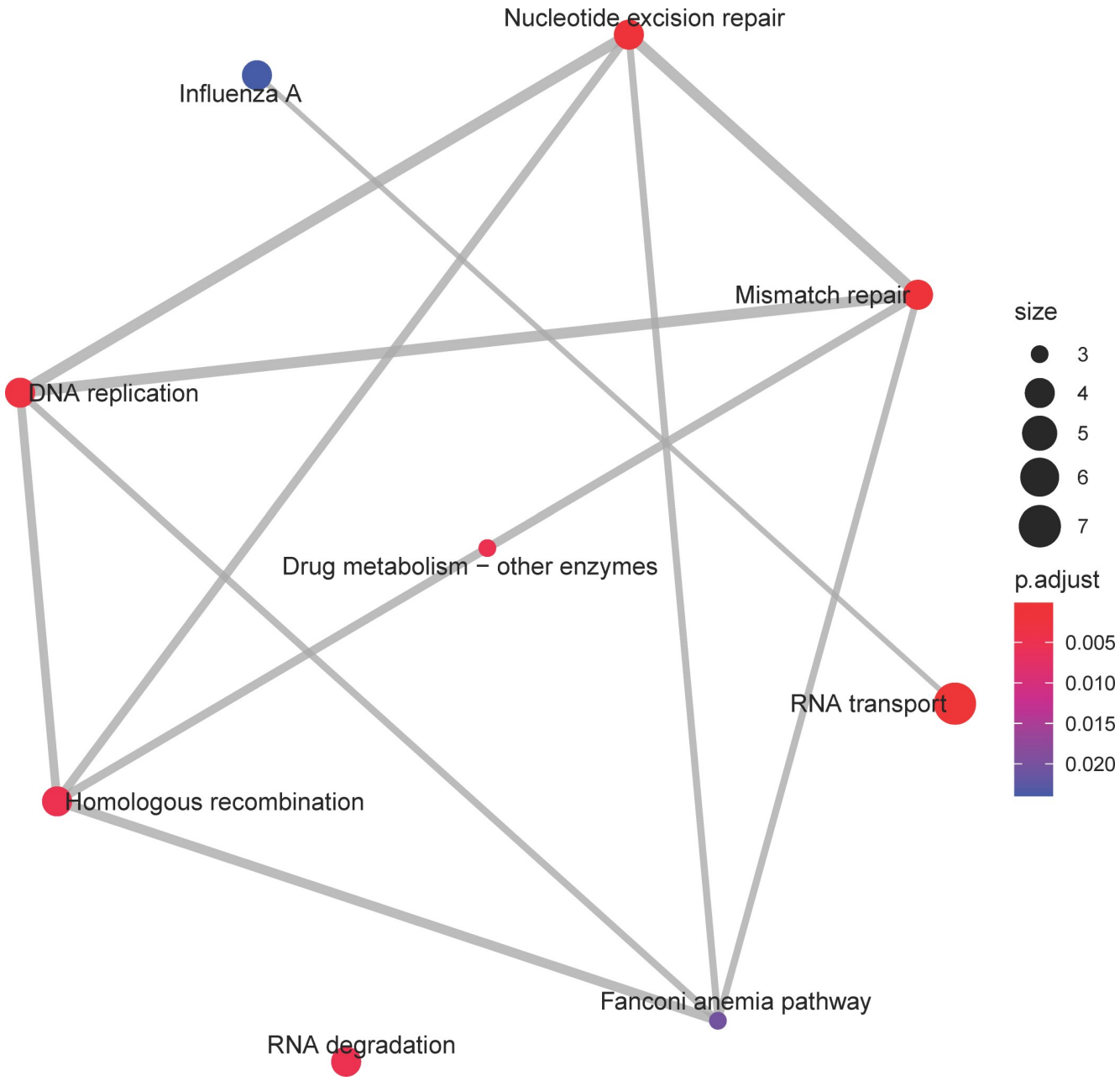

Fig 6. Enrichment map of Kyoto Encyclopedia of Genes and Genomes (KEGG) pathways for the *darkgreen* consensus co-expression module. Symbol explanation as in Fig 4. Several pathways dealing with nucleic acid metabolism, such as *DNA replication* and *RNA degradation* are significant in this pathway. The expression trend of this module increased linearly until age 10 months after which it stabilized, suggesting increasing activity of these pathways until a stable activity level is reach in old age.

https://doi.org/10.1371/journal.pone.0252647.g006

Ca^{2+} reservoirs and dysfunctional mitochondria can lead to perturbed Ca^{2+} dynamics. This is further suggested by downregulation of orthologs of *C1orf194* and *CALM2* which act to maintain Ca^{2+} homeostasis [50,53]. Homeostasis of Ca^{2+} is critical to the proper function of neurons suggesting that knock-on effects of energy metabolism impairment may have adverse effects on the proper functioning of these sensory neurons with aging. Similarly, the presence of two potassium channels orthologs, *KCNC2* and *KCNAB2*, a delayed rectifier K channel and

Table 5. Selection of transcripts with highest correlation to transcript co-expression module eigengene (module membership, MM) in the *darkgreen* consensus module identified in *Aplysia californica* sensory neurons by *WGCNA*.

Refseq ID	MM	MM p value	TAS	TAS P value	Human Ortholog	Ortholog Name	Ortholog Function
XM_013082889.1	0.96	9.81E-41	0.39	6.56E-04	RPA2	Replication protein A 32 kDa subunit	DNA replication [158], DNA damage repair [159,160]
XM_005094195.2	0.95	3.60E-37	0.51	4.61E-06	TRIM3	Tripartite motif-containing protein 3	E3 ubiquitin-protein ligase, negative regulator of inflammation [161–163], inhibits synaptic plasticity [164]
XM_013086128.1	0.94	2.71E-34	0.47	2.42E-05	TIPARP	Poly [ADP-ribose] polymerase	Inhibitor of AHR-dependent transcription [165], suppressor of INF due to AHR activation [166], activator of INF due to ROS [167]
XM_005113357.2!	0.93	7.35E-33	0.53	1.71E-06	SOCS2	Suppressor of cytokine signaling 2[160]	Inhibits JAK/STAT signaling, promotes neurite outgrowth [168], regulates cytokine signaling [169,170]
XM_005092855.1!	0.91	3.77E-28	0.46	3.57E-05			
XM_005108083.2!	0.85	4.32E-21	0.42	2.17E-04			
XM_005092772.2	0.93	1.77E-32	0.29	1.39E-02	ENDOG	Endonuclease G, mitochondrial	mitochondrial biogenenesis and homeostasis [171,172], apoptosis [173,174]
*XM_005107816.2**	0.93	3.24E-32	0.52	2.29E-06	HENMT1	Small RNA 2'-O-methyltransferase	piRNA biogenesis [175]
*XM_005095515.2**	0.93	3.35E-32	0.60	2.12E-08	ICE2	Little elongation complex subunit 2	snRNA transcription [176]
XM_005101982.2	0.93	1.01E-31	0.38	8.51E-04	LGALS4	Galectin-4	Reduced pro-inflammatory cytokine secretion [177], inhibits myelination [178]
*XM_013087261.1**	0.92	3.26E-31	0.48	1.80E-05	GALC	Galactocerebrosidase	Lysosomal degradation of galactocerebrosides [179]
XM_013084530.1	0.92	1.26E-30	0.43	1.36E-04	SMARCD1	SWI/SNF-related matrix-associated actin-dependent regulator of chromatin subfamily D member 1	Transcription activation and repression via chromatin remodeling as part of SWI/SNF complex [180], immune regulation [181]
XM_005102729.2	0.92	5.39E-30	0.28	1.59E-02	WDR53	WD repeat-containing protein 53	unknown
XM_005105962.2	0.92	8.43E-30	0.46	4.99E-05	EPSTI1	Epithelial-stromal interaction protein 1	Macrophage differentiation [182]
XM_005111022.2	0.92	1.03E-29	0.52	2.03E-06	RBBP9	Putative hydrolase RBBP9	Inhibits TGF-beta growth-inhibition [183]
XM_005101042.1	0.91	1.34E-29	0.44	9.85E-05	RPA3	Replication protein A 14 kDa subunit	DNA damage repair [184]
XM_005108381.2	0.91	1.78E-29	0.43	1.39E-04	MOV10L1	RNA helicase Mov10l1	piRNA biogenesis [185]
XM_013088805.1	0.91	2.10E-29	0.47	3.26E-05	SLC16A14	Monocarboxylate transporter 14	Neuronal aromatic-amino-acid transporter [186]
*XM_005100427.2**	0.91	3.91E-29	0.50	6.50E-06	NSMCE1	Non-structural maintenance of chromosomes element 1 homolog	E3 ubiquitin-protein ligase, DNA damage response, and iron homeostasis [187]
XM_013084495.1	0.91	5.14E-29	0.42	1.84E-04	DDX58	Probable ATP-dependent RNA helicase DDX58	RIG 1, antiviral immune receptor [188]
*XM_005091253.2**	0.91	9.96E-29	0.56	2.70E-07	TENT4A	Terminal nucleotidyltransferase 4A	mRNA stability and quality control [189,190]
XM_013090188.1!	0.91	1.24E-28	0.56	2.35E-07	MPEG1	Macrophage-expressed gene 1 protein	Antibacterial protein, pore-forming protein, innate immunity [191]
XM_005088804.2	0.91	1.75E-28	0.44	1.00E-04	PLA2G16	HRAS-like suppressor 3	Phospholipid metabolism [192], sensor for sites of viral entry [193]
XM_013082099.1	0.90	1.24E-27	0.42	1.97E-04	NUP214	Nuclear pore complex protein Nup214	Nuclear pore formation and protein import into nucleus [194,195]

(*Continued*)

Table 5. (Continued)

Refseq ID	MM	MM p value	TAS	TAS P value	Human Ortholog	Ortholog Name	Ortholog Function
XM_013088902.1!	0.89	1.45E-26	0.50	8.27E-06	DIS3L2	DIS3-like exonuclease 2	Mediates degradation of polyuridylated RNAs [196], mRNA metabolism [197]
XM_005089228.2	0.89	2.04E-26	0.48	2.03E-05	SSUH2	Protein SSUH2 homolog	Odontogenesis, upstream of several transcriptional regulators [163]
XM_005107110.2	0.89	2.47E-26	0.43	1.52E-04	PARP14	Protein mono-ADP-ribosyltransferase PARP14	Suppresses IFN-gamma response, induces IL-4 response, counteracts PARP9 [198]
XM_013081916.1	0.89	6.38E-26	0.53	1.16E-06	NUP98	Nuclear pore complex protein Nup98-Nup96	Nuclear pore formation, gene expression regulation [199]
*XM_005106449.2**!	0.89	1.87E-25	0.57	1.31E-07	ZRANB3	DNA annealing helicase and endonuclease ZRANB3	Rewinds DNA and maintains genome stability, replication stress response [200,201]
XM_005106672.2!	0.88	3.94E-25	0.44	1.18E-04	JAK2	Tyrosine-protein kinase JAK2	JAK/STAT signaling, interferon gamma response [202]
XM_005106450.2	0.88	5.72E-25	0.46	3.81E-05	BANF1	Barrier-to-autointegration factor	Chromatin organization and gene expression [203], blocks viral DNA replication [204]
XM_013085923.1	0.87	7.99E-24	0.42	2.17E-04	TREX2	Three prime repair exonuclease 2	DNA repair, mRNA export, transcription [205–207]
*XM_013080704.1**	0.87	8.51E-24	0.52	2.95E-06	VRK1	Serine/threonine-protein kinase VRK1	Regulates BANF1 [208], activates ATF2 [209]
XM_005107122.2!	0.87	4.34E-23	0.35	2.44E-03	GLE1	Nucleoporin GLE1	Export of mRNA from nucleus [210]
XM_005110865.2	0.86	5.48E-22	0.41	2.70E-04	DXO	Decapping and exoribonuclease protein	Pre-mRNA quality control [211]
XM_005113277.2!	0.85	6.73E-22	0.28	1.77E-02	NUP88	Nuclear pore complex protein Nup88	Nuclear pore formation [212]
XM_005099732.2	0.85	9.14E-22	0.35	2.59E-03	MTPAP	Poly(A) RNA polymerase, mitochondrial	mtDNA stabilization [213,214], histone mRNA degradation [215]
XM_013087644.1	0.77	3.02E-15	0.39	7.51E-04	RPUSD3	Mitochondrial mRNA pseudouridine synthase RPUSD3	mtRNA translation, mitochondrial ribosome biogenesis via pseudouridylation [216,217]
XM_005104572.2	0.74	1.10E-13	0.41	2.66E-04	GIMAP1	GTPase IMAP family member 1	Immune cell development [218]
XM_005109614.2!	0.73	1.84E-13	0.30	9.16E-03	XIAP	E3 ubiquitin-protein ligase XIAP	E3 protein-ubiquitin ligase, apoptosis inhibitor [219], NFkB activation [220]
XM_005109011.2	0.72	5.24E-13	0.25	2.98E-02	STRA6	Receptor for retinol uptake STRA6	Retinol importer [221]

See Table 2 for description of organization. Common functions include nuclear pore formation, DNA damage repair, immune and inflammation signaling. The expression trend of this module increased linearly until age 10 months after which it stabilized, suggesting increasing activity of these in early age and stable, heightened activity in old age.

https://doi.org/10.1371/journal.pone.0252647.t005

a subunit of fast-inactivating A-type K channels, respectively, that repolarize neurons during firing and thus play important roles in membrane excitability, further suggests impaired neuronal function [63,74].

A facet of this module that was not captured in the expression clusters is the presence of many downregulated transcripts involved in cellular cargo transport. Orthologs of several proteins involved in retrograde transport, including *DCTN6*, *CCDC151*, and *EFCAB1*, and anterograde transport orthologs like *BLOC1S1* and *KIF3A*, suggest disruptions in communication from soma to synapse and vice versa [38,44,51,56,66,76,259]. Downregulation of *STAU2*, which plays a key role in transport of RNA from the cell body to dendrites for local translation, suggests disruption of transcription/translation events necessary for long term memory in these sensory neurons [77,260]. Other processes in cellular cargo transport, such as ER to

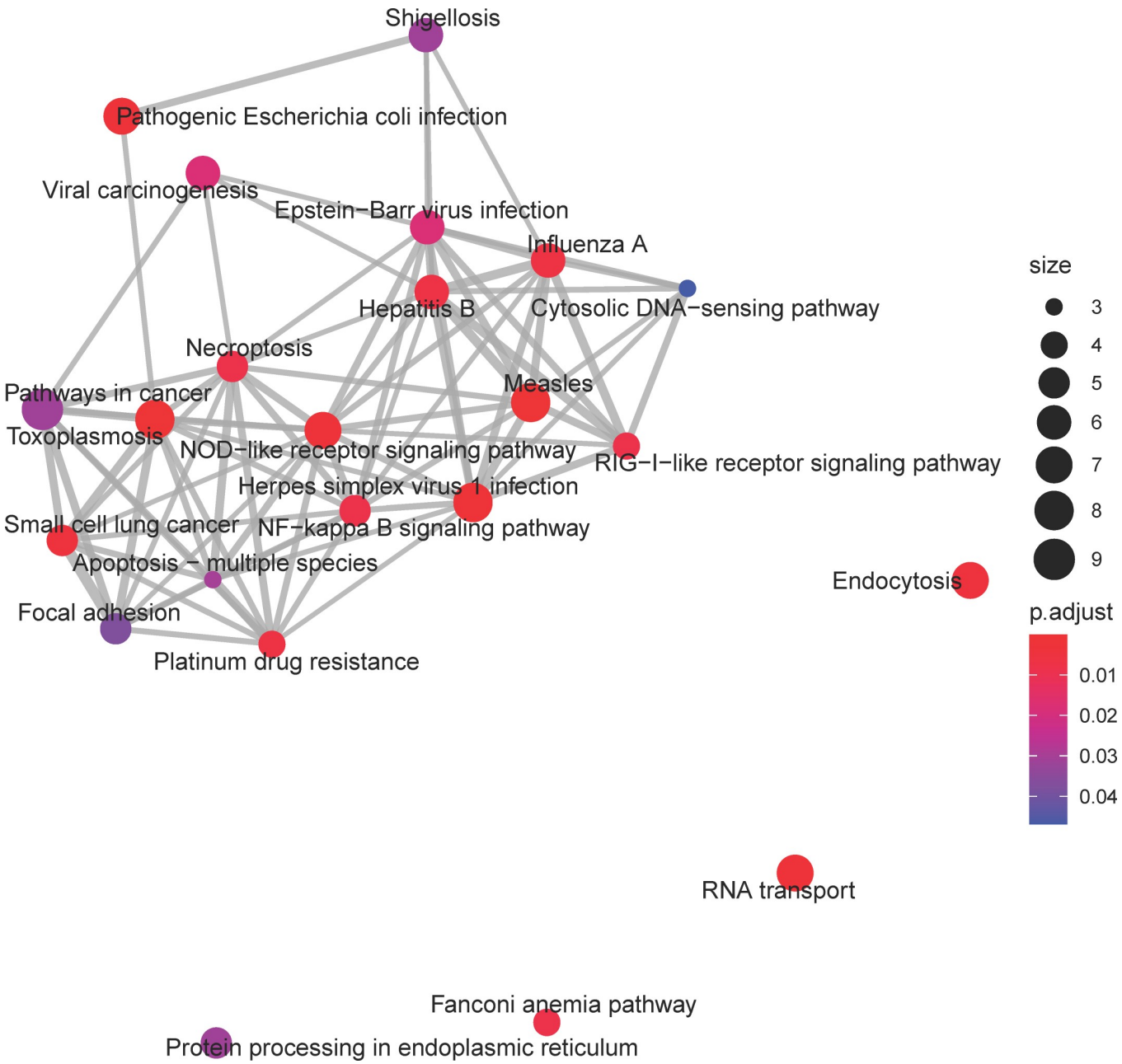

Fig 7. Enrichment map of KEGG pathways for the *greenyellow* consensus co-expression module. Symbol explanation as in Fig 4. Many of the significant pathways in this module have overlapping gene sets, many of which are associated with immune activation, such as *NOD-like receptor signaling*, *RIG-I-like receptor signaling*, *and NF-Kappa-B signaling pathway*. The increasing expression trend of this module's eigengene throughout aging suggests consistently increased activation of these pathways in aging.

https://doi.org/10.1371/journal.pone.0252647.g007

Golgi transport, endocytosis and exocytosis are also represented by downregulated orthologs to *NAPG*, *EXOC2*, *SNX30*, *PDCD6*, *CHMP6*, *VPS26B*, and *SYT4* [52,60,68,72]. Proper vesicle transport and recycling are crucial for the signaling function of neurons, and disruptions in timing of these vesicle mediated events can impact neuronal function. The diversity of biological functions present in this module demonstrates the tight coupling of neuronal metabolism, transport of cellular cargo, and signaling.

Table 6. Selection of transcripts with highest correlation to transcript co-expression module eigengene (module membership, MM) in the *greenyellow* consensus module identified in *Aplysia californica* sensory neurons by *WGCNA*.

Refseq ID	MM	MM p value	TAS	TAS p value	Human Ortholog	Ortholog Name	Ortholog Function
XM_005110768.2!	0.95	1.8E-36	0.44	1.1E-04	**ZNFX1**	**NFX1-type zinc finger-containing protein 1**	Virus detection, IFN response [222], epigenetics [223]
XM_005097053.2!	0.92	6.8E-31	0.44	8.8E-05			
XM_005105124.2!	0.86	2.9E-22	0.53	1.4E-06			
XM_013083625.1	0.94	4.2E-35	0.42	1.9E-04	DTX3L	E3 ubiquitin-protein ligase DTX3L	E3 ubiquitin-protein ligase [224], DNA damage repair [225], INF response [226]
XM_005102017.2	0.94	1.8E-34	0.52	2.2E-06	SAMD9	Sterile alpha motif domain-containing protein 9	Antiviral stress response [227]
*XM_005090189.2**	0.93	2.2E-32	0.45	5.9E-05	MRE11	Double-strand break repair protein	DNA damage repair [228], INF response [229]
XM_005105514.2	0.93	3.7E-32	0.46	4.5E-05	TRANK1	TPR and ankyrin repeat-containing protein 1	Interferon- stimulated gene [230]
XM_013082259.1!	0.93	1.1E-31	0.48	2.1E-05	TUT4	Terminal uridylyltransferase 4	mRNA decay [231], innate immunity [232]
XM_005110839.2	0.91	5.6E-29	0.47	2.5E-05	IL17RD	Interleukin-17 receptor D	ERK inhibitor [233], negative regulation of TLR signaling [234]
XM_005099718.2	0.90	7.9E-28	0.45	7.5E-05	VCPIP1	Deubiquitinating protein VCIP135	Deubiquitination [235]
XM_005090454.2	0.90	1.0E-27	0.56	3.4E-07	SACS	Sacsin	Chaperone [236], INF response in oyster
*XM_005106324.2**	0.90	1.7E-27	0.60	2.6E-08	ZNF598	E3 ubiquitin-protein ligase ZNF598	E3 ubiquitin-protein ligase and Ribosome quality control [237], translation repression [238], Attenuation of innate immune response [239]
XM_005093151.2	0.90	2.7E-27	0.36	1.6E-03	TRIM2	Tripartite motif-containing protein 2	E3 ubiquitin-protein ligase [240], antiviral [241]
*XM_013081468.1**	0.90	3.4E-27	0.52	2.0E-06	ASCC3	Activating signal cointegrator 1 complex subunit 3	DNA repair [242], NFkB, ATF-1, and SRF signaling [243]
XM_005107621.2!	0.90	4.2E-27	0.34	3.0E-03	CMTR1	Cap-specific mRNA (nucleoside-2'-O-)-methyltransferase 1	IFN signaling, antiviral state establishment [244]
XM_013084387.1!	0.90	6.5E-27	0.36	2.0E-03	STAT5B	Signal transducer and activator of transcription 5B	GH signaling [245], Il-2 cytokine signaling [246]
XM_005095848.2	0.90	1.3E-26	0.25	3.4E-02	ANK1	Ankyrin-1	Diverse, including protein localization to membranes [247]
*XM_005108543.2**!	0.89	1.9E-26	0.63	2.2E-09	HERC4	Probable E3 ubiquitin-protein ligase HERC4	E3 ubiquitin-protein ligase [87]
XM_005094842.2!	0.89	4.7E-26	0.47	2.9E-05	IRF1	Interferon regulatory factor 1	IFN signaling [248]
XM_005096699.2	0.89	8.4E-26	0.31	7.1E-03	PARP12	Protein mono-ADP-ribosyltransferase PARP12	Interferon induced gens, negative regulation of translation, NFkB singaling [249]
*XM_005102776.2**	0.88	4.5E-25	0.41	2.7E-04	DDX58	Probable ATP-dependent RNA helicase DDX58	RIG 1, antiviral immune receptor [188]
XM_005104216.2!	0.83	5.0E-20					
XM_005098154.2!	0.88	4.6E-25	0.55	5.7E-07	SMG1	Serine/threonine-protein kinase SMG1	Nonsense mediated mRNA decay [250], restriction of viral replication [251]
XM_005101113.2	0.88	7.1E-25	0.54	8.0E-07	ZC3HAV1L	Zinc finger CCCH-type antiviral protein 1-like	Same family as ZNFX1, unknown function [252]
XM_013086154.1	0.87	1.95E-23	0.32	5.2E-03	BIRC2	Baculoviral IAP repeat-containing protein 2	E3 ubiquitin-protein ligase, NF-kappa-B signaling regulation [83], innate immunity regulation [84]
XM_013086147.1	0.84	1.57E-20					
XM_013089793.1!	0.86	7.8E-23	0.43	1.7E-04	CASP8	Caspase-8	Apoptosis [253], inflammatory homeostasis via RIPK1 [254]
XM_005111821.2	0.85	1.6E-21	0.42	2.1E-04	HIST1H3A	Histone H3.1	Nucleosome formation, transcription regulation [255]
XM_013079365.1	0.83	6.6E-20	0.34	2.9E-03	TLR1	Toll-like receptor 1	Innate immune response [256,257]
XM_013079178.1!	0.83	7.2E-20	0.39	6.5E-04	IRF8	Interferon regulatory factor 8	Microglia activation and neuroinflammation [113]

See Table 2 for description of organization. Common functions include ubiquitination, interferon signaling (IFN), and inflammation. The roughly monotonic increasing trend of this module's eigengene throughout aging suggests consistently increased activation of these processes in aging.

https://doi.org/10.1371/journal.pone.0252647.t006

Table 7. Aplysia co-expression module enrichment for orthologs differentially expressed after immune priming and viral challenge in pacific oyster *Crassostrea gigas*.

	Aplysia transcripts in C. gigas (m +n)	**Transcripts in LaFont (m)**	**Transcripts not in Lafont (n)**	**signif threshold (α)**	**Bonferroni (α'= α/14)**
	7359	697	6662	0.05	0.00385
Module	**Transcripts in module (k)**	**Module transcripts in LaFont (x)**	**Proportion (x/k)**	**p-value (p = Σp(x-1: k))**	**Sig (p<α')**
greenyellow	224	45	0.20	4.37E-06	*
darkgreen	156	29	0.19	1.41E-03	*
pink	906	111	0.12	3.71E-03	*
purple	2203	206	0.09	6.72E-01	-
blue	1170	109	0.09	6.78E-01	-
violet	24	2	0.08	1.00E+00	-
royalblue	410	34	0.08	9.01E-01	-
grey	190	15	0.08	9.22E-01	-
green	1838	133	0.07	1.00E+00	-
orange	125	9	0.07	9.59E-01	-
steelblue	39	2	0.05	1.00E+00	-
paleturquoise	23	1	0.04	1.00E+00	-
saddlebrown	51	1	0.02	1.00E+00	-

Module enrichment for *C. gigas* immune genes in Aplysia co-expression modules was assessed via Fisher's exact test. Of the 7359 Aplysia transcripts that were annotated as *C. gigas* orthologs and present in Aplysia co-expression modules, 697 were present in *C. gigas* (Lafont et al (2020) [37] m = 697, n = 6662). For each module, the number of transcripts in that module that were marked as *C. gigas* orthologs (k) and the proportion of those also present in Lafont et al (2020) [37] (x) were used to calculate the hypergeometric distribution in R. The p value was calculated as the sum of all probabilities at least as extreme as k (Σp(x-1:k) which was compared to a significance threshold of 0.05 with Bonferroni multiple test correction for 14 tests. Three modules (*greenyellow*, *darkgreen*, and *pink*) were identified as significantly enriched for *C. gigas* immune response orthologs.

https://doi.org/10.1371/journal.pone.0252647.t007

While the *pink* module was identified as having an increasing eigengene expression trajectory and a largely a transcriptional and proteostatic character by KEGG enrichment analysis similar to several clusters in Kron et al (2020) [24], the transcripts with the highest module membership, including the hub gene *NFKBIA*, suggest inflammation plays a central role in this module. Many of these upregulated transcripts mapped to human genes known to be induced by NFkB, including *CSTL*, *BIRC3*, *FTH1*, *CYLD*, and the hub gene *NFKBIA* [261–266]. Furthermore, several of these orthologs activate or permit NFkB signaling, including *CSTL*, *BIRC3*, *GM2A*, and NAT10 [83,97,267–270]. The *pink* module also contains several dampeners of the NFkB signaling cascade and innate immunity, such as *NFKBIA*, *CYLD*, *PDE12*, *SIGIRR*, *RIOK1*, *RIOK3 JKAMP*, and *TNIP1*, likely to maintain homeostatic control and prevent over-inflammation [118,122,126,129–132,271,272]. While an upregulation of *NFKBIA* would seem to suggest a decrease in NFkB signaling, the degradation of *NKFBIA* is a key step in the release of NFkB, allowing translocation to the nucleus [272]. This may suggest that these neurons are upregulating NFKBIA to keep up with growing rates of *NKFBIA* degradation as a result of increased NFkB signaling [122].

The *pink* module also contains upregulated translation modulators. This includes genes that promote rRNA maturation and recruitment such as *EFL1*, *NAT10*, *RIOK1*, *RIOK3*, and *HEATR1* [96,97,110,125,127]. Although known for its role in ribosome biogenesis and translation efficiency [97,273,274], *NAT10* is also responsible for N^4-acetylcytoside (N4A) driven INF and NFkB inflammatory signaling via *HMGB1* and *NLRP3* inflammasomes, perhaps playing a dual role in this module [270]. Chronic, low grade inflammation as a result of N4A accumulation due to consistent activity of *NAT10* may contribute to aging in these neurons.

Table 8. Mapping between Aplysia transcripts with high module membership in the greenyellow, darkgreen, and pink modules and genes differentially expressed as a result of immune priming and viral exposure in *C. gigas*.

Module	Aplysia transcript	*C. gigas* Gene	Antimicrobial activity	Pathways	Human Ortholog	Ortholog Name
greenyellow	XM_005110768.2	CGI_10023396	virus	IFN-like pathway and RLR recognition	ZNFX1	NFX1-type zinc finger-containing protein 1
greenyellow	XM_013082259.1	CGI_10020126	V/B	other	TUT4	Terminal uridylyltransferase 4
greenyellow	XM_005097053.2	CGI_10003301	virus	IFN-like pathway and RLR recognition	ZNFX1	NFX1-type zinc finger-containing protein 1
greenyellow	XM_005107621.2	CGI_10013977	other	other	CMTR1	Cap-specific mRNA (nucleoside-2'-O-)-methyltransferase 1
greenyellow	XM_013084387.1	CGI_10028719	virus	JAK/STAT	STAT5B	Signal transducer and activator of transcription 5B
greenyellow	XM_005098154.2	CGI_10024989	V/B	signaling	SMG1	Serine/threonine-protein kinase SMG1 (Fragment)
greenyellow	XM_005101016.2	CGI_10021954	virus	IFN-like pathway and RLR recognition	DHX38	Pre-mRNA-splicing factor ATP-dependent RNA helicase PRP16
greenyellow	XM_013089793.1	CGI_10023960	virus	apoptosis	CASP8	Caspase-8
greenyellow	XM_005105124.2	CGI_10023396	virus	IFN-like pathway and RLR recognition	ZNFX1	NFX1-type zinc finger-containing protein 1
greenyellow	XM_005104216.2	CGI_10024392	virus	IFN-like pathway and RLR recognition	DDX58	Probable ATP-dependent RNA helicase DDX58
greenyellow	XM_013079178.1	CGI_10003270	virus	IFN-like pathway and RLR recognition	IRF8	Interferon regulatory factor 8 (Fragment)
greenyellow	XM_013085543.1	CGI_10018479	V/B	signaling	COL21A1	Collagen alpha-1(XXI) chain
greenyellow	XM_013081218.1	CGI_10021954	virus	IFN-like pathway and RLR recognition	DHX16	Pre-mRNA-splicing factor ATP-dependent RNA helicase DHX16
greenyellow	XM_005104310.2	CGI_10010459	virus	IFN-like pathway and RLR recognition	DDX58	Probable ATP-dependent RNA helicase DDX58
greenyellow	XM_005110422.2	CGI_10003270	virus	IFN-like pathway and RLR recognition	IRF8	Interferon regulatory factor 8
greenyellow	XM_005109293.2	CGI_10002009	other	other	ELF5	ETS-related transcription factor Elf-5
greenyellow	XM_005108818.2	CGI_10020752	virus	RNAi	DDX58	Probable ATP-dependent RNA helicase DDX58
darkgreen	XM_005113357.2	CGI_10019528	virus	JAK/STAT	SOCS2	Suppressor of cytokine signaling 2
darkgreen	XM_013090188.1	CGI_10002181	bacteria	other	MPEG1	Macrophage-expressed gene 1 protein
darkgreen	XM_005092855.1	CGI_10019528	virus	JAK/STAT	SOCS2	Suppressor of cytokine signaling 2
darkgreen	XM_013088902.1	CGI_10019733	virus	other	DIS3L2	DIS3-like exonuclease 2
darkgreen	XM_005108083.2	CGI_10019528	virus	JAK/STAT	SOCS2	Suppressor of cytokine signaling 2
darkgreen	XM_013091162.1	CGI_10028125	virus	other	RANBP2	E3 SUMO-protein ligase RanBP2
darkgreen	XM_013088005.1	CGI_10027619	virus	other	TYMP	Thymidine phosphorylase
pink	XM_005088796.2	CGI_10003270	virus	IFN-like pathway and RLR recognition	IRF8	Interferon regulatory factor 8 (Fragment)
pink	XM_005097229.2	CGI_10023430	other	other	FNIP2	Folliculin-interacting protein 2 (Fragment)
pink	XM_005110283.2	CGI_10026985	bacteria	other	PRSS12	Neurotrypsin
pink	XM_013081403.1	CGI_10026606	other	other	CBX4	E3 SUMO-protein ligase CBX4
pink	XM_005099789.2	CGI_10021954	virus	IFN-like pathway and RLR recognition	DHX16	Pre-mRNA-splicing factor ATP-dependent RNA helicase DHX16
pink	XM_013082526.1	CGI_10025856	virus	other	MSH2	DNA mismatch repair protein Msh2
pink	XM_005102215.2	CGI_10013829	V/B	other	ANGPTL6	Angiopoietin-related protein 6

(*Continued*)

Table 8. (Continued)

Module	Aplysia transcript	*C. gigas* Gene	Antimicrobial activity	Pathways	Human Ortholog	Ortholog Name
pink	XM_005107413.2	CGI_10005182	virus	IFN-like pathway and RLR recognition	ADAR	Double-stranded RNA-specific adenosine deaminase (Fragment)

Transcripts (column 2) from the *greenyellow*, *darkgreen*, and *pink* (column 1) modules alongside the *C. gigas* gene to which they mapped (column 3) during BLAST comparison of Aplysia and *C. gigas* proteomes. Transcripts were selected if they exhibited module membership greater than or equal to 0.8 for their respective module and the *C. gigas* ortholog exhibited a log 2 fold change of at least 1 in Lafont et al (2020) [37] as a result of immune priming or virus exposure. Columns 4 and 5 list the antimicrobial function and pathway identified by Lafont et al (2020) [37] for each *C. gigas* gene. Columns 6 and 7 list the gene symbol and gene name for the human ortholog of each Aplysia transcript. A full mapping of Aplysia transcripts to *C. gigas* genes from Lafont et al (2020) [37] can be found in supplementary file **S3 Dataset**.

https://doi.org/10.1371/journal.pone.0252647.t008

Translation attenuating orthologs are also present in this module, such as *INTS1*, *GCN1*, and *EIF4A2* [91,92]. Under amino acid starvation conditions, *GCN1* activates *GCN2* which in turn phosphorylates *EIF4A*, which restricts translation [94,275–277]. However, this cascade has also been shown to be part of the antiviral response, specifically to prevent translation of viral RNAs [278,279]. Considering the preponderance of inflammatory genes in the *pink* module and the methodology that these animals were fed an *ad libitum* diet, the antiviral function of this cascade is the more likely here. Interestingly, this cascade also modulates synaptic plasticity and memory by inhibiting *CREB* in the hippocampus. Because *CREB* is essential for synaptic plasticity, increased *CREB* inhibition as a result of increased activity of the *GCN1-EIF4A* cascade during an inflammatory response may have knock-on effects that inhibit synaptic plasticity in these neurons [280].

Like the *pink* module, the *orange* module is similar to expression profile clusters found in Kron et al (2020) [24] as it exhibits increasing eigengene expression trajectory in age and classic signatures of ER stress. The hub transcript *CREB3L3* (*CREBH*) and the ortholog with fourth highest module membership *EIF2AK3* (*PERK*) are critical in the ER stress response cascade, while others like *UGGT1*, *STT3B* and *TNXDC16* are involved in ERAD [135,139,154,155,157]. Interestingly, several of the transcripts in the *pink* module with high module membership are involved in sphingolipid metabolism, such as PSAP and SPLITC2 [114,281,282]. Sphingolipids, particularly ceramides, play central roles in pro-inflammatory signaling and ER stress, suggesting this module also participates in pro-inflammatory signaling [283]. *SPLITC2* in particular has been shown to be upregulated by NFkB, suggesting NFkB signaling also plays a role in the *orange* module [281].

Several transcripts in the *orange* module regulate NFkB, such as *BCL3* and *BIRC3*, similar to the *pink* module [83,149,150]. In addition, upregulation of the *orange* module hub gene *CREB3L3* itself suggests neuro-inflammation as a central component of this module due to the role of this ortholog in the acute inflammatory response [135]. The similarities in the *pink* and *orange* modules suggest that each represents a different element of a proteostatic response to inflammation. Interestingly, the *darkgreen* module has a monotonic increasing eigengene expression trend early in the aging process and then stabilizes when the *orange* and *pink* modules enter their monotonic phase.

Many upregulated transcripts in the *darkgreen* module are orthologous to human genes associated with DNA damage response, including the hub transcript *RPA2*, *RPA3*, *NSMCE1*, *ZRANB3*, and *TREX2* suggesting mounting DNA damage with age in these neurons [160,184,187,201,205]. The presence of several upregulated transcripts orthologous to genes critical to the formation of the nuclear pore such as *NUP214*, *NUP98*, and *NUP88* as well as the stability and export of mRNA such as *TREX2*, *GLE1*, and *TENT4A*, and transcription and

translation regulators like *SMARCD1* may suggest this module maintains a particular transcriptional program [180,189,190,206,207,210]. Interestingly, this module contains several upregulated orthologs known to inhibit inflammatory or immune signaling, such as *TRIM3*, *TIPARP*, *SOCS2*, *SMARCD1*, and *LGALS4*. This could suggest this module is either acting to suppress or modulate inflammatory signaling to prevent over-inflammation as seen in the *pink* and *orange* modules [162,166,170,177,181]. However, several other member orthologs exhibit pro-inflammatory functions, such as the hub transcript *RPA2* and *XIAP* which activate NFkB [220,284], viral RNA sensor and activator of the interferon response pathway DDX58/RIG-1 [285], and genes that support differentiation and maturation of immune cells such as *EPSTI1*, *RBBP9*, *SSUH2* and *GIMAP1* [163,182,183,218]. Aplysia immune hemocyte aggregates are known to play a pivotal role in neuron injury-associated inflammation and perhaps are similarly involved in the inflammatory response suggested by the orthologs present in the pink, orange, and *darkgreen* modules [286–289]. Curiously, *TIPARP* and *PARP14* function to suppress and activate different cytokine signaling cascades depending on context and could be counted among other previously listed groups [166,167,198]. Upregulation of orthologs to the aforementioned viral RNA sensor *RIG-1*, sensor of viral entry *PLA2G16*, antimicrobial peptide *MPEG1*, and blocker of viral DNA replication *BANF1* may suggest a role for this module in the detection of and initial response to viral infection in these neurons [191,193,204]. Interestingly, this may be further supported by the orthologs *HENMT1* and *MOV10L1* which mediate the formation of PIWI interacting RNAs (piRNA), noncoding RNAs that have antiviral activities in the innate immune systems of insects and possibly all eukaryotes [175,185,290,291]. The final module of interest, the *greenyellow* module, exhibits a monotonic increase in eigengene expression during the aging process, in parallel with the *darkgreen* module from age 6–9 months, and then parallel to the *pink* and *orange* modules thereafter.

Transcripts with highest module membership in the *greenyellow* module all represent orthologs to elements of the Interferon (IFN) Mediated response to RNA viruses. Several innate immune mobilized antiviral zinc finger protein orthologs are represented in this module, including *PARP12*, *ZC3HAVIL*, *TUT4*, and three orthologs of *ZNFX1*, one of which is the hub transcript [249,252,292,293]. Other transcripts are orthologs of interferon-stimulated genes (ISG) that stimulate or facilitate the expression of other ISG, including *ZNFX1*, *MRE11*, *DTX3L*, *CMTR1*, and *IRF1* [222,226,229,244,248]. Among these ISG orthologs are viral dsRNA sensors *ZNFX1* and *DDX58*/*RIG1* [222,285]. Other ISG orthologs upregulated in this module are IFN effector genes that have specific antiviral action: *SAMD9* triggers anti-viral granule formation, *TUT4* uridylates viral RNAs thus tagging them for degradation, *SMG1* restricts viral replication, and *TRIM2* prevents viral internalization [227,232,241,251]. The upregulation of *TLR1* and *STAT5b* orthologs in the *greenyellow* module, which cooperate with *STRA6* and *JAK2* from the *darkgreen*, capture elements of the pattern recognition signaling cascade needed to mobilize an immune response [246,256,257]. A proper immune response also requires modulators to prevent over-inflammation or to dampen ISG expression once the viral challenge has been dealt with to allow clearance of waste. Several such immune regulator orthologs are also upregulated in the *greenyellow* module, including *IL17RD* which exists as part of a larger family of proteins that regulate interleukin (IL) and Toll-like receptor (TLR) signaling, *ZNF598*, and *ASCC3* [234,239,243]. Whereas the *pink* module contains translation modulators, several of these upregulated transcripts are also orthologs of proteins known to have epigenetic and/or transcription attenuating effects, including *PARP12*, *ZNFX1*, and *H3.1*, possibly to mute global transcription in favor of anti-viral transcriptional programs [223,249,255].

Several of these transcripts also participate in NFkB signaling, promoting inflammation as part of the immune response. These include *IRF1* and *IRF8* which activate the Type-I

Interferon response, *CASP8*, *ASCC3* which is indispensable for NFkB signaling, and *PARP12* which activates NFkB [243,249,254,294]. Ubiquitination dynamics are crucial for IFN and NFkB signaling [295], and many of the included upregulated transcripts are orthologs of genes that act as E3 ubiquitin-protein ligases such as *DTX3L*, *ZNF598*, *TRIM2*, and *HERC4*; as well as the Deubiquitinating enzymes *VCPIP1*. The multitude of orthologs involved in initiating the NFkB signaling cascade in response to viral infection in the *greenyellow* module may suggest this module may act upstream of the NFkB stimulated *pink* and *orange* modules.

While the discussed results appear to present a convincing picture of the function of these co-expression networks, it is important to approach these inferences with a degree of caution. Genes marked as orthologous by statistical means, such as BLAST or ghostKOALA, do not always perform the same functions in the target species as they do in the annotated species. Very few of these transcripts discussed have been independently investigated in Aplysia and their functions in Aplysia neurons and associated cells are not known. While several orthologs are generally understood to perform conserved roles across genera and their inferred function can be reasonably assumed, such as those involved in glycolysis or the TCA cycle, others involved in more idiosyncratic systems such as the immune response may have a large degree of divergence, especially when comparing the complex immune system of vertebrates such as human to that of evolutionarily distant mollusks.

Although the function of the orthologs discussed were characterized in human, mouse, *C. elegans*, and/or Drosophila, similar expression patterns to those captured by the *pink*, *orange*, *darkgreen*, and *greenyellow* modules have also been documented in other mollusks. Both *Cathepsin L* and *MPEG1* orthologs have been shown to take part in the innate immune response of two species of abalone [296–298]. Immune challenge in oysters with viral RNA also resulted in upregulation of common NFkB and JAK/STAT signaling components observed in *darkgreen* and *greenyellow* modules, including orthologs to *ZNFX1*, *Sacsin*, and *MPEG1* along with various IAP, *TRIM*, caspases, and IRF proteins *[37]*. To assess to what degree the transcripts inferred to play a role in the neural immune and inflammatory response via annotation to human orthologs represent a bonafide immune response, we further compared our module transcript sets to the transcriptional signature of an acute immune response to immune priming and RNA virus exposure in another mollusk, the Pacific oyster *Crassostrea gigas* [37]. The *pink*, *greenyellow*, and *darkgreen* modules were significantly enriched for orthologs to putative *C. gigas* immune response genes, supporting the notion that these modules do indeed represent a component of the Aplysia immune response. Indeed, several DE genes in the *C. gigas* immune response were orthologs of transcripts with high module membership in the *pink*, *darkgreen*, and/or *greenyellow* modules, such as the aforementioned orthologs of HERK4, BIRC3, IRF1, IRF8, MPEG1, DDX58/RIG-I, and most importantly all three orthologs of ZNFX1, including the *greenyellow* hub gene. Furthermore, several more transcripts, although not identified as orthologs of genes demonstrated to be DE in Lafont et al (2020) [37], do still map to the same human ortholog as genes identified in Lafont et al (2020) [37], such as *sacsin*. However, when comparing the list of significantly differentially expressed genes as a result of poly(I·C) in *C. gigas* to Aplysia orthologous genes significantly upregulated in sensory neuron aging as reported in our previous study, only two orthologs are shared. This suggest that, while the *greenyellow* and *darkreen* modules may capture an immune transcriptional program, viral infection and associated immune response are not drivers of transcriptional change in Aplysia sensory neurons. Moreover, this lack of correlation with oyster genes chronically upregulated after exposure to a virus analog indicates the need for caution in interpreting changes in module expression. Even when specific modules that show an increase in expression with aging include transcript members with anti-inflammatory or antiviral functions, these specific genes may not individually exhibit age-related expression changes. On the

other hand, a majority of transcripts with high module membership in the *royalblue*, *pink*, and *orange* modules were identified as differentially expressed in our previous study, suggesting inflammation may result in proteostatic stress and mitochondrial dysfunction rather than infection.

Several transcripts from the *royalblue* module interact with the *pink* and *orange* modules, primarily as inhibitors. *MTFS2* specifically inhibits the activity of *EIF2AK3* from the *orange* module, which functions to maintain mitochondrial morphology, Ca^{2+} homeostasis, and limit ROS production [299]. *ITCH*, via its interaction with *TXNIP*, promotes an antioxidant state, prevents pro-inflammatory signaling through ROS and NFkB, and prevents *TXNIP* from inhibiting glycolysis [300,301]. Similarly, *PARK7* also inhibits NFkB signaling and the astrocyte inflammatory response [302,303]. Finally, GPS2 also exhibits strong anti-inflammatory activity [304,305]. Conversely, *PDE12* from the *pink* module is known to suppresses mitochondrial translation and contribute to respiratory incompetence [306]. Perhaps the eigengene expression perturbation at 9 months of age common to these expression modules may represent a transition from a state of healthy metabolic activity and antioxidant capacity exemplified by the transcripts of the *royalblue* module towards an aged state typified by inflammation and protein dyshomeostasis suggested by the transcript sets of the *pink* and *orange* modules. The role of ROS represents a potentially interesting link between these modules.

Decreased activity of mitochondrial homeostasis and metabolism mechanism suggested by the *royalblue* module suggest mitochondrial dysfunction with age, a well-known source of ROS [307]. Furthermore, downregulation of several antioxidant proteins in the *royalblue* module would suggest decreased capacity for ROS defense. Overexpression of SOD2 and GPX have been demonstrated to inhibit NFkB activation [308,309], thus the downregulation of these and other antioxidants in the *royalblue* module may in fact potentiate NFkB activation as suggested by the *pink* and *orange* modules via increased ROS levels. While the role of ROS in NFkB signaling is complex and cell type specific, prolonged oxidative stress has been shown to increased NFkB signaling and contribute to a pro-inflammatory state [310,311]. Upregulation of FTH by NFkB, as seen in the *pink* module, has also been suggested to be a major component of the NFkB derived antioxidant response against high H_2O_2 levels during chronic inflammation and oxidative stress [312]. Furthermore, ER stress resulting from increases in misfolded proteins due to oxidative stress, signatures of which were identified in our previous study and are also suggested by the *orange* module, has been shown to activate NFkB as well. Specifically, the activity of PERK, which is among the top orthologs in the *orange* module, plays a crucial role in activation of NFkB during ER stress [313]. In addition to downregulation of antioxidants, co-temporal upregulation of ROS producers like the two *DUOX1* orthologs in the *pink* module suggest an increased in ROS, [88,134].

Indeed, chronic, low-grade inflammation has been suggested to be both cause and consequence of mitochondrial dysfunction and resulting metabolic impairment in neuronal aging [314–316]. These data suggest that chronic inflammation contributes to an increasingly oxidative environment in these neurons, exacerbating mitochondrial dysfunction that is known to occur in aging.

Supporting information

S1 Fig. Scale free topology and mean connectivity calculated for expression data from PVC and BSC sensory neurons. For each cutout, the scale free topology model fit (A), median connectivity (B), mean connectivity (C), and max connectivity (D) of a co-expression matrix (y-axis) at a selected soft threshold power (x-axis) is plotted for both BSC (black) and PVC (Red). A soft power of 16 was selected for both sensory neuron types to achieve a scale free topology

fit above 0.9 and to minimize the mean connectivity.
(TIF)

S2 Fig. Hierarchical cluster of consensus co-expression module eigengenes derived from expression data from PVC and BSC sensory neuron clusters. Module eigengene names are arbitrarily assigned. Red horizontal line represents 0.25 branch height threshold for similarity, below which modules are merged.
(TIF)

S3 Fig. Hierarchical cluster of consensus expression data from PVC and BSC sensory neuron clusters. Colored bars at the bottom represent module assignments for each transcript. Module colors are arbitrarily assigned. The top color set represents the module assignment before merging similar of similar modules, while bottom bar represents module assignment post merge (see S2 Fig). In total, 13 co-expression modules were identified.
(TIF)

S4 Fig. Consensus co-expression module eigengene correlation with external phenotype calculated individually for constituent sensory neuron types (PVC and BSC sensory neurons). Each cell of the heatmap represents the correlation between a module eigengene (row) and phenotype (column). The top number in a cell is the value of Pearson correlation between two eigengenes. The p-value significance of module-trait correlation is the bottom number in each cell in parentheses. The phenotypes are animal weight at sacrifice (weight), latency of two reflex behaviors described in Greer et al 2018: Tail withdrawal reflex time (TWRT) and time to right (TTR), and chronological age of the animal in months at sacrifice (Age). Correlations for age are similar between sensory neuron types for the *royalblue*, *saddlebrown*, *greenyellow*, *orange*, *pink*, and *darkgreen* modules.
(TIF)

S1 Table. Software. All Software and respective versions used for RNA sequencing read quality control and quality assurance, mapping and abundance estimation, and downstream analysis.
(DOCX)

S2 Table. Transcript set overlap between co-expression modules (modules) and transcript expression profile clusters (clusters) from Kron et al (2020) [24]. Each cell represents the number of transcripts shared between respective module (row) and cluster (column). The "n" column represents the number of transcripts in a given module, and the "n" row represents the number of transcripts in a given cluster. Values in the "Sum" columns are row sums, e.g. the total number of transcripts in each respective module also present in the clusters. The "% of module" columns represent percentage values calculated by dividing the "Sum" columns by the total number of transcripts in a cluster set (1106 for B clusters, and 1198 for P clusters). Values in the "Sum" row are column sums, e.g. the total number of transcripts in each respective cluster that are also present in the modules. The "cluster %" row represent percentage values calculated by dividing the "Sum" row by the total number of transcripts among all modules (10012).
(DOCX)

S1 File. R session. All R packages and respective versions used for clustering, analysis, and visualization of RNA sequencing transcript abundances.
(TXT)

S1 Dataset. Full module KEGG enrichment results. Full results for all modules of KEGG enrichment of co-expression modules using clusterProfiler.
(XLSX)

S2 Dataset. Full module membership results. Per module module-membership values and significance for all transcripts assigned to each module.
(XLSX)

S3 Dataset. Module transcript overlap with genes DE in C. gigas immune response. This file contains the results of mapping *Aplysia californica* transcript IDs to *Crassostrea gigas* gene IDs for transcripts in Aplysia age associated co-expression modules that mapped to C. gigas genes identified as DE in immune priming and viral challenge by Laont et al 2020.
(XLSX)

S4 Dataset. Evaluation of shared, upregulated orthologs in *C. gigas* immune response and Aplysia sensory neuron aging. This file contains a list of genes upregulated genes in *C. gigas* immune respone to viral analogue poly(IC) as reported in Lafont et al. 2020 [37] that have orthologs with evalue of >1E-20 in Aplysia. Aplysia orthologs are annotated with transcript, protein, and gene RefSeq identifiers as well as neuron type-specific adjusted pvalues, expression cluster assignment, and expression cluster direction reported in our previous publication. Only two Aplysia orthologs were identified as significantly upregulated in aging sensory neurons.
(XLSX)

Acknowledgments

We gratefully acknowledge the University of Miami Aplysia Resource staff for their assistance. We are indebted to Dr. Douglas Crawford and Dr. Marjorie Oleksiak for use of their Nanodrop and Bioanalyzer. We thank Dr. Justin Greer for his assistance in RNA extraction and invaluable advice.

Author Contributions

Conceptualization: N. S. Kron, L. A. Fieber.

Data curation: N. S. Kron.

Formal analysis: N. S. Kron.

Funding acquisition: L. A. Fieber.

Investigation: N. S. Kron.

Methodology: N. S. Kron.

Project administration: L. A. Fieber.

Resources: L. A. Fieber.

Software: N. S. Kron.

Supervision: L. A. Fieber.

Validation: N. S. Kron.

Visualization: N. S. Kron.

Writing – original draft: N. S. Kron.

Writing – review & editing: N. S. Kron, L. A. Fieber.

References

1. Grimm A, Eckert A. Brain aging and neurodegeneration: from a mitochondrial point of view. Journal of Neurochemistry. 2017; 143(4):418–31. https://doi.org/10.1111/jnc.14037 WOS:000415368800004. PMID: 28397282
2. Poddar J, Pradhan M, Ganguly G, Chakrabarti S. Biochemical deficits and cognitive decline in brain aging: Intervention by dietary supplements. J Chem Neuroanat. 2019; 95:70–80. https://doi.org/10.1016/j.jchemneu.2018.04.002 PMID: 29678666.
3. Lopez-Otin C, Blasco MA, Partridge L, Serrano M, Kroemer G. The hallmarks of aging. Cell. 2013; 153 (6):1194–217. https://doi.org/10.1016/j.cell.2013.05.039 PMID: 23746838; PubMed Central PMCID: PMC3836174.
4. Watts ME, Pocock R, Claudianos C. Brain Energy and Oxygen Metabolism: Emerging Role in Normal Function and Disease. Front Mol Neurosci. 2018; 11:216. https://doi.org/10.3389/fnmol.2018.00216 PMID: 29988368; PubMed Central PMCID: PMC6023993.
5. Mattson MP, Arumugam TV. Hallmarks of Brain Aging: Adaptive and Pathological Modification by https://doi.org/10.1016/j.cmet.2018.05.011 PMID: 29874566 States. Cell Metabolism. 2018; 27 (6):1176–99. WOS:000434480000007.
6. Yankner BA, Lu T, Loerch P. The aging brain. Annu Rev Pathol. 2008; 3:41–66. https://doi.org/10.1146/annurev.pathmechdis.2.010506.092044 PMID: 18039130.
7. Buffenstein R, Edrey YH, Yang T, Mele J. The oxidative stress theory of aging: embattled or invincible? Insights from non-traditional model organisms. Age. 2008; 30(2–3):99–109. https://doi.org/10.1007/s11357-008-9058-z WOS:000258881300004. PMID: 19424860
8. Gems D, Partridge L. Genetics of longevity in model organisms: debates and paradigm shifts. Annu Rev Physiol. 2013; 75:621–44. https://doi.org/10.1146/annurev-physiol-030212-183712 PMID: 23190075.
9. Capo TR, Fieber LA, Stommes DL, Walsh PJ. Reproductive output in the hatchery-reared California sea hare at different stocking densities. Contemp Top Lab Anim. 2003; 42(5):31–5. WOS:000185698300007. PMID: 14510522
10. Moroz LL. Aplysia. Curr Biol. 2011; 21(2):R60–1. https://doi.org/10.1016/j.cub.2010.11.028 PMID: 21256433; PubMed Central PMCID: PMC4024469.
11. Audesirk TE. A Field Study of Growth and Reproduction in Aplysia Californica. Biol Bull. 1979; 157 (3):407–21. https://doi.org/10.2307/1541026 PMID: 29324028.
12. Kempsell AT, Fieber LA. Behavioral aging is associated with reduced sensory neuron excitability in Aplysia californica. Front Aging Neurosci. 2014;6. https://doi.org/10.3389/fnagi.2014.00006 WOS:000339432000001. PMID: 24570662
13. Gerdes R, Fieber LA. Life history and aging of captive-reared California sea hares (Aplysia californica). J Am Assoc Lab Anim. 2006; 45(1):40–7. WOS:000236461200006.
14. Bailey CH, Castellucci VF, Koester J, Chen M. Behavioral changes in aging Aplysia: a model system for studying the cellular basis of age-impaired learning, memory, and arousal. Behav Neural Biol. 1983; 38(1):70–81. https://doi.org/10.1016/s0163-1047(83)90399-0 PMID: 6626101.
15. Rattan KS, Peretz B. Age-dependent behavioral changes and physiological changes in identified neurons in Aplysia californica. J Neurobiol. 1981; 12(5):469–78. https://doi.org/10.1002/neu.480120506 PMID: 7276930.
16. Papka R, Peretz B, Tudor J, Becker J. Age-Dependent Anatomical Changes in an Identified Neuron in the Cns of Aplysia-Californica. Journal of Neurobiology. 1981; 12(5):455–68. https://doi.org/10.1002/neu.480120505 WOS:A1981MD97800004. PMID: 7276929
17. Kempsell AT, Fieber LA. Habituation in the Tail Withdrawal Reflex Circuit is Impaired During Aging in Aplysia californica. Front Aging Neurosci. 2016;8. https://doi.org/10.3389/fnagi.2016.00008 WOS:000369905200001. PMID: 26858639
18. Kempsell AT, Fieber LA. Aging in Sensory and Motor Neurons Results in Learning Failure in Aplysia californica. Plos One. 2015; 10(5). https://doi.org/10.1371/journal.pone.0127056 WOS:000354544200147. PMID: 25970633
19. Kempsell AT, Fieber LA. Age-related deficits in synaptic plasticity rescued by activating PKA or PKC in sensory neurons of Aplysia californica. Front Aging Neurosci. 2015;7. https://doi.org/10.3389/fnagi.2015.00007 WOS:000361232000001. PMID: 25762930
20. Greer JB, Schmale MC, Fieber LA. Whole-transcriptome changes in gene expression accompany aging of sensory neurons in Aplysia californica. BMC genomics. 2018; 19(1):529. https://doi.org/10.1186/s12864-018-4909-1 PMID: 29996779; PubMed Central PMCID: PMC6042401.

21. Moroz LL, Kohn AB. Single-neuron transcriptome and methylome sequencing for epigenomic analysis of aging. Methods Mol Biol. 2013; 1048:323–52. https://doi.org/10.1007/978-1-62703-556-9_21 PMID: 23929113; PubMed Central PMCID: PMC4045448.

22. Moroz LL, Kohn AB. Do different neurons age differently? Direct genome-wide analysis of aging in single identified cholinergic neurons. Front Aging Neurosci. 2010;2. https://doi.org/10.3389/neuro.24.002.2010 PMID: 20552042; PubMed Central PMCID: PMC2910937.

23. Kadakkuzha BM, Akhmedov K, Capo TR, Carvalloza AC, Fallahi M, Puthanveettil SV. Age-associated bidirectional modulation of gene expression in single identified R15 neuron of Aplysia. BMC genomics. 2013; 14:880. https://doi.org/10.1186/1471-2164-14-880 PMID: 24330282; PubMed Central PMCID: PMC3909179.

24. Kron NS, Schmale MC, Fieber LA. Changes in Metabolism and Proteostasis Drive Aging Phenotype in Aplysia californica Sensory Neurons. Front Aging Neurosci. 2020; 12(280).https://doi.org/10.3389/fnagi.2020.573764

25. Song Y, Pan Y, Liu J. The relevance between the immune response-related gene module and clinical traits in head and neck squamous cell carcinoma. Cancer Manag Res. 2019; 11:7455–72. https://doi.org/10.2147/CMAR.S201177 PMID: 31496804; PubMed Central PMCID: PMC6689548.

26. Langfelder P, Horvath S. WGCNA: an R package for weighted correlation network analysis. Bmc Bioinformatics. 2008;9. https://doi.org/10.1186/1471-2105-9-9 WOS:000262999900002. PMID: 18182098

27. Nam D, Kim SY. Gene-set approach for expression pattern analysis. Brief Bioinform. 2008; 9(3):189–97. https://doi.org/10.1093/bib/bbn001 PMID: 18202032.

28. Oldham MC, Konopka G, Iwamoto K, Langfelder P, Kato T, Horvath S, et al. Functional organization of the transcriptome in human brain. Nat Neurosci. 2008; 11(11):1271–82. https://doi.org/10.1038/nn.2207 PMID: 18849986; PubMed Central PMCID: PMC2756411.

29. Serin EAR, Nijveen H, Hilhorst HWM, Ligterink W. Learning from Co-expression Networks: Possibilities and Challenges. Front Plant Sci. 2016;7. https://doi.org/10.3389/fpls.2016.00007 WOS:000373600300001. PMID: 26870046

30. Bushnell B. BBMap. 37.90 ed. sourceforge.net/projects/bbmap/2014.

31. Patro R, Duggal G, Love MI, Irizarry RA, Kingsford C. Salmon provides fast and bias-aware quantification of transcript expression. Nat Methods. 2017; 14(4):417–9. https://doi.org/10.1038/nmeth.4197 PMID: 28263959.

32. Soneson C, Love MI, Robinson MD. Differential analyses for RNA-seq: transcript-level estimates improve gene-level inferences. F1000Res. 2015; 4:1521. https://doi.org/10.12688/f1000research.7563.2 PMID: 26925227; PubMed Central PMCID: PMC4712774.

33. Gentleman R, Carey V, Huber W, Hahne F. genefilter: genefilter: methods for filtering genes from high-throughput experiments. 1.70.0 ed2020.

34. Leek JT. svaseq: removing batch effects and other unwanted noise from sequencing data. Nucleic Acids Res. 2014;42(21). WOS:000347914600002. https://doi.org/10.1093/nar/gku864 PMID: 25294822

35. Love MI, Huber W, Anders S. Moderated estimation of fold change and dispersion for RNA-seq data with DESeq2. Genome Biol. 2014; 15(12). https://doi.org/10.1186/s13059-014-0550-8 WOS:000346609500022. PMID: 25516281

36. Yu GC, Wang LG, Han YY, He QY. clusterProfiler: an R Package for Comparing Biological Themes Among Gene Clusters. Omics-a Journal of Integrative Biology. 2012; 16(5):284–7. https://doi.org/10.1089/omi.2011.0118 WOS:000303653300007. PMID: 22455463

37. Lafont M, Vergnes A, Vidal-Dupiol J, de Lorgeril J, Gueguen Y, Haffner P, et al. A Sustained Immune Response Supports Long-Term Antiviral Immune Priming in the Pacific Oyster, Crassostrea gigas. mBio. 2020; 11(2). https://doi.org/10.1128/mBio.02777-19 PMID: 32156821; PubMed Central PMCID: PMC7064767.

38. Deacon SW, Serpinskaya AS, Vaughan PS, Lopez Fanarraga M, Vernos I, Vaughan KT, et al. Dynactin is required for bidirectional organelle transport. J Cell Biol. 2003; 160(3):297–301. https://doi.org/10.1083/jcb.200210066 PMID: 12551954; PubMed Central PMCID: PMC2172679.

39. Faik P, Walker JI, Redmill AA, Morgan MJ. Mouse glucose-6-phosphate isomerase and neuroleukin have identical 3' sequences. Nature. 1988; 332(6163):455–7. https://doi.org/10.1038/332455a0 PMID: 3352745.

40. Imai H, Nakagawa Y. Biological significance of phospholipid hydroperoxide glutathione peroxidase (PHGPx, GPx4) in mammalian cells. Free Radic Biol Med. 2003; 34(2):145–69. https://doi.org/10.1016/s0891-5849(02)01197-8 PMID: 12521597.

41. Hao HX, Khalimonchuk O, Schraders M, Dephoure N, Bayley JP, Kunst H, et al. SDH5, a gene required for flavination of succinate dehydrogenase, is mutated in paraganglioma. Science. 2009; 325 (5944):1139–42. https://doi.org/10.1126/science.1175689 PMID: 19628817; PubMed Central PMCID: PMC3881419.

42. Weir ML, Xie H, Klip A, Trimble WS. VAP-A binds promiscuously to both v- and tSNAREs. Biochem Biophys Res Commun. 2001; 286(3):616–21. https://doi.org/10.1006/bbrc.2001.5437 PMID: 11511104.

43. Ikeda Y, Okamura-Ikeda K, Tanaka K. Purification and characterization of short-chain, medium-chain, and long-chain acyl-CoA dehydrogenases from rat liver mitochondria. Isolation of the holo- and apoenzymes and conversion of the apoenzyme to the holoenzyme. J Biol Chem. 1985; 260(2):1311–25. PMID: 3968063.

44. Jerber J, Baas D, Soulavie F, Chhin B, Cortier E, Vesque C, et al. The coiled-coil domain containing protein CCDC151 is required for the function of IFT-dependent motile cilia in animals. Hum Mol Genet. 2014; 23(3):563–77. https://doi.org/10.1093/hmg/ddt445 PMID: 24067530.

45. Taira T, Saito Y, Niki T, Iguchi-Ariga SM, Takahashi K, Ariga H. DJ-1 has a role in antioxidative stress to prevent cell death. Embo Rep. 2004; 5(2):213–8. https://doi.org/10.1038/sj.embor.7400074 PMID: 14749723; PubMed Central PMCID: PMC1298985.

46. Junn E, Jang WH, Zhao X, Jeong BS, Mouradian MM. Mitochondrial localization of DJ-1 leads to enhanced neuroprotection. J Neurosci Res. 2009; 87(1):123–9. https://doi.org/10.1002/jnr.21831 PMID: 18711745; PubMed Central PMCID: PMC2752655.

47. Clements CM, McNally RS, Conti BJ, Mak TW, Ting JP. DJ-1, a cancer- and Parkinson's disease-associated protein, stabilizes the antioxidant transcriptional master regulator Nrf2. Proc Natl Acad Sci U S A. 2006; 103(41):15091–6. https://doi.org/10.1073/pnas.0607260103 PMID: 17015834; PubMed Central PMCID: PMC1586179.

48. Niemann A, Ruegg M, La Padula V, Schenone A, Suter U. Ganglioside-induced differentiation associated protein 1 is a regulator of the mitochondrial network: new implications for Charcot-Marie-Tooth disease. J Cell Biol. 2005; 170(7):1067–78. https://doi.org/10.1083/jcb.200507087 PMID: 16172208; PubMed Central PMCID: PMC2171517.

49. Carpenter K, Pollitt RJ, Middleton B. Human liver long-chain 3-hydroxyacyl-coenzyme A dehydrogenase is a multifunctional membrane-bound beta-oxidation enzyme of mitochondria. Biochem Biophys Res Commun. 1992; 183(2):443–8. https://doi.org/10.1016/0006-291x(92)90501-b PMID: 1550553.

50. Sun SC, Ma D, Li MY, Zhang RX, Huang C, Huang HJ, et al. Mutations in C1orf194, encoding a calcium regulator, cause dominant Charcot-Marie-Tooth disease. Brain. 2019; 142(8):2215–29. https://doi.org/10.1093/brain/awz151 PMID: 31199454.

51. Sasaki K, Shiba K, Nakamura A, Kawano N, Satouh Y, Yamaguchi H, et al. Calaxin is required for cilia-driven determination of vertebrate laterality. Commun Biol. 2019; 2:226. https://doi.org/10.1038/s42003-019-0462-y PMID: 31240264; PubMed Central PMCID: PMC6586612.

52. Yorikawa C, Shibata H, Waguri S, Hatta K, Horii M, Katoh K, et al. Human CHMP6, a myristoylated ESCRT-III protein, interacts directly with an ESCRT-II component EAP20 and regulates endosomal cargo sorting. Biochem J. 2005; 387(Pt 1):17–26. https://doi.org/10.1042/BJ20041227 PMID: 15511219; PubMed Central PMCID: PMC1134928.

53. Chin D, Means AR. Calmodulin: a prototypical calcium sensor. Trends Cell Biol. 2000; 10(8):322–8. https://doi.org/10.1016/s0962-8924(00)01800-6 WOS:000088382600004. PMID: 10884684

54. Zelko IN, Mariani TJ, Folz RJ. Superoxide dismutase multigene family: a comparison of the CuZn-SOD (SOD1), Mn-SOD (SOD2), and EC-SOD (SOD3) gene structures, evolution, and expression. Free Radic Biol Med. 2002; 33(3):337–49. https://doi.org/10.1016/s0891-5849(02)00905-x PMID: 12126755.

55. Schriner SE, Linford NJ, Martin GM, Treuting P, Ogburn CE, Emond M, et al. Extension of murine life span by overexpression of catalase targeted to mitochondria. Science. 2005; 308(5730):1909–11. https://doi.org/10.1126/science.1106653 WOS:000230120000040. PMID: 15879174

56. Setty SR, Tenza D, Truschel ST, Chou E, Sviderskaya EV, Theos AC, et al. BLOC-1 is required for cargo-specific sorting from vacuolar early endosomes toward lysosome-related organelles. Mol Biol Cell. 2007; 18(3):768–80. https://doi.org/10.1091/mbc.e06-12-1066 PMID: 17182842; PubMed Central PMCID: PMC1805088.

57. Cardamone MD, Tanasa B, Cederquist CT, Huang J, Mahdaviani K, Li W, et al. Mitochondrial Retrograde Signaling in Mammals Is Mediated by the Transcriptional Cofactor GPS2 via Direct Mitochondria-to-Nucleus Translocation. Mol Cell. 2018; 69(5):757–72 e7. https://doi.org/10.1016/j.molcel.2018.01.037 PMID: 29499132; PubMed Central PMCID: PMC6022402.

58. Hua T, Wu D, Ding W, Wang J, Shaw N, Liu ZJ. Studies of human 2,4-dienoyl CoA reductase shed new light on peroxisomal beta-oxidation of unsaturated fatty acids. J Biol Chem. 2012; 287

(34):28956–65. https://doi.org/10.1074/jbc.M112.385351 PMID: 22745130; PubMed Central PMCID: PMC3436514.

59. Olsen RK, Andresen BS, Christensen E, Bross P, Skovby F, Gregersen N. Clear relationship between ETF/ETFDH genotype and phenotype in patients with multiple acyl-CoA dehydrogenation deficiency. Hum Mutat. 2003; 22(1):12–23. https://doi.org/10.1002/humu.10226 PMID: 12815589.

60. Yoshihara M, Adolfsen B, Galle KT, Littleton JT. Retrograde signaling by Syt 4 induces presynaptic release and synapse-specific growth. Science. 2005; 310(5749):858–63. https://doi.org/10.1126/science.1117541 PMID: 16272123.

61. Korkut C, Li Y, Koles K, Brewer C, Ashley J, Yoshihara M, et al. Regulation of postsynaptic retrograde signaling by presynaptic exosome release. Neuron. 2013; 77(6):1039–46. https://doi.org/10.1016/j.neuron.2013.01.013 PMID: 23522040; PubMed Central PMCID: PMC3626103.

62. Chen M, Chen ZH, Wang YY, Tan Z, Zhu CZ, Li YJ, et al. Mitophagy receptor FUNDC1 regulates mitochondrial dynamics and mitophagy. Autophagy. 2016; 12(4):689–702. https://doi.org/10.1080/15548627.2016.1151580 WOS:000373983600007. PMID: 27050458

63. Yan L, Herrington J, Goldberg E, Dulski PM, Bugianesi RM, Slaughter RS, et al. Stichodactyla helianthus peptide, a pharmacological tool for studying Kv3.2 channels. Mol Pharmacol. 2005; 67(5):1513–21. https://doi.org/10.1124/mol.105.011064 PMID: 15709110.

64. Cao YL, Meng S, Chen Y, Feng JX, Gu DD, Yu B, et al. MFN1 structures reveal nucleotide-triggered dimerization critical for mitochondrial fusion. Nature. 2017; 542(7641):372–6. https://doi.org/10.1038/nature21077 PMID: 28114303; PubMed Central PMCID: PMC5319402.

65. Santel A, Fuller MT. Control of mitochondrial morphology by a human mitofusin. J Cell Sci. 2001; 114(Pt 5):867–74. 11181170. PMID: 11181170

66. Merveille AC, Davis EE, Becker-Heck A, Legendre M, Amirav I, Bataille G, et al. CCDC39 is required for assembly of inner dynein arms and the dynein regulatory complex and for normal ciliary motility in humans and dogs. Nat Genet. 2011; 43(1):72–8. https://doi.org/10.1038/ng.726 PMID: 21131972; PubMed Central PMCID: PMC3509786.

67. Bugarcic A, Zhe Y, Kerr MC, Griffin J, Collins BM, Teasdale RD. Vps26A and Vps26B subunits define distinct retromer complexes. Traffic. 2011; 12(12):1759–73. https://doi.org/10.1111/j.1600-0854.2011.01284.x PMID: 21920005.

68. Kim E, Lee Y, Lee HJ, Kim JS, Song BS, Huh JW, et al. Implication of mouse Vps26b-Vps29-Vps35 retromer complex in sortilin trafficking. Biochem Biophys Res Commun. 2010; 403(2):167–71. https://doi.org/10.1016/j.bbrc.2010.10.121 PMID: 21040701.

69. Jaillard C, Mouret A, Niepon ML, Clerin E, Yang Y, Lee-Rivera I, et al. Nxnl2 splicing results in dual functions in neuronal cell survival and maintenance of cell integrity. Hum Mol Genet. 2012; 21(10):2298–311. https://doi.org/10.1093/hmg/dds050 PMID: 22343139; PubMed Central PMCID: PMC3664437.

70. Stroud DA, Surgenor EE, Formosa LE, Reljic B, Frazier AE, Dibley MG, et al. Accessory subunits are integral for assembly and function of human mitochondrial complex I. Nature. 2016; 538(7623):123–6. https://doi.org/10.1038/nature19754 PMID: 27626371.

71. Ogilvie I, Kennaway NG, Shoubridge EA. A molecular chaperone for mitochondrial complex I assembly is mutated in a progressive encephalopathy. J Clin Invest. 2005; 115(10):2784–92. https://doi.org/10.1172/JCI26020 PMID: 16200211; PubMed Central PMCID: PMC1236688.

72. Inuzuka T, Suzuki H, Kawasaki M, Shibata H, Wakatsuki S, Maki M. Molecular basis for defect in Alix-binding by alternatively spliced isoform of ALG-2 (ALG-2DeltaGF122) and structural roles of F122 in target recognition. BMC Struct Biol. 2010; 10:25. https://doi.org/10.1186/1472-6807-10-25 PMID: 20691033; PubMed Central PMCID: PMC2927601.

73. Li Y, Jourdain AA, Calvo SE, Liu JS, Mootha VK. CLIC, a tool for expanding biological pathways based on co-expression across thousands of datasets. Plos Comput Biol. 2017; 13(7):e1005653. https://doi.org/10.1371/journal.pcbi.1005653 PMID: 28719601; PubMed Central PMCID: PMC5546725.

74. McCormack K, McCormack T, Tanouye M, Rudy B, Stuhmer W. Alternative splicing of the human Shaker K+ channel beta 1 gene and functional expression of the beta 2 gene product. FEBS Lett. 1995; 370(1–2):32–6. https://doi.org/10.1016/0014-5793(95)00785-8 PMID: 7649300.

75. Floyd BJ, Wilkerson EM, Veling MT, Minogue CE, Xia C, Beebe ET, et al. Mitochondrial Protein Interaction Mapping Identifies Regulators of Respiratory Chain Function. Mol Cell. 2016; 63(4):621–32. https://doi.org/10.1016/j.molcel.2016.06.033 PMID: 27499296; PubMed Central PMCID: PMC4992456.

76. Kondo S, Sato-Yoshitake R, Noda Y, Aizawa H, Nakata T, Matsuura Y, et al. KIF3A is a new microtubule-based anterograde motor in the nerve axon. J Cell Biol. 1994; 125(5):1095–107. https://doi.org/10.1083/jcb.125.5.1095 PMID: 7515068; PubMed Central PMCID: PMC2120052.

77. Tang SJ, Meulemans D, Vazquez L, Colaco N, Schuman E. A role for a rat homolog of staufen in the transport of RNA to neuronal dendrites. Neuron. 2001; 32(3):463–75. https://doi.org/10.1016/s0896-6273(01)00493-7 PMID: 11709157.

78. Zhang P, Wang C, Gao K, Wang D, Mao J, An J, et al. The ubiquitin ligase itch regulates apoptosis by targeting thioredoxin-interacting protein for ubiquitin-dependent degradation. J Biol Chem. 2010; 285 (12):8869–79. https://doi.org/10.1074/jbc.M109.063321 PMID: 20068034; PubMed Central PMCID: PMC2838308.

79. You F, Sun H, Zhou X, Sun W, Liang S, Zhai Z, et al. PCBP2 mediates degradation of the adaptor MAVS via the HECT ubiquitin ligase AIP4. Nat Immunol. 2009; 10(12):1300–8. https://doi.org/10.1038/ni.1815 PMID: 19881509.

80. Yamashita H, Avraham S, Jiang S, London R, Van Veldhoven PP, Subramani S, et al. Characterization of human and murine PMP20 peroxisomal proteins that exhibit antioxidant activity in vitro. J Biol Chem. 1999; 274(42):29897–904. https://doi.org/10.1074/jbc.274.42.29897 PMID: 10514471.

81. Scherer DC, Brockman JA, Chen Z, Maniatis T, Ballard DW. Signal-induced degradation of I kappa B alpha requires site-specific ubiquitination. Proc Natl Acad Sci U S A. 1995; 92(24):11259–63. https://doi.org/10.1073/pnas.92.24.11259 PMID: 7479976; PubMed Central PMCID: PMC40611.

82. Xiao C, Ghosh S. NF-kappaB, an evolutionarily conserved mediator of immune and inflammatory responses. Adv Exp Med Biol. 2005; 560:41–5. https://doi.org/10.1007/0-387-24180-9_5 PMID: 15932018.

83. Mahoney DJ, Cheung HH, Mrad RL, Plenchette S, Simard C, Enwere E, et al. Both cIAP1 and cIAP2 regulate TNFalpha-mediated NF-kappaB activation. Proc Natl Acad Sci U S A. 2008; 105(33):11778–83. https://doi.org/10.1073/pnas.0711122105 PMID: 18697935; PubMed Central PMCID: PMC2575330.

84. Bertrand MJ, Doiron K, Labbe K, Korneluk RG, Barker PA, Saleh M. Cellular inhibitors of apoptosis cIAP1 and cIAP2 are required for innate immunity signaling by the pattern recognition receptors NOD1 and NOD2. Immunity. 2009; 30(6):789–801. https://doi.org/10.1016/j.immuni.2009.04.011 PMID: 19464198.

85. Haahr P, Borgermann N, Guo X, Typas D, Achuthankutty D, Hoffmann S, et al. ZUFSP Deubiquitylates K63-Linked Polyubiquitin Chains to Promote Genome Stability. Mol Cell. 2018; 70(1):165–74 e6. https://doi.org/10.1016/j.molcel.2018.02.024 PMID: 29576528.

86. Huang F, Kirkpatrick D, Jiang X, Gygi S, Sorkin A. Differential regulation of EGF receptor internalization and degradation by multiubiquitination within the kinase domain. Mol Cell. 2006; 21(6):737–48. https://doi.org/10.1016/j.molcel.2006.02.018 PMID: 16543144.

87. Rodriguez CI, Stewart CL. Disruption of the ubiquitin ligase HERC4 causes defects in spermatozoon maturation and impaired fertility. Dev Biol. 2007; 312(2):501–8. https://doi.org/10.1016/j.ydbio.2007.09.053 PMID: 17967448.

88. Schenk G, Mitić N, Hanson GR, Comba P. Purple acid phosphatase: A journey into the function and mechanism of a colorful enzyme. Coordination Chemistry Reviews. 2013; 257(2):473–82. https://doi.org/10.1016/j.ccr.2012.03.020

89. Rienzo M, Casamassimi A. Integrator complex and transcription regulation: Recent findings and pathophysiology. Biochim Biophys Acta. 2016; 1859(10):1269–80. https://doi.org/10.1016/j.bbagrm.2016.07.008 PMID: 27427483.

90. Lai F, Gardini A, Zhang A, Shiekhattar R. Integrator mediates the biogenesis of enhancer RNAs. Nature. 2015; 525(7569):399–403. https://doi.org/10.1038/nature14906 PMID: 26308897; PubMed Central PMCID: PMC4718573.

91. Tatomer DC, Elrod ND, Liang D, Xiao MS, Jiang JZ, Jonathan M, et al. The Integrator complex cleaves nascent mRNAs to attenuate transcription. Genes Dev. 2019; 33(21–22):1525–38. https://doi.org/10.1101/gad.330167.119 PMID: 31530651; PubMed Central PMCID: PMC6824465.

92. Elrod ND, Henriques T, Huang KL, Tatomer DC, Wilusz JE, Wagner EJ, et al. The Integrator Complex Attenuates Promoter-Proximal Transcription at Protein-Coding Genes. Mol Cell. 2019; 76(5):738–52 e7. https://doi.org/10.1016/j.molcel.2019.10.034 PMID: 31809743; PubMed Central PMCID: PMC6952639.

93. Mahuran DJ. The GM2 activator protein, its roles as a co-factor in GM2 hydrolysis and as a general glycolipid transport protein. Biochim Biophys Acta. 1998; 1393(1):1–18. https://doi.org/10.1016/s0005-2760(98)00057-5 PMID: 9714704.

94. Marton MJ, Crouch D, Hinnebusch AG. GCN1, a translational activator of GCN4 in Saccharomyces cerevisiae, is required for phosphorylation of eukaryotic translation initiation factor 2 by protein kinase GCN2. Mol Cell Biol. 1993; 13(6):3541–56. https://doi.org/10.1128/mcb.13.6.3541-3556.1993 PMID: 8497269; PubMed Central PMCID: PMC359824.

95. Jones RS, Tu C, Zhang M, Qu J, Morris ME. Characterization and Proteomic-Transcriptomic Investigation of Monocarboxylate Transporter 6 Knockout Mice: Evidence of a Potential Role in Glucose and Lipid Metabolism. Mol Pharmacol. 2019; 96(3):364–76. https://doi.org/10.1124/mol.119.116731 PMID: 31436537; PubMed Central PMCID: PMC6693307.

96. Finch AJ, Hilcenko C, Basse N, Drynan LF, Goyenechea B, Menne TF, et al. Uncoupling of GTP hydrolysis from eIF6 release on the ribosome causes Shwachman-Diamond syndrome. Genes Dev. 2011; 25(9):917–29. https://doi.org/10.1101/gad.623011 PMID: 21536732. PubMed Central PMCID: PMC3084026.

97. Ito S, Horikawa S, Suzuki T, Kawauchi H, Tanaka Y, Suzuki T, et al. Human NAT10 is an ATP-dependent RNA acetyltransferase responsible for N4-acetylcytidine formation in 18 S ribosomal RNA (rRNA). J Biol Chem. 2014; 289(52):35724–30. https://doi.org/10.1074/jbc.C114.602698 PMID: 25411247; PubMed Central PMCID: PMC4276842.

98. Liu X, Tan Y, Zhang C, Zhang Y, Zhang L, Ren P, et al. NAT10 regulates p53 activation through acetylating p53 at K120 and ubiquitinating Mdm2. Embo Rep. 2016; 17(3):349–66. https://doi.org/10.15252/embr.201540505 PMID: 26882543; PubMed Central PMCID: PMC4772976.

99. Arango D, Sturgill D, Alhusaini N, Dillman AA, Sweet TJ, Hanson G, et al. Acetylation of Cytidine in mRNA Promotes Translation Efficiency. Cell. 2018; 175(7):1872–86 e24. https://doi.org/10.1016/j.cell.2018.10.030 PMID: 30449621; PubMed Central PMCID: PMC6295233.

100. Singh B, Arlinghaus RB. Mos and the cell cycle. Prog Cell Cycle Res. 1997; 3:251–9. https://doi.org/10.1007/978-1-4615-5371-7_20 PMID: 9552420.

101. Ma L, Huang Y, Song Z, Feng S, Tian X, Du W, et al. Livin promotes Smac/DIABLO degradation by ubiquitin-proteasome pathway. Cell Death Differ. 2006; 13(12):2079–88. https://doi.org/10.1038/sj.cdd.4401959 PMID: 16729033.

102. Schnell S, Demolliere C, van den Berk P, Jacobs H. Gimap4 accelerates T-cell death. Blood. 2006; 108(2):591–9. https://doi.org/10.1182/blood-2005-11-4616 PMID: 16569770.

103. Heinonen MT, Kanduri K, Lahdesmaki HJ, Lahesmaa R, Henttinen TA. Tubulin- and actin-associating GIMAP4 is required for IFN-gamma secretion during Th cell differentiation. Immunol Cell Biol. 2015; 93(2):158–66. https://doi.org/10.1038/icb.2014.86 PMID: 25287446; PubMed Central PMCID: PMC4355353.

104. Frolova L, Le Goff X, Rasmussen HH, Cheperegin S, Drugeon G, Kress M, et al. A highly conserved eukaryotic protein family possessing properties of polypeptide chain release factor. Nature. 1994; 372(6507):701–3. https://doi.org/10.1038/372701a0 PMID: 7990965.

105. Greulich W, Wagner M, Gaidt MM, Stafford C, Cheng Y, Linder A, et al. TLR8 Is a Sensor of RNase T2 Degradation Products. Cell. 2019; 179(6):1264–75 e13. https://doi.org/10.1016/j.cell.2019.11.001 PMID: 31778653.

106. Liu P, Huang J, Zheng Q, Xie L, Lu X, Jin J, et al. Mammalian mitochondrial RNAs are degraded in the mitochondrial intermembrane space by RNASET2. Protein Cell. 2017; 8(10):735–49. https://doi.org/10.1007/s13238-017-0448-9 PMID: 28730546; PubMed Central PMCID: PMC5636749.

107. Jin Y, Tan YJ, Chen LP, Liu Y, Ren ZQ. Reactive Oxygen Species Induces Lipid Droplet Accumulation in HepG2 Cells by Increasing Perilipin 2 Expression. Int J Mol Sci. 2018; 19(11). https://doi.org/10.3390/ijms19113445 WOS:000451528500161. PMID: 30400205

108. Gingras AC, Raught B, Sonenberg N. eIF4 initiation factors: effectors of mRNA recruitment to ribosomes and regulators of translation. Annu Rev Biochem. 1999; 68:913–63. https://doi.org/10.1146/annurev.biochem.68.1.913 PMID: 10872469.

109. David R. eIF4A2 helps silence mRNAs. Nat Rev Mol Cell Bio. 2013; 14(5):266–. https://doi.org/10.1038/nrm3573

110. Prieto JL, McStay B. Recruitment of factors linking transcription and processing of pre-rRNA to NOR chromatin is UBF-dependent and occurs independent of transcription in human cells. Genes Dev. 2007; 21(16):2041–54. https://doi.org/10.1101/gad.436707 PMID: 17699751; PubMed Central PMCID: PMC1948859.

111. Januszyk K, Liu Q, Lima CD. Activities of human RRP6 and structure of the human RRP6 catalytic domain. Rna. 2011; 17(8):1566–77. https://doi.org/10.1261/rna.2763111 PMID: 21705430; PubMed Central PMCID: PMC3153979.

112. Dowd S, Sneddon AA, Keyse SM. Isolation of the human genes encoding the pyst1 and Pyst2 phosphatases: characterisation of Pyst2 as a cytosolic dual-specificity MAP kinase phosphatase and its catalytic activation by both MAP and SAP kinases. J Cell Sci. 1998; 111 (Pt 22):3389–99. PMID: 9788880.

113. Yoshida Y, Yoshimi R, Yoshii H, Kim D, Dey A, Xiong H, et al. The transcription factor IRF8 activates integrin-mediated TGF-beta signaling and promotes neuroinflammation. Immunity. 2014; 40(2):187–

98. https://doi.org/10.1016/j.immuni.2013.11.022 PMID: 24485804; PubMed Central PMCID: PMC4105266.

114. Kishimoto Y, Hiraiwa M, O'Brien JS. Saposins: structure, function, distribution, and molecular genetics. J Lipid Res. 1992; 33(9):1255–67. PMID: 1402395.

115. Kaul G, Pattan G, Rafeequi T. Eukaryotic elongation factor-2 (eEF2): its regulation and peptide chain elongation. Cell Biochem Funct. 2011; 29(3):227–34. https://doi.org/10.1002/cbf.1740 PMID: 21394738.

116. Brix K, Dunkhorst A, Mayer K, Jordans S. Cysteine cathepsins: cellular roadmap to different functions. Biochimie. 2008; 90(2):194–207. https://doi.org/10.1016/j.biochi.2007.07.024 PMID: 17825974.

117. Funkelstein L, Beinfeld M, Minokadeh A, Zadina J, Hook V. Unique biological function of cathepsin L in secretory vesicles for biosynthesis of neuropeptides. Neuropeptides. 2010; 44(6):457–66. https://doi.org/10.1016/j.npep.2010.08.003 PMID: 21047684; PubMed Central PMCID: PMC3058267.

118. Trompouki E, Hatzivassiliou E, Tsichritzis T, Farmer H, Ashworth A, Mosialos G. CYLD is a deubiquitinating enzyme that negatively regulates NF-kappaB activation by TNFR family members. Nature. 2003; 424(6950):793–6. https://doi.org/10.1038/nature01803 PMID: 12917689.

119. Friedman CS O'Donnell MA, Legarda-Addison D, Ng A, Cardenas WB, Yount JS, et al. The tumour suppressor CYLD is a negative regulator of RIG-I-mediated antiviral response. Embo Rep. 2008; 9 (9):930–6. https://doi.org/10.1038/embor.2008.136 PMID: 18636086; PubMed Central PMCID: PMC2529351.

120. Nicholson DW, Ali A, Thornberry NA, Vaillancourt JP, Ding CK, Gallant M, et al. Identification and inhibition of the ICE/CED-3 protease necessary for mammalian apoptosis. Nature. 1995; 376(6535):37–43. https://doi.org/10.1038/376037a0 PMID: 7596430.

121. Tanaka Y, Suzuki G, Matsuwaki T, Hosokawa M, Serrano G, Beach TG, et al. Progranulin regulates lysosomal function and biogenesis through acidification of lysosomes. Hum Mol Genet. 2017; 26 (5):969–88. https://doi.org/10.1093/hmg/ddx011 PMID: 28073925.

122. Qin J, Qian Y, Yao J, Grace C, Li X. SIGIRR inhibits interleukin-1 receptor- and toll-like receptor 4-mediated signaling through different mechanisms. J Biol Chem. 2005; 280(26):25233–41. https://doi.org/10.1074/jbc.M501363200 PMID: 15866876.

123. Arosio P, Elia L, Poli M. Ferritin, Cellular Iron Storage and Regulation. Iubmb Life. 2017; 69(6):414–22. https://doi.org/10.1002/iub.1621 WOS:000403902700005. PMID: 28349628

124. Waterfield MR, Zhang M, Norman LP, Sun SC. NF-kappaB1/p105 regulates lipopolysaccharide-stimulated MAP kinase signaling by governing the stability and function of the Tpl2 kinase. Mol Cell. 2003; 11(3):685–94. https://doi.org/10.1016/s1097-2765(03)00070-4 PMID: 12667451.

125. Widmann B, Wandrey F, Badertscher L, Wyler E, Pfannstiel J, Zemp I, et al. The kinase activity of human Rio1 is required for final steps of cytoplasmic maturation of 40S subunits. Mol Biol Cell. 2012; 23(1):22–35. https://doi.org/10.1091/mbc.E11-07-0639 PMID: 22072790; PubMed Central PMCID: PMC3248900.

126. Chen YW, Ko WC, Chen CS, Chen PL. RIOK-1 Is a Suppressor of the p38 MAPK Innate Immune Pathway in Caenorhabditis elegans. Front Immunol. 2018; 9:774. https://doi.org/10.3389/fimmu.2018.00774 PMID: 29719537; PubMed Central PMCID: PMC5913292.

127. Baumas K, Soudet J, Caizergues-Ferrer M, Faubladier M, Henry Y, Mougin A. Human RioK3 is a novel component of cytoplasmic pre-40S pre-ribosomal particles. Rna Biol. 2012; 9(2):162–74. https://doi.org/10.4161/rna.18810 PMID: 22418843; PubMed Central PMCID: PMC3346313.

128. Feng J, De Jesus PD, Su V, Han S, Gong D, Wu NC, et al. RIOK3 is an adaptor protein required for IRF3-mediated antiviral type I interferon production. J Virol. 2014; 88(14):7987–97. https://doi.org/10.1128/JVI.00643-14 PMID: 24807708; PubMed Central PMCID: PMC4097797.

129. Shan J, Wang P, Zhou J, Wu D, Shi H, Huo K. RIOK3 interacts with caspase-10 and negatively regulates the NF-kappaB signaling pathway. Mol Cell Biochem. 2009; 332(1–2):113–20. https://doi.org/10.1007/s11010-009-0180-8 PMID: 19557502.

130. Takashima K, Oshiumi H, Takaki H, Matsumoto M, Seya T. RIOK3-mediated phosphorylation of MDA5 interferes with its assembly and attenuates the innate immune response. Cell Rep. 2015; 11 (2):192–200. https://doi.org/10.1016/j.celrep.2015.03.027 PMID: 25865883.

131. Kadoya T, Khurana A, Tcherpakov M, Bromberg KD, Didier C, Broday L, et al. JAMP, a Jun N-terminal kinase 1 (JNK1)-associated membrane protein, regulates duration of JNK activity. Mol Cell Biol. 2005; 25(19):8619–30. https://doi.org/10.1128/MCB.25.19.8619-8630.2005 PMID: 16166642; PubMed Central PMCID: PMC1265750.

132. Mauro C, Pacifico F, Lavorgna A, Mellone S, Iannetti A, Acquaviva R, et al. ABIN-1 binds to NEMO/IKKgamma and co-operates with A20 in inhibiting NF-kappaB. J Biol Chem. 2006; 281(27):18482–8. https://doi.org/10.1074/jbc.M601502200 PMID: 16684768.

133. Ashida H, Kim M, Schmidt-Supprian M, Ma A, Ogawa M, Sasakawa C. A bacterial E3 ubiquitin ligase IpaH9.8 targets NEMO/IKKgamma to dampen the host NF-kappaB-mediated inflammatory response. Nat Cell Biol. 2010; 12(1):66–73; sup pp 1–9. https://doi.org/10.1038/ncb2006 PMID: 20010814; PubMed Central PMCID: PMC3107189.

134. McCallum KC, Garsin DA. The Role of Reactive Oxygen Species in Modulating the Caenorhabditis elegans Immune Response. Plos Pathog. 2016; 12(11):e1005923. https://doi.org/10.1371/journal.ppat.1005923 PMID: 27832190; PubMed Central PMCID: PMC5104326.

135. Zhang K, Shen X, Wu J, Sakaki K, Saunders T, Rutkowski DT, et al. Endoplasmic reticulum stress activates cleavage of CREBH to induce a systemic inflammatory response. Cell. 2006; 124(3):587–99. https://doi.org/10.1016/j.cell.2005.11.040 PMID: 16469704.

136. Tu H, Nelson O, Bezprozvanny A, Wang Z, Lee SF, Hao YH, et al. Presenilins form ER Ca2+ leak channels, a function disrupted by familial Alzheimer's disease-linked mutations. Cell. 2006; 126 (5):981–93. https://doi.org/10.1016/j.cell.2006.06.059 PMID: 16959576; PubMed Central PMCID: PMC3241869.

137. Zampese E, Fasolato C, Kipanyula MJ, Bortolozzi M, Pozzan T, Pizzo P. Presenilin 2 modulates endoplasmic reticulum (ER)-mitochondria interactions and Ca2+ cross-talk. Proc Natl Acad Sci U S A. 2011; 108(7):2777–82. https://doi.org/10.1073/pnas.1100735108 PMID: 21285369; PubMed Central PMCID: PMC3041131.

138. Chen JM, Dando PM, Stevens RA, Fortunato M, Barrett AJ. Cloning and expression of mouse legumain, a lysosomal endopeptidase. Biochem J. 1998; 335 (Pt 1):111–7. https://doi.org/10.1042/bj3350111 PMID: 9742219; PubMed Central PMCID: PMC1219758.

139. Rozpedek W, Pytel D, Mucha B, Leszczynska H, Diehl JA, Majsterek I. The Role of the PERK/eIF2alpha/ATF4/CHOP Signaling Pathway in Tumor Progression During Endoplasmic Reticulum Stress. Curr Mol Med. 2016; 16(6):533–44. https://doi.org/10.2174/1566524016666160523143937 PMID: 27211800; PubMed Central PMCID: PMC5008685.

140. Miyara A, Ohta A, Okochi Y, Tsukada Y, Kuhara A, Mori I. Novel and conserved protein macoilin is required for diverse neuronal functions in Caenorhabditis elegans. PLoS Genet. 2011; 7(5):e1001384. https://doi.org/10.1371/journal.pgen.1001384 PMID: 21589894; PubMed Central PMCID: PMC3093358.

141. Xie X, Wang X, Jiang D, Wang J, Fei R, Cong X, et al. PPPDE1 is a novel deubiquitinase belonging to a cysteine isopeptidase family. Biochem Biophys Res Commun. 2017; 488(2):291–6. https://doi.org/10.1016/j.bbrc.2017.04.161 PMID: 28483520.

142. Ban N, Matsumura Y, Sakai H, Takanezawa Y, Sasaki M, Arai H, et al. ABCA3 as a lipid transporter in pulmonary surfactant biogenesis. J Biol Chem. 2007; 282(13):9628–34. https://doi.org/10.1074/jbc.M611767200 PMID: 17267394.

143. Zhang X, Lei K, Yuan X, Wu X, Zhuang Y, Xu T, et al. SUN1/2 and Syne/Nesprin-1/2 complexes connect centrosome to the nucleus during neurogenesis and neuronal migration in mice. Neuron. 2009; 64(2):173–87. https://doi.org/10.1016/j.neuron.2009.08.018 PMID: 19874786; PubMed Central PMCID: PMC2788510.

144. Ding X, Xu R, Yu J, Xu T, Zhuang Y, Han M. SUN1 is required for telomere attachment to nuclear envelope and gametogenesis in mice. Dev Cell. 2007; 12(6):863–72. https://doi.org/10.1016/j.devcel.2007.03.018 PMID: 17543860.

145. Gijon MA, Riekhof WR, Zarini S, Murphy RC, Voelker DR. Lysophospholipid acyltransferases and arachidonate recycling in human neutrophils. J Biol Chem. 2008; 283(44):30235–45. https://doi.org/10.1074/jbc.M806194200 PMID: 18772128; PubMed Central PMCID: PMC2573059.

146. Lee HC, Inoue T, Imae R, Kono N, Shirae S, Matsuda S, et al. Caenorhabditis elegans mboa-7, a member of the MBOAT family, is required for selective incorporation of polyunsaturated fatty acids into phosphatidylinositol. Mol Biol Cell. 2008; 19(3):1174–84. https://doi.org/10.1091/mbc.e07-09-0893 PMID: 18094042; PubMed Central PMCID: PMC2262980.

147. Wu YJ, La Pierre DP, Wu J, Yee AJ, Yang BB. The interaction of versican with its binding partners. Cell Res. 2005; 15(7):483–94. https://doi.org/10.1038/sj.cr.7290318 PMID: 16045811.

148. Wight TN, Kang I, Merrilees MJ. Versican and the control of inflammation. Matrix Biol. 2014; 35:152–61. https://doi.org/10.1016/j.matbio.2014.01.015 PMID: 24513039; PubMed Central PMCID: PMC4039577.

149. Zhang Q, Didonato JA, Karin M, McKeithan TW. BCL3 encodes a nuclear protein which can alter the subcellular location of NF-kappa B proteins. Mol Cell Biol. 1994; 14(6):3915–26. https://doi.org/10.1128/mcb.14.6.3915-3926.1994 PMID: 8196632; PubMed Central PMCID: PMC358758.

150. Bundy DL, McKeithan TW. Diverse effects of BCL3 phosphorylation on its modulation of NF-kappaB p52 homodimer binding to DNA. J Biol Chem. 1997; 272(52):33132–9. https://doi.org/10.1074/jbc.272.52.33132 PMID: 9407099.

151. Mogha A, Benesh AE, Patra C, Engel FB, Schoneberg T, Liebscher I, et al. Gpr126 functions in Schwann cells to control differentiation and myelination via G-protein activation. J Neurosci. 2013; 33 (46):17976–85. https://doi.org/10.1523/JNEUROSCI.1809-13.2013 PMID: 24227709; PubMed Central PMCID: PMC3828454.

152. McNally KE, Faulkner R, Steinberg F, Gallon M, Ghai R, Pim D, et al. Retriever is a multiprotein complex for retromer-independent endosomal cargo recycling. Nat Cell Biol. 2017; 19(10):1214–25. https://doi.org/10.1038/ncb3610 PMID: 28892079; PubMed Central PMCID: PMC5790113.

153. Ruiz-Canada C, Kelleher DJ, Gilmore R. Cotranslational and posttranslational N-glycosylation of polypeptides by distinct mammalian OST isoforms. Cell. 2009; 136(2):272–83. https://doi.org/10.1016/j.cell.2008.11.047 PMID: 19167329; PubMed Central PMCID: PMC2859625.

154. Sato T, Sako Y, Sho M, Momohara M, Suico MA, Shuto T, et al. STT3B-dependent posttranslational N-glycosylation as a surveillance system for secretory protein. Mol Cell. 2012; 47(1):99–110. https://doi.org/10.1016/j.molcel.2012.04.015 PMID: 22607976.

155. Riemer J, Hansen HG, Appenzeller-Herzog C, Johansson L, Ellgaard L. Identification of the PDI-family member ERp90 as an interaction partner of ERFAD. Plos One. 2011; 6(2):e17037. https://doi.org/10.1371/journal.pone.0017037 PMID: 21359175; PubMed Central PMCID: PMC3040216.

156. Harz C, Ludwig N, Lang S, Werner TV, Galata V, Backes C, et al. Secretion and immunogenicity of the meningioma-associated antigen TXNDC16. J Immunol. 2014; 193(6):3146–54. https://doi.org/10.4049/jimmunol.1303098 PMID: 25122923.

157. Arnold SM, Fessler LI, Fessler JH, Kaufman RJ. Two homologues encoding human UDP-glucose:glycoprotein glucosyltransferase differ in mRNA expression and enzymatic activity. Biochemistry. 2000; 39(9):2149–63. https://doi.org/10.1021/bi9916473 PMID: 10694380.

158. Erdile LF, Wold MS, Kelly TJ. The primary structure of the 32-kDa subunit of human replication protein A. J Biol Chem. 1990; 265(6):3177–82. PMID: 2406247.

159. Sleeth KM, Sorensen CS, Issaeva N, Dziegielewski J, Bartek J, Helleday T. RPA mediates recombination repair during replication stress and is displaced from DNA by checkpoint signalling in human cells. J Mol Biol. 2007; 373(1):38–47. https://doi.org/10.1016/j.jmb.2007.07.068 PMID: 17765923.

160. He Z, Henricksen LA, Wold MS, Ingles CJ. RPA involvement in the damage-recognition and incision steps of nucleotide excision repair. Nature. 1995; 374(6522):566–9. https://doi.org/10.1038/374566a0 PMID: 7700386.

161. Kawai T, Akira S. Regulation of innate immune signalling pathways by the tripartite motif (TRIM) family proteins. EMBO Mol Med. 2011; 3(9):513–27. https://doi.org/10.1002/emmm.201100160 PMID: 21826793; PubMed Central PMCID: PMC3377094.

162. Wang M, Wu J, Zhou E, Chang X, Gan J, Cheng T. Forkhead box o3a suppresses lipopolysaccharide-stimulated proliferation and inflammation in fibroblast-like synoviocytes through regulating tripartite motif-containing protein 3. J Cell Physiol. 2019; 234(11):20139–48. https://doi.org/10.1002/jcp.28615 PMID: 30980385.

163. Xiong F, Ji Z, Liu Y, Zhang Y, Hu L, Yang Q, et al. Mutation in SSUH2 Causes Autosomal-Dominant Dentin Dysplasia Type I. Hum Mutat. 2017; 38(1):95–104. https://doi.org/10.1002/humu.23130 PMID: 27680507.

164. Schreiber J, Vegh MJ, Dawitz J, Kroon T, Loos M, Labonte D, et al. Ubiquitin ligase TRIM3 controls hippocampal plasticity and learning by regulating synaptic gamma-actin levels. J Cell Biol. 2015; 211 (3):569–86. https://doi.org/10.1083/jcb.201506048 PMID: 26527743. PubMed Central PMCID: PMC4639863.

165. MacPherson L, Tamblyn L, Rajendra S, Bralha F, McPherson JP, Matthews J. 2,3,7,8-Tetrachlorodibenzo-p-dioxin poly(ADP-ribose) polymerase (TiPARP, ARTD14) is a mono-ADP-ribosyltransferase and repressor of aryl hydrocarbon receptor transactivation. Nucleic Acids Res. 2013; 41(3):1604–21. https://doi.org/10.1093/nar/gks1337 PMID: 23275542; PubMed Central PMCID: PMC3562000.

166. Yamada T, Horimoto H, Kameyama T, Hayakawa S, Yamato H, Dazai M, et al. Constitutive aryl hydrocarbon receptor signaling constrains type I interferon-mediated antiviral innate defense. Nat Immunol. 2016; 17(6):687–94. https://doi.org/10.1038/ni.3422 PMID: 27089381.

167. Kozaki T, Komano J, Kanbayashi D, Takahama M, Misawa T, Satoh T, et al. Mitochondrial damage elicits a TCDD-inducible poly(ADP-ribose) polymerase-mediated antiviral response. Proc Natl Acad Sci U S A. 2017; 114(10):2681–6. https://doi.org/10.1073/pnas.1621508114 PMID: 28213497; PubMed Central PMCID: PMC5347618.

168. Goldshmit Y, Walters CE, Scott HJ, Greenhalgh CJ, Turnley AM. SOCS2 induces neurite outgrowth by regulation of epidermal growth factor receptor activation. J Biol Chem. 2004; 279(16):16349–55. https://doi.org/10.1074/jbc.M312873200 PMID: 14764607.

169. Letellier E, Haan S. SOCS2: physiological and pathological functions. Front Biosci (Elite Ed). 2016; 8:189–204. PMID: 26709655.

170. Kazi JU, Ronnstrand L. Suppressor of cytokine signaling 2 (SOCS2) associates with FLT3 and negatively regulates downstream signaling. Mol Oncol. 2013; 7(3):693–703. https://doi.org/10.1016/j.molonc.2013.02.020 PMID: 23548639; PubMed Central PMCID: PMC5528470.

171. Tiranti V, Rossi E, Ruiz-Carrillo A, Rossi G, Rocchi M, DiDonato S, et al. Chromosomal localization of mitochondrial transcription factor A (TCF6), single-stranded DNA-binding protein (SSBP), and endonuclease G (ENDOG), three human housekeeping genes involved in mitochondrial biogenesis. Genomics. 1995; 25(2):559–64. https://doi.org/10.1016/0888-7543(95)80058-t PMID: 7789991.

172. Duguay BA, Smiley JR. Mitochondrial nucleases ENDOG and EXOG participate in mitochondrial DNA depletion initiated by herpes simplex virus 1 UL12.5. J Virol. 2013; 87(21):11787–97. https://doi.org/10.1128/JVI.02306-13 PMID: 23986585; PubMed Central PMCID: PMC3807374.

173. Zhdanov DD, Fahmi T, Wang X, Apostolov EO, Sokolov NN, Javadov S, et al. Regulation of Apoptotic Endonucleases by EndoG. DNA Cell Biol. 2015; 34(5):316–26. https://doi.org/10.1089/dna.2014.2772 PMID: 25849439; PubMed Central PMCID: PMC4426297.

174. Kim JS, Lee JH, Jeong WW, Choi DH, Cha HJ, Kim DH, et al. Reactive oxygen species-dependent EndoG release mediates cisplatin-induced caspase-independent apoptosis in human head and neck squamous carcinoma cells. Int J Cancer. 2008; 122(3):672–80. https://doi.org/10.1002/ijc.23158 PMID: 17955488.

175. Kirino Y, Mourelatos Z. 2'-O-methyl modification in mouse piRNAs and its methylase. Nucleic Acids Symp Ser (Oxf). 2007;(51):417–8. https://doi.org/10.1093/nass/nrm209 PMID: 18029764.

176. Hu D, Smith ER, Garruss AS, Mohaghegh N, Varberg JM, Lin C, et al. The little elongation complex functions at initiation and elongation phases of snRNA gene transcription. Mol Cell. 2013; 51(4):493–505. https://doi.org/10.1016/j.molcel.2013.07.003 PMID: 23932780; PubMed Central PMCID: PMC4104523.

177. Paclik D, Danese S, Berndt U, Wiedenmann B, Dignass A, Sturm A. Galectin-4 controls intestinal inflammation by selective regulation of peripheral and mucosal T cell apoptosis and cell cycle. Plos One. 2008; 3(7):e2629. https://doi.org/10.1371/journal.pone.0002629 PMID: 18612433; PubMed Central PMCID: PMC2440804.

178. Stancic M, Slijepcevic D, Nomden A, Vos MJ, de Jonge JC, Sikkema AH, et al. Galectin-4, a novel neuronal regulator of myelination. Glia. 2012; 60(6):919–35. https://doi.org/10.1002/glia.22324 PMID: 22431161.

179. Chen YQ, Rafi MA, de Gala G, Wenger DA. Cloning and expression of cDNA encoding human galactocerebrosidase, the enzyme deficient in globoid cell leukodystrophy. Hum Mol Genet. 1993; 2 (11):1841–5. https://doi.org/10.1093/hmg/2.11.1841 PMID: 8281145.

180. Wang W, Xue Y, Zhou S, Kuo A, Cairns BR, Crabtree GR. Diversity and specialization of mammalian SWI/SNF complexes. Genes Dev. 1996; 10(17):2117–30. https://doi.org/10.1101/gad.10.17.2117 PMID: 8804307.

181. Chi T. A BAF-centred view of the immune system. Nat Rev Immunol. 2004; 4(12):965–77. https://doi.org/10.1038/nri1501 PMID: 15573131.

182. Kim YH, Lee JR, Hahn MJ. Regulation of inflammatory gene expression in macrophages by epithelial-stromal interaction 1 (Epsti1). Biochem Biophys Res Commun. 2018; 496(2):778–83. https://doi.org/10.1016/j.bbrc.2017.12.014 PMID: 29217193.

183. Woitach JT, Zhang M, Niu CH, Thorgeirsson SS. A retinoblastoma-binding protein that affects cell-cycle control and confers transforming ability. Nat Genet. 1998; 19(4):371–4. https://doi.org/10.1038/1258 PMID: 9697699.

184. Lin YL, Shivji MK, Chen C, Kolodner R, Wood RD, Dutta A. The evolutionarily conserved zinc finger motif in the largest subunit of human replication protein A is required for DNA replication and mismatch repair but not for nucleotide excision repair. J Biol Chem. 1998; 273(3):1453–61. https://doi.org/10.1074/jbc.273.3.1453 PMID: 9430682.

185. Zheng K, Xiol J, Reuter M, Eckardt S, Leu NA, McLaughlin KJ, et al. Mouse MOV10L1 associates with Piwi proteins and is an essential component of the Piwi-interacting RNA (piRNA) pathway. Proc Natl Acad Sci U S A. 2010; 107(26):11841–6. https://doi.org/10.1073/pnas.1003953107 PMID: 20534472; PubMed Central PMCID: PMC2900664.

186. Roshanbin S, Lindberg FA, Lekholm E, Eriksson MM, Perland E, Ahlund J, et al. Histological characterization of orphan transporter MCT14 (SLC16A14) shows abundant expression in mouse CNS and kidney. Bmc Neurosci. 2016; 17(1):43. https://doi.org/10.1186/s12868-016-0274-7 PMID: 27364523; PubMed Central PMCID: PMC4929735.

187. Weon JL, Yang SW, Potts PR. Cytosolic Iron-Sulfur Assembly Is Evolutionarily Tuned by a Cancer-Amplified Ubiquitin Ligase. Mol Cell. 2018; 69(1):113–25 e6. https://doi.org/10.1016/j.molcel.2017.11.010 PMID: 29225034.

188. Shi Y, Yuan B, Zhu W, Zhang R, Li L, Hao X, et al. Ube2D3 and Ube2N are essential for RIG-I-mediated MAVS aggregation in antiviral innate immunity. Nat Commun. 2017; 8:15138. https://doi.org/10.1038/ncomms15138 PMID: 28469175; PubMed Central PMCID: PMC5418627.

189. Ogami K, Cho R, Hoshino S. Molecular cloning and characterization of a novel isoform of the non-canonical poly(A) polymerase PAPD7. Biochem Biophys Res Commun. 2013; 432(1):135–40. https://doi.org/10.1016/j.bbrc.2013.01.072 PMID: 23376078.

190. Lim J, Kim D, Lee YS, Ha M, Lee M, Yeo J, et al. Mixed tailing by TENT4A and TENT4B shields mRNA from rapid deadenylation. Science. 2018; 361(6403):701–4. https://doi.org/10.1126/science.aam5794 PMID: 30026317.

191. McCormack RM, de Armas LR, Shiratsuchi M, Fiorentino DG, Olsson ML, Lichtenheld MG, et al. Perforin-2 is essential for intracellular defense of parenchymal cells and phagocytes against pathogenic bacteria. Elife. 2015;4. https://doi.org/10.7554/eLife.06508 PMID: 26402460; PubMed Central PMCID: PMC4626811.

192. Uyama T, Jin XH, Tsuboi K, Tonai T, Ueda N. Characterization of the human tumor suppressors TIG3 and HRASLS2 as phospholipid-metabolizing enzymes. Biochim Biophys Acta. 2009; 1791(12):1114–24. https://doi.org/10.1016/j.bbalip.2009.07.001 PMID: 19615464.

193. Staring J, von Castelmur E, Blomen VA, van den Hengel LG, Brockmann M, Baggen J, et al. PLA2G16 represents a switch between entry and clearance of Picornaviridae. Nature. 2017; 541 (7637):412–6. https://doi.org/10.1038/nature21032 PMID: 28077878.

194. Kraemer D, Wozniak RW, Blobel G, Radu A. The human CAN protein, a putative oncogene product associated with myeloid leukemogenesis, is a nuclear pore complex protein that faces the cytoplasm. Proc Natl Acad Sci U S A. 1994; 91(4):1519–23. https://doi.org/10.1073/pnas.91.4.1519 PMID: 8108440; PubMed Central PMCID: PMC43191.

195. Fornerod M, van Deursen J, van Baal S, Reynolds A, Davis D, Murti KG, et al. The human homologue of yeast CRM1 is in a dynamic subcomplex with CAN/Nup214 and a novel nuclear pore component Nup88. Embo J. 1997; 16(4):807–16. https://doi.org/10.1093/emboj/16.4.807 PMID: 9049309; PubMed Central PMCID: PMC1169681.

196. Ustianenko D, Hrossova D, Potesil D, Chalupnikova K, Hrazdilova K, Pachernik J, et al. Mammalian DIS3L2 exoribonuclease targets the uridylated precursors of let-7 miRNAs. Rna. 2013; 19(12):1632–8. https://doi.org/10.1261/rna.040055.113 PMID: 24141620; PubMed Central PMCID: PMC3884668.

197. Lubas M, Damgaard CK, Tomecki R, Cysewski D, Jensen TH, Dziembowski A. Exonuclease hDIS3L2 specifies an exosome-independent 3'-5' degradation pathway of human cytoplasmic mRNA. Embo J. 2013; 32(13):1855–68. https://doi.org/10.1038/emboj.2013.135 PMID: 23756462; PubMed Central PMCID: PMC3981170.

198. Iwata H, Goettsch C, Sharma A, Ricchiuto P, Goh WW, Halu A, et al. PARP9 and PARP14 cross-regulate macrophage activation via STAT1 ADP-ribosylation. Nat Commun. 2016; 7:12849. https://doi.org/10.1038/ncomms12849 PMID: 27796300; PubMed Central PMCID: PMC5095532.

199. Capitanio JS, Montpetit B, Wozniak RW. Human Nup98 regulates the localization and activity of DExH/D-box helicase DHX9. Elife. 2017;6. https://doi.org/10.7554/eLife.18825 PMID: 28221134; PubMed Central PMCID: PMC5338925.

200. Weston R, Peeters H, Ahel D. ZRANB3 is a structure-specific ATP-dependent endonuclease involved in replication stress response. Genes Dev. 2012; 26(14):1558–72. https://doi.org/10.1101/gad.193516.112 PMID: 22759634; PubMed Central PMCID: PMC3404384.

201. Ciccia A, Nimonkar AV, Hu Y, Hajdu I, Achar YJ, Izhar L, et al. Polyubiquitinated PCNA recruits the ZRANB3 translocase to maintain genomic integrity after replication stress. Mol Cell. 2012; 47(3):396–409. https://doi.org/10.1016/j.molcel.2012.05.024 PMID: 22704558; PubMed Central PMCID: PMC3613862.

202. Sakatsume M, Igarashi K, Winestock KD, Garotta G, Larner AC, Finbloom DS. The Jak kinases differentially associate with the alpha and beta (accessory factor) chains of the interferon gamma receptor to form a functional receptor unit capable of activating STAT transcription factors. J Biol Chem. 1995; 270(29):17528–34. https://doi.org/10.1074/jbc.270.29.17528 PMID: 7615558.

203. Segura-Totten M, Kowalski AK, Craigie R, Wilson KL. Barrier-to-autointegration factor: major roles in chromatin decondensation and nuclear assembly. J Cell Biol. 2002; 158(3):475–85. https://doi.org/10.1083/jcb.200202019 PMID: 12163470; PubMed Central PMCID: PMC2173821.

204. Wiebe MS, Traktman P. Poxviral B1 kinase overcomes barrier to autointegration factor, a host defense against virus replication. Cell Host Microbe. 2007; 1(3):187–97. https://doi.org/10.1016/j.chom.2007.03.007 PMID: 18005698; PubMed Central PMCID: PMC1978190.

205. Mazur DJ, Perrino FW. Excision of 3' termini by the Trex1 and TREX2 3'—>5' exonucleases. Characterization of the recombinant proteins. J Biol Chem. 2001; 276(20):17022–9. https://doi.org/10.1074/jbc.M100623200 PMID: 11279105.

206. Schneider M, Hellerschmied D, Schubert T, Amlacher S, Vinayachandran V, Reja R, et al. The Nuclear Pore-Associated TREX-2 Complex Employs Mediator to Regulate Gene Expression. Cell. 2015; 162(5):1016–28. https://doi.org/10.1016/j.cell.2015.07.059 PMID: 26317468; PubMed Central PMCID: PMC4644235.

207. Garcia-Oliver E, Garcia-Molinero V, Rodriguez-Navarro S. mRNA export and gene expression: the SAGA-TREX-2 connection. Biochim Biophys Acta. 2012; 1819(6):555–65. https://doi.org/10.1016/j.bbagrm.2011.11.011 PMID: 22178374.

208. Nichols RJ, Wiebe MS, Traktman P. The vaccinia-related kinases phosphorylate the N' terminus of BAF, regulating its interaction with DNA and its retention in the nucleus. Mol Biol Cell. 2006; 17 (5):2451–64. https://doi.org/10.1091/mbc.e05-12-1179 PMID: 16495336; PubMed Central PMCID: PMC1446082.

209. Sevilla A, Santos CR, Vega FM, Lazo PA. Human vaccinia-related kinase 1 (VRK1) activates the ATF2 transcriptional activity by novel phosphorylation on Thr-73 and Ser-62 and cooperates with JNK. J Biol Chem. 2004; 279(26):27458–65. https://doi.org/10.1074/jbc.M401009200 PMID: 15105425.

210. Watkins JL, Murphy R, Emtage JL, Wente SR. The human homologue of Saccharomyces cerevisiae Gle1p is required for poly(A)+ RNA export. Proc Natl Acad Sci U S A. 1998; 95(12):6779–84. https://doi.org/10.1073/pnas.95.12.6779 PMID: 9618489; PubMed Central PMCID: PMC22633.

211. Jiao X, Chang JH, Kilic T, Tong L, Kiledjian M. A mammalian pre-mRNA 5' end capping quality control mechanism and an unexpected link of capping to pre-mRNA processing. Mol Cell. 2013; 50(1):104–15. https://doi.org/10.1016/j.molcel.2013.02.017 PMID: 23523372; PubMed Central PMCID: PMC3630477.

212. Bonnin E, Cabochette P, Filosa A, Juhlen R, Komatsuzaki S, Hezwani M, et al. Biallelic mutations in nucleoporin NUP88 cause lethal fetal akinesia deformation sequence. PLoS Genet. 2018; 14(12): e1007845. https://doi.org/10.1371/journal.pgen.1007845 PMID: 30543681; PubMed Central PMCID: PMC6307818.

213. Tomecki R, Dmochowska A, Gewartowski K, Dziembowski A, Stepien PP. Identification of a novel human nuclear-encoded mitochondrial poly(A) polymerase. Nucleic Acids Res. 2004; 32(20):6001–14. https://doi.org/10.1093/nar/gkh923 PMID: 15547249; PubMed Central PMCID: PMC534615.

214. Nagaike T, Suzuki T, Katoh T, Ueda T. Human mitochondrial mRNAs are stabilized with polyadenylation regulated by mitochondria-specific poly(A) polymerase and polynucleotide phosphorylase. J Biol Chem. 2005; 280(20):19721–7. https://doi.org/10.1074/jbc.M500804200 PMID: 15769737.

215. Mullen TE, Marzluff WF. Degradation of histone mRNA requires oligouridylation followed by decapping and simultaneous degradation of the mRNA both 5' to 3' and 3' to 5'. Genes Dev. 2008; 22(1):50–65. https://doi.org/10.1101/gad.1622708 PMID: 18172165; PubMed Central PMCID: PMC2151014.

216. Antonicka H, Choquet K, Lin ZY, Gingras AC, Kleinman CL, Shoubridge EA. A pseudouridine synthase module is essential for mitochondrial protein synthesis and cell viability. Embo Rep. 2017; 18 (1):28–38. https://doi.org/10.15252/embr.201643391 PMID: 27974379; PubMed Central PMCID: PMC5210091.

217. Arroyo JD, Jourdain AA, Calvo SE, Ballarano CA, Doench JG, Root DE, et al. A Genome-wide CRISPR Death Screen Identifies Genes Essential for Oxidative Phosphorylation. Cell Metab. 2016; 24 (6):875–85. https://doi.org/10.1016/j.cmet.2016.08.017 PMID: 27667664; PubMed Central PMCID: PMC5474757.

218. Saunders A, Webb LM, Janas ML, Hutchings A, Pascall J, Carter C, et al. Putative GTPase GIMAP1 is critical for the development of mature B and T lymphocytes. Blood. 2010; 115(16):3249–57. https://doi.org/10.1182/blood-2009-08-237586 PMID: 20194894.

219. Deveraux QL, Takahashi R, Salvesen GS, Reed JC. X-linked IAP is a direct inhibitor of cell-death proteases. Nature. 1997; 388(6639):300–4. https://doi.org/10.1038/40901 PMID: 9230442.

220. Lu M, Lin SC, Huang Y, Kang YJ, Rich R, Lo YC, et al. XIAP induces NF-kappaB activation via the BIR1/TAB1 interaction and BIR1 dimerization. Mol Cell. 2007; 26(5):689–702. https://doi.org/10.1016/j.molcel.2007.05.006 PMID: 17560374; PubMed Central PMCID: PMC1991276.

221. Isken A, Golczak M, Oberhauser V, Hunzelmann S, Driever W, Imanishi Y, et al. RBP4 disrupts vitamin A uptake homeostasis in a STRA6-deficient animal model for Matthew-Wood syndrome. Cell Metab. 2008; 7(3):258–68. https://doi.org/10.1016/j.cmet.2008.01.009 PMID: 18316031; PubMed Central PMCID: PMC2561276.

222. Wang Y, Yuan S, Jia X, Ge Y, Ling T, Nie M, et al. Mitochondria-localised ZNFX1 functions as a dsRNA sensor to initiate antiviral responses through MAVS. Nat Cell Biol. 2019; 21(11):1346–56. https://doi.org/10.1038/s41556-019-0416-0 PMID: 31685995.

223. Ishidate T, Ozturk AR, Durning DJ, Sharma R, Shen EZ, Chen H, et al. ZNFX-1 Functions within Perinuclear Nuage to Balance Epigenetic Signals. Mol Cell. 2018; 70(4):639–49 e6. https://doi.org/10.1016/j.molcel.2018.04.009 PMID: 29775580; PubMed Central PMCID: PMC5994929.

224. Takeyama K, Aguiar RC, Gu L, He C, Freeman GJ, Kutok JL, et al. The BAL-binding protein BBAP and related Deltex family members exhibit ubiquitin-protein isopeptide ligase activity. J Biol Chem. 2003; 278(24):21930–7. https://doi.org/10.1074/jbc.M301157200 PMID: 12670957.

225. Yan Q, Dutt S, Xu R, Graves K, Juszczynski P, Manis JP, et al. BBAP monoubiquitylates histone H4 at lysine 91 and selectively modulates the DNA damage response. Mol Cell. 2009; 36(1):110–20. https://doi.org/10.1016/j.molcel.2009.08.019 PMID: 19818714; PubMed Central PMCID: PMC2913878.

226. Zhang Y, Mao D, Roswit WT, Jin X, Patel AC, Patel DA, et al. PARP9-DTX3L ubiquitin ligase targets host histone H2BJ and viral 3C protease to enhance interferon signaling and control viral infection. Nat Immunol. 2015; 16(12):1215–27. https://doi.org/10.1038/ni.3279 PMID: 26479788; PubMed Central PMCID: PMC4653074.

227. Liu J, McFadden G. SAMD9 is an innate antiviral host factor with stress response properties that can be antagonized by poxviruses. J Virol. 2015; 89(3):1925–31. https://doi.org/10.1128/JVI.02262-14 PMID: 25428864; PubMed Central PMCID: PMC4300762.

228. Carney JP, Maser RS, Olivares H, Davis EM, Le Beau M, Yates JR, 3rd, et al. The hMre11/hRad50 protein complex and Nijmegen breakage syndrome: linkage of double-strand break repair to the cellular DNA damage response. Cell. 1998; 93(3):477–86. https://doi.org/10.1016/s0092-8674(00)81175-7 PMID: 9590181.

229. Kondo T, Kobayashi J, Saitoh T, Maruyama K, Ishii KJ, Barber GN, et al. DNA damage sensor MRE11 recognizes cytosolic double-stranded DNA and induces type I interferon by regulating STING trafficking. Proc Natl Acad Sci U S A. 2013; 110(8):2969–74. https://doi.org/10.1073/pnas.1222694110 PMID: 23388631; PubMed Central PMCID: PMC3581880.

230. Irudayam JI, Contreras D, Spurka L, Subramanian A, Allen J, Ren S, et al. Characterization of type I interferon pathway during hepatic differentiation of human pluripotent stem cells and hepatitis C virus infection. Stem Cell Res. 2015; 15(2):354–64. https://doi.org/10.1016/j.scr.2015.08.003 PMID: 26313525; PubMed Central PMCID: PMC4600668.

231. Lim J, Ha M, Chang H, Kwon SC, Simanshu DK, Patel DJ, et al. Uridylation by TUT4 and TUT7 marks mRNA for degradation. Cell. 2014; 159(6):1365–76. https://doi.org/10.1016/j.cell.2014.10.055 PMID: 25480299; PubMed Central PMCID: PMC4720960.

232. Le Pen J, Jiang H, Di Domenico T, Kneuss E, Kosalka J, Leung C, et al. Terminal uridylyltransferases target RNA viruses as part of the innate immune system. Nat Struct Mol Biol. 2018; 25(9):778–86. https://doi.org/10.1038/s41594-018-0106-9 PMID: 30104661; PubMed Central PMCID: PMC6130846.

233. Torii S, Kusakabe M, Yamamoto T, Maekawa M, Nishida E. Sef is a spatial regulator for Ras/MAP kinase signaling. Dev Cell. 2004; 7(1):33–44. https://doi.org/10.1016/j.devcel.2004.05.019 PMID: 15239952.

234. Mellett M, Atzei P, Bergin R, Horgan A, Floss T, Wurst W, et al. Orphan receptor IL-17RD regulates Toll-like receptor signalling via SEFIR/TIR interactions. Nat Commun. 2015; 6:6669. https://doi.org/10.1038/ncomms7669 PMID: 25808990.

235. Wang Y, Satoh A, Warren G, Meyer HH. VCIP135 acts as a deubiquitinating enzyme during p97-p47-mediated reassembly of mitotic Golgi fragments. J Cell Biol. 2004; 164(7):973–8. https://doi.org/10.1083/jcb.200401010 PMID: 15037600; PubMed Central PMCID: PMC2172062.

236. Anderson JF, Siller E, Barral JM. The neurodegenerative-disease-related protein sacsin is a molecular chaperone. J Mol Biol. 2011; 411(4):870–80. https://doi.org/10.1016/j.jmb.2011.06.016 PMID: 21726565.

237. Sundaramoorthy E, Leonard M, Mak R, Liao J, Fulzele A, Bennett EJ. ZNF598 and RACK1 Regulate Mammalian Ribosome-Associated Quality Control Function by Mediating Regulatory 40S Ribosomal Ubiquitylation. Mol Cell. 2017; 65(4):751–60 e4. https://doi.org/10.1016/j.molcel.2016.12.026 PMID: 28132843; PubMed Central PMCID: PMC5321136.

238. Morita M, Ler LW, Fabian MR, Siddiqui N, Mullin M, Henderson VC, et al. A novel 4EHP-GIGYF2 translational repressor complex is essential for mammalian development. Mol Cell Biol. 2012; 32(17):3585–93. https://doi.org/10.1128/MCB.00455-12 PMID: 22751931; PubMed Central PMCID: PMC3422012.

239. Wang G, Kouwaki T, Okamoto M, Oshiumi H. Attenuation of the Innate Immune Response against Viral Infection Due to ZNF598-Promoted Binding of FAT10 to RIG-I. Cell Rep. 2019; 28(8):1961–70 e4. https://doi.org/10.1016/j.celrep.2019.07.081 PMID: 31433974.

240. Balastik M, Ferraguti F, Pires-da Silva A, Lee TH, Alvarez-Bolado G, Lu KP, et al. Deficiency in ubiquitin ligase TRIM2 causes accumulation of neurofilament light chain and neurodegeneration. Proc Natl Acad Sci U S A. 2008; 105(33):12016–21. https://doi.org/10.1073/pnas.0802261105 PMID: 18687884; PubMed Central PMCID: PMC2575299.

241. Sarute N, Ibrahim N, Medegan Fagla B, Lavanya M, Cuevas C, Stavrou S, et al. TRIM2, a novel member of the antiviral family, limits New World arenavirus entry. PLoS Biol. 2019; 17(2):e3000137. https://doi.org/10.1371/journal.pbio.3000137 PMID: 30726215; PubMed Central PMCID: PMC6380604.

242. Dango S, Mosammaparast N, Sowa ME, Xiong LJ, Wu F, Park K, et al. DNA unwinding by ASCC3 helicase is coupled to ALKBH3-dependent DNA alkylation repair and cancer cell proliferation. Mol Cell. 2011; 44(3):373–84. https://doi.org/10.1016/j.molcel.2011.08.039 PMID: 22055184; PubMed Central PMCID: PMC3258846.

243. Jung DJ, Sung HS, Goo YW, Lee HM, Park OK, Jung SY, et al. Novel transcription coactivator complex containing activating signal cointegrator 1. Mol Cell Biol. 2002; 22(14):5203–11. https://doi.org/10.1128/MCB.22.14.5203-5211.2002 PMID: 12077347; PubMed Central PMCID: PMC139772.

244. Williams GD, Gokhale NS, Snider DL, Horner SM. The mRNA Cap 2'-O-Methyltransferase CMTR1 Regulates the Expression of Certain Interferon-Stimulated Genes. mSphere. 2020; 5(3). https://doi.org/10.1128/mSphere.00202-20 PMID: 32404510; PubMed Central PMCID: PMC7227766.

245. Silva CM, Lu H, Day RN. Characterization and cloning of STAT5 from IM-9 cells and its activation by growth hormone. Mol Endocrinol. 1996; 10(5):508–18. https://doi.org/10.1210/mend.10.5.8732682 PMID: 8732682.

246. Lin JX, Leonard WJ. The role of Stat5a and Stat5b in signaling by IL-2 family cytokines. Oncogene. 2000; 19(21):2566–76. https://doi.org/10.1038/sj.onc.1203523 PMID: 10851055.

247. Bennett V, Baines AJ. Spectrin and ankyrin-based pathways: metazoan inventions for integrating cells into tissues. Physiol Rev. 2001; 81(3):1353–92. https://doi.org/10.1152/physrev.2001.81.3.1353 PMID: 11427698.

248. Pine R. Constitutive expression of an ISGF2/IRF1 transgene leads to interferon-independent activation of interferon-inducible genes and resistance to virus infection. J Virol. 1992; 66(7):4470–8. https://doi.org/10.1128/JVI.66.7.4470-4478.1992 PMID: 1376370; PubMed Central PMCID: PMC241256.

249. Welsby I, Hutin D, Gueydan C, Kruys V, Rongvaux A, Leo O. PARP12, an interferon-stimulated gene involved in the control of protein translation and inflammation. J Biol Chem. 2014; 289(38):26642–57. https://doi.org/10.1074/jbc.M114.589515 PMID: 25086041; PubMed Central PMCID: PMC4176246.

250. Yamashita A. Role of SMG-1-mediated Upf1 phosphorylation in mammalian nonsense-mediated mRNA decay. Genes Cells. 2013; 18(3):161–75. https://doi.org/10.1111/gtc.12033 PMID: 23356578.

251. Balistreri G, Horvath P, Schweingruber C, Zund D, McInerney G, Merits A, et al. The host nonsense-mediated mRNA decay pathway restricts Mammalian RNA virus replication. Cell Host Microbe. 2014; 16(3):403–11. https://doi.org/10.1016/j.chom.2014.08.007 PMID: 25211080.

252. Fu M, Blackshear PJ. RNA-binding proteins in immune regulation: a focus on CCCH zinc finger proteins. Nat Rev Immunol. 2017; 17(2):130–43. https://doi.org/10.1038/nri.2016.129 PMID: 27990022; PubMed Central PMCID: PMC5556700.

253. Boldin MP, Goncharov TM, Goltsev YV, Wallach D. Involvement of MACH, a novel MORT1/FADD-interacting protease, in Fas/APO-1- and TNF receptor-induced cell death. Cell. 1996; 85(6):803–15. https://doi.org/10.1016/s0092-8674(00)81265-9 PMID: 8681376.

254. Lalaoui N, Boyden SE, Oda H, Wood GM, Stone DL, Chau D, et al. Mutations that prevent caspase cleavage of RIPK1 cause autoinflammatory disease. Nature. https://doi.org/10.1038/s41586-019-1828-5 PMID: 31827281; 577(7788):103–8. PubMed Central PMCID: PMC6930849.

255. Tagami H, Ray-Gallet D, Almouzni G, Nakatani Y. Histone H3.1 and H3.3 complexes mediate nucleosome assembly pathways dependent or independent of DNA synthesis. Cell. 2004; 116(1):51–61. https://doi.org/10.1016/s0092-8674(03)01064-x PMID: 14718166.

256. Medzhitov R. Toll-like receptors and innate immunity. Nat Rev Immunol. 2001; 1(2):135–45. https://doi.org/10.1038/35100529 PMID: 11905821.

257. Kaisho T, Akira S. Toll-like receptors and their signaling mechanism in innate immunity. Acta Odontol Scand. 2001; 59(3):124–30. https://doi.org/10.1080/000163501750266701 PMID: 11501880.

258. Mitacek RM, Ke YL, Prenni JE, Jadeja R, VanOverbeke DL, Mafi GG, et al. Mitochondrial Degeneration, Depletion of NADH, and Oxidative Stress Decrease Color Stability of Wet-Aged Beef Longissimus Steaks. J Food Sci. 2019; 84(1):38–50. https://doi.org/10.1111/1750-3841.14396 WOS:000455527800006. PMID: 30496612

259. Ross JL, Wallace K, Shuman H, Goldman YE, Holzbaur EL. Processive bidirectional motion of dynein-dynactin complexes in vitro. Nat Cell Biol. 2006; 8(6):562–70. https://doi.org/10.1038/ncb1421 PMID: 16715075.

260. Heraud-Farlow JE, Sharangdhar T, Li X, Pfeifer P, Tauber S, Orozco D, et al. Staufen2 regulates neuronal target RNAs. Cell Rep. 2013; 5(6):1511–8. https://doi.org/10.1016/j.celrep.2013.11.039 PMID: 24360961.

261. Hay RT, Vuillard L, Desterro JM, Rodriguez MS. Control of NF-kappa B transcriptional activation by signal induced proteolysis of I kappa B alpha. Philos Trans R Soc Lond B Biol Sci. 1999; 354 (1389):1601–9. https://doi.org/10.1098/rstb.1999.0504 PMID: 10582246; PubMed Central PMCID: PMC1692667.

262. Gaur U, Aggarwal BB. Regulation of proliferation, survival and apoptosis by members of the TNF superfamily. Biochem Pharmacol. 2003; 66(8):1403–8. https://doi.org/10.1016/s0006-2952(03)00490-8 PMID: 14555214.

263. James MA, Lee JH, Klingelhutz AJ. Human papillomavirus type 16 E6 activates NF-kappaB, induces cIAP-2 expression, and protects against apoptosis in a PDZ binding motif-dependent manner. J Virol. 2006; 80(11):5301–7. https://doi.org/10.1128/JVI.01942-05 PMID: 16699010; PubMed Central PMCID: PMC1472131.

264. Kwak EL, Larochelle DA, Beaumont C, Torti SV, Torti FM. Role for NF-kappa B in the regulation of ferritin H by tumor necrosis factor-alpha. J Biol Chem. 1995; 270(25):15285–93. https://doi.org/10.1074/jbc.270.25.15285 PMID: 7797515.

265. Biswas G, Guha M, Avadhani NG. Mitochondria-to-nucleus stress signaling in mammalian cells: nature of nuclear gene targets, transcription regulation, and induced resistance to apoptosis. Gene. 2005; 354:132–9. https://doi.org/10.1016/j.gene.2005.03.028 PMID: 15978749; PubMed Central PMCID: PMC3800739.

266. Jono H, Lim JH, Chen LF, Xu H, Trompouki E, Pan ZK, et al. NF-kappaB is essential for induction of CYLD, the negative regulator of NF-kappaB: evidence for a novel inducible autoregulatory feedback pathway. J Biol Chem. 2004; 279(35):36171–4. https://doi.org/10.1074/jbc.M406638200 PMID: 15226292.

267. Xu SQ, Zhang H, Yang XD, Qian YW, Xiao Q. Inhibition of cathepsin L alleviates the microglia-mediated neuroinflammatory responses through caspase-8 and NF-kappa B pathways. Neurobiol Aging. 2018; 62:159–67. https://doi.org/10.1016/j.neurobiolaging.2017.09.030 WOS:000418478600014. PMID: 29154036

268. Wang YR, Qin S, Han R, Wu JC, Liang ZQ, Qin ZH, et al. Cathepsin L plays a role in quinolinic acid-induced NF-Kappab activation and excitotoxicity in rat striatal neurons. Plos One. 2013; 8(9):e75702. https://doi.org/10.1371/journal.pone.0075702 PMID: 24073275; PubMed Central PMCID: PMC3779166.

269. Wendeler M, Hoernschemeyer J, Hoffmann D, Kolter T, Schwarzmann G, Sandhoff K. Photoaffinity labelling of the human GM2-activator protein. Mechanistic insight into ganglioside GM2 degradation. Eur J Biochem. 2004; 271(3):614–27. https://doi.org/10.1111/j.1432-1033.2003.03964.x PMID: 14728689.

270. Duan J, Zhang Q, Hu X, Lu D, Yu W, Bai H. N(4)-acetylcytidine is required for sustained NLRP3 inflammasome activation via HMGB1 pathway in microglia. Cell Signal. 2019; 58:44–52. https://doi.org/10.1016/j.cellsig.2019.03.007 PMID: 30853521.

271. Wood ER, Bledsoe R, Chai J, Daka P, Deng H, Ding Y, et al. The Role of Phosphodiesterase 12 (PDE12) as a Negative Regulator of the Innate Immune Response and the Discovery of Antiviral Inhibitors. J Biol Chem. 2015; 290(32):19681–96. https://doi.org/10.1074/jbc.M115.653113 PMID: 26055709; PubMed Central PMCID: PMC4528132.

272. Krappmann D, Scheidereit C. Regulation of NF-kappa B activity by I kappa B alpha and I kappa B beta stability. Immunobiology. 1997; 198(1–3):3–13. https://doi.org/10.1016/s0171-2985(97)80022-8 PMID: 9442373.

273. Dominissini D, Rechavi G. N(4)-acetylation of Cytidine in mRNA by NAT10 Regulates Stability and Translation. Cell. 2018; 175(7):1725–7. https://doi.org/10.1016/j.cell.2018.11.037 PMID: 30550783.

274. Cai S, Liu X, Zhang C, Xing B, Du X. Autoacetylation of NAT10 is critical for its function in rRNA transcription activation. Biochem Biophys Res Commun. 2017; 483(1):624–9. https://doi.org/10.1016/j.bbrc.2016.12.092 PMID: 27993683.

275. Cambiaghi TD, Pereira CM, Shanmugam R, Bolech M, Wek RC, Sattlegger E, et al. Evolutionarily conserved IMPACT impairs various stress responses that require GCN1 for activating the eIF2 kinase GCN2. Biochem Biophys Res Commun. 2014; 443(2):592–7. https://doi.org/10.1016/j.bbrc.2013.12.021 PMID: 24333428.

276. Pereira CM, Sattlegger E, Jiang HY, Longo BM, Jaqueta CB, Hinnebusch AG, et al. IMPACT, a protein preferentially expressed in the mouse brain, binds GCN1 and inhibits GCN2 activation. J Biol Chem. 2005; 280(31):28316–23. https://doi.org/10.1074/jbc.M408571200 PMID: 15937339.

277. Roobol A, Roobol J, Bastide A, Knight JR, Willis AE, Smales CM. p58IPK is an inhibitor of the eIF2alpha kinase GCN2 and its localization and expression underpin protein synthesis and ER processing capacity. Biochem J. 2015; 465(2):213–25. https://doi.org/10.1042/BJ20140852 PMID: 25329545.

278. del Pino J, Jimenez JL, Ventoso I, Castello A, Munoz-Fernandez MA, de Haro C, et al. GCN2 has inhibitory effect on human immunodeficiency virus-1 protein synthesis and is cleaved upon viral infection. Plos One. 2012; 7(10):e47272. https://doi.org/10.1371/journal.pone.0047272 PMID: 23110064; PubMed Central PMCID: PMC3479103.

279. Berlanga JJ, Ventoso I, Harding HP, Deng J, Ron D, Sonenberg N, et al. Antiviral effect of the mammalian translation initiation factor 2alpha kinase GCN2 against RNA viruses. Embo J. 2006; 25(8):1730–40. https://doi.org/10.1038/sj.emboj.7601073 PMID: 16601681; PubMed Central PMCID: PMC1440839.

280. Costa-Mattioli M, Gobert D, Harding H, Herdy B, Azzi M, Bruno M, et al. Translational control of hippocampal synaptic plasticity and memory by the eIF2alpha kinase GCN2. Nature. 2005; 436 (7054):1166–73. https://doi.org/10.1038/nature03897 PMID: 16121183; PubMed Central PMCID: PMC1464117.

281. Chang ZQ, Lee SY, Kim HJ, Kim JR, Kim SJ, Hong IK, et al. Endotoxin activates de novo sphingolipid biosynthesis via nuclear factor kappa B-mediated upregulation of Sptlc2. Prostaglandins Other Lipid Mediat. 2011; 94(1–2):44–52. https://doi.org/10.1016/j.prostaglandins.2010.12.003 PMID: 21167294; PubMed Central PMCID: PMC3366150.

282. Hornemann T, Penno A, Rutti MF, Ernst D, Kivrak-Pfiffner F, Rohrer L, et al. The SPTLC3 subunit of serine palmitoyltransferase generates short chain sphingoid bases. J Biol Chem. 2009; 284 (39):26322–30. https://doi.org/10.1074/jbc.M109.023192 PMID: 19648650; PubMed Central PMCID: PMC2785320.

283. Pralhada Rao R, Vaidyanathan N, Rengasamy M, Mammen Oommen A, Somaiya N, Jagannath MR. Sphingolipid metabolic pathway: an overview of major roles played in human diseases. J Lipids. 2013; 2013:178910. https://doi.org/10.1155/2013/178910 PMID: 23984075; PubMed Central PMCID: PMC3747619.

284. Chen CC, Juan CW, Chen KY, Chang YC, Lee JC, Chang MC. Upregulation of RPA2 promotes NF-kappaB activation in breast cancer by relieving the antagonistic function of menin on NF-kappaB-regulated transcription. Carcinogenesis. 2017; 38(2):196–206. https://doi.org/10.1093/carcin/bgw123 PMID: 28007956.

285. Hagele H, Allam R, Pawar RD, Anders HJ. Double-stranded RNA activates type I interferon secretion in glomerular endothelial cells via retinoic acid-inducible gene (RIG)-1. Nephrol Dial Transplant. 2009; 24(11):3312–8. https://doi.org/10.1093/ndt/gfp339 PMID: 19608629.

286. Farr M, Zhu D-F, Povelones M, Valcich D, Ambron RT. Direct interactions between immunocytes and neurons after axotomy in Aplysia. Journal of Neurobiology. 2001; 46(2):89–96. https://doi.org/10.1002/1097-4695(20010205)46:2<89::AID-NEU20>3.0.CO;2-D. PMID: 11153011

287. Farr M, Mathews J, Zhu DF, Ambron RT. Inflammation causes a long-term hyperexcitability in the nociceptive sensory neurons of Aplysia. Learn Mem. 1999; 6(3):331–40. PMID: 10492014; PubMed Central PMCID: PMC311296.

288. Abrams TW. Studies on Aplysia neurons suggest treatments for chronic human disorders. Curr Biol. 2012; 22(17):R705–11. https://doi.org/10.1016/j.cub.2012.08.011 PMID: 22975001.

289. Clatworthy A, Castro G, Budelmann B, Walters E. Induction of a cellular defense reaction is accompanied by an increase in sensory neuron excitability in Aplysia. The Journal of Neuroscience. 1994; 14 (5):3263–70. https://doi.org/10.1523/jneurosci.14-05-03263.1994 PMID: 8182470

290. Aravin AA, Hannon GJ, Brennecke J. The Piwi-piRNA pathway provides an adaptive defense in the transposon arms race. Science. 2007; 318(5851):761–4. https://doi.org/10.1126/science.1146484 PMID: 17975059.

291. Parrish NF, Fujino K, Shiromoto Y, Iwasaki YW, Ha H, Xing J, et al. piRNAs derived from ancient viral processed pseudogenes as transgenerational sequence-specific immune memory in mammals. Rna. 2015; 21(10):1691–703. https://doi.org/10.1261/rna.052092.115 PMID: 26283688; PubMed Central PMCID: PMC4574747.

292. Hamada H, Yamamura M, Ohi H, Kobayashi Y, Niwa K, Oyama T, et al. Characterization of the human zinc finger nfx1type containing 1 encoding ZNFX1 gene and its response to 12Otetradecanoyl13acetate in HL60 cells. Int J Oncol. 2019; 55(4):896–904. https://doi.org/10.3892/ijo.2019.4860 PMID: 31432148.

293. Minoda Y, Saeki K, Aki D, Takaki H, Sanada T, Koga K, et al. A novel Zinc finger protein, ZCCHC11, interacts with TIFA and modulates TLR signaling. Biochem Biophys Res Commun. 2006; 344 (3):1023–30. https://doi.org/10.1016/j.bbrc.2006.04.006 PMID: 16643855.

294. Simon PS, Sharman SK, Lu C, Yang D, Paschall AV, Tulachan SS, et al. The NF-kappaB p65 and p50 homodimer cooperate with IRF8 to activate iNOS transcription. BMC Cancer. 2015; 15:770. https://doi.org/10.1186/s12885-015-1808-6 PMID: 26497740; PubMed Central PMCID: PMC4619452.

295. Chen J, Chen ZJ. Regulation of NF-kappaB by ubiquitination. Curr Opin Immunol. 2013; 25(1):4–12. https://doi.org/10.1016/j.coi.2012.12.005 PMID: 23312890; PubMed Central PMCID: PMC3594545.

296. Kemp IK, Coyne VE. Identification and characterisation of the Mpeg1 homologue in the South African abalone, Haliotis midae. Fish Shellfish Immunol. 2011; 31(6):754–64. https://doi.org/10.1016/j.fsi.2011.07.010 PMID: 21803160.

297. Bathige SD, Umasuthan N, Whang I, Lim BS, Won SH, Lee J. Antibacterial activity and immune responses of a molluscan macrophage expressed gene-1 from disk abalone, Haliotis discus discus. Fish Shellfish Immunol. 2014; 39(2):263–72. https://doi.org/10.1016/j.fsi.2014.05.012 PMID: 24852343.

298. Shen JD, Cai QF, Yan LJ, Du CH, Liu GM, Su WJ, et al. Cathepsin L is an immune-related protein in Pacific abalone (Haliotis discus hannai)—Purification and characterization. Fish Shellfish Immunol. 2015; 47(2):986–95. https://doi.org/10.1016/j.fsi.2015.11.004 PMID: 26549175.

299. Munoz JP, Ivanova S, Sanchez-Wandelmer J, Martinez-Cristobal P, Noguera E, Sancho A, et al. Mfn2 modulates the UPR and mitochondrial function via repression of PERK. Embo J. 2013; 32(17):2348–61. https://doi.org/10.1038/emboj.2013.168 PMID: 23921556; PubMed Central PMCID: PMC3770335.

300. Muoio DM. TXNIP links redox circuitry to glucose control. Cell Metabolism. 2007; 5(6):412–4. https://doi.org/10.1016/j.cmet.2007.05.011 WOS:000247115400004. PMID: 17550776

301. Shembade N, Parvatiyar K, Harhaj NS, Harhaj EW. The ubiquitin-editing enzyme A20 requires RNF11 to downregulate NF-kappaB signalling. Embo J. 2009; 28(5):513–22. https://doi.org/10.1038/emboj.2008.285 PMID: 19131965; PubMed Central PMCID: PMC2657574.

302. McNally RS, Davis BK, Clements CM, Accavitti-Loper MA, Mak TW, Ting JP. DJ-1 enhances cell survival through the binding of Cezanne, a negative regulator of NF-kappaB. J Biol Chem. 2011; 286(6):4098–106. https://doi.org/10.1074/jbc.M110.147371 PubMed Central PMCID: PMC3039338. PMID: 21097510

303. Kim KS, Kim JS, Park JY, Suh YH, Jou I, Joe EH, et al. DJ-1 associates with lipid rafts by palmitoylation and regulates lipid rafts-dependent endocytosis in astrocytes. Hum Mol Genet. 2013; 22(23):4805–17. https://doi.org/10.1093/hmg/ddt332 PMID: 23847046.

304. Cardamone MD, Krones A, Tanasa B, Taylor H, Ricci L, Ohgi KA, et al. A protective strategy against hyperinflammatory responses requiring the nontranscriptional actions of GPS2. Mol Cell. 2012; 46(1):91–104. https://doi.org/10.1016/j.molcel.2012.01.025 PMID: 22424771; PubMed Central PMCID: PMC3327812.

305. Fan R, Toubal A, Goni S, Drareni K, Huang Z, Alzaid F, et al. Loss of the co-repressor GPS2 sensitizes macrophage activation upon metabolic stress induced by obesity and type 2 diabetes. Nat Med. 2016; 22(7):780–91. https://doi.org/10.1038/nm.4114 PMID: 27270589.

306. Rorbach J, Nicholls TJ, Minczuk M. PDE12 removes mitochondrial RNA poly(A) tails and controls translation in human mitochondria. Nucleic Acids Res. 2011; 39(17):7750–63. https://doi.org/10.1093/nar/gkr470 PMID: 21666256; PubMed Central PMCID: PMC3177208.

307. Boveris A, Navarro A. Brain mitochondrial dysfunction in aging. Iubmb Life. 2008; 60(5):308–14. https://doi.org/10.1002/iub.46 WOS:000255598500014. PMID: 18421773

308. Manna SK, Zhang HJ, Yan T, Oberley LW, Aggarwal BB. Overexpression of manganese superoxide dismutase suppresses tumor necrosis factor-induced apoptosis and activation of nuclear transcription factor-kappaB and activated protein-1. J Biol Chem. 1998; 273(21):13245–54. https://doi.org/10.1074/jbc.273.21.13245 PMID: 9582369.

309. Kretz-Remy C, Mehlen P, Mirault ME, Arrigo AP. Inhibition of I kappa B-alpha phosphorylation and degradation and subsequent NF-kappa B activation by glutathione peroxidase overexpression. J Cell Biol. 1996; 133(5):1083–93. https://doi.org/10.1083/jcb.133.5.1083 PMID: 8655581; PubMed Central PMCID: PMC2120847.

310. Lingappan K. NF-kappaB in Oxidative Stress. Curr Opin Toxicol. 2018; 7:81–6. https://doi.org/10.1016/j.cotox.2017.11.002 PMID: 29862377; PubMed Central PMCID: PMC5978768.

311. Li N, Karin M. Is NF-κB the sensor of oxidative stress? The FASEB Journal. 1999; 13(10):1137–43. https://doi.org/10.1096/fasebj.13.10.1137. PMID: 10385605

312. Papa S, Bubici C, Pham CG, Zazzeroni F, Franzoso G. NF-kappaB meets ROS: an 'iron-ic' encounter. Cell Death Differ. 2005; 12(10):1259–62. https://doi.org/10.1038/sj.cdd.4401694 PMID: 15947786.

313. Deng J, Lu PD, Zhang Y, Scheuner D, Kaufman RJ, Sonenberg N, et al. Translational repression mediates activation of nuclear factor kappa B by phosphorylated translation initiation factor 2. Mol Cell Biol. 2004; 24(23):10161–8. https://doi.org/10.1128/MCB.24.23.10161-10168.2004 PMID: 15542827; PubMed Central PMCID: PMC529034.

314. Deleidi M, Jaggle M, Rubino G. Immune aging, dysmetabolism, and inflammation in neurological diseases. Front Neurosci. 2015; 9:172. https://doi.org/10.3389/fnins.2015.00172 PMID: 26089771; PubMed Central PMCID: PMC4453474.

315. Currais A. Ageing and inflammation—A central role for mitochondria in brain health and disease. Ageing Res Rev. 2015; 21:30–42. https://doi.org/10.1016/j.arr.2015.02.001 WOS:000355037900003. PMID: 25684584

316. Garaschuk O, Semchyshyn HM, Lushchak VI. Healthy brain aging: Interplay between reactive species, inflammation and energy supply. Ageing Res Rev. 2018; 43:26–45. https://doi.org/10.1016/j.arr.2018.02.003 WOS:000433016300004. PMID: 29452266